

## CHAPTER 3

A SIMULATION MODEL FOR SULFATE FORMATION AND TRANSPORT  
UNDER UNSTEADY METEOROLOGICAL CONDITIONS3.1 Introduction

An appropriate means must be constructed for relating sulfur oxides pollutant emissions to observed sulfate air quality over the central portion of the Los Angeles Basin. In the preceding chapter, it was decided that our understanding of emissions-air quality relationships would be verified by simulating monthly average sulfate concentrations observed during the years 1972 through 1974. For this reason, an air quality model capable of simulating long-term average sulfate concentrations must be selected.

Techniques in current use for modeling long-term average emissions-air quality relationships first will be reviewed. Commonly employed modeling methods lack the ability to calculate long-term average pollutant concentrations in a geographic region like Los Angeles which is characterized by unsteady meteorological conditions (e.g. light and variable winds). To resolve this problem, a simulation model will be constructed which calculates long-run average pollutant levels using a Lagrangian marked particle technique. The model will be derived for first-order chemical reaction and dry deposition of sulfur oxides dispersing in an airshed which experiences a temperature inversion aloft. Then a series of approximations will be made which permit the model

to be applied to simulation of long-run average sulfate concentrations in Los Angeles using readily available meteorological data.

### 3.2 An Overview of Long-Term Average Air Quality Models

Long-term average air quality models in current use are of two general types: empirical models based on statistical analysis of air quality data, and deterministic models based on the atmospheric diffusion equation.

#### 3.2.1 Empirical Emissions to Air Quality Models

Statistical techniques have been widely applied as the primary means of developing empirical emissions-air quality relationships. The frequency distribution of existing air pollutant levels in the air basin of interest is first established from ambient air monitoring data by methods such as those of Larsen (1971). Then linear or non-linear rollback techniques are used to make air quality projections. Linear rollback models assume that current air quality levels are proportional to current basin-wide emissions levels, and that ambient pollutant concentrations will decline in proportion to emission reductions until background air quality is reached at zero emissions. Non-linear rollback models hold that air quality response to an emission change for a reactive contaminant is some stated non-linear function of current contaminant emissions or air quality levels. Examples of linear and non-linear rollback models recommended by the U.S. Environmental Protection Agency are found in the Federal Register, (36 F.R. 158, August 14, 1971, pp. 15489-15491 and Appendix J). The sulfate air

pollution control strategy study conducted by Trijonis, et al. (1975) depends on a linear rollback calculation.

Linear rollback models assume uniform proportionate response at all receptor points due to a change in emissions anywhere in the air basin. Thus linear rollback models are likely to be valid only under a very limited set of circumstances. Situations in which a simple rollback air quality projection is likely to fail include cases where

- (a) the relative spatial distribution of emission source strength is to be changed;
- (b) changes are made in source effective stack height;
- (c) atmospheric chemical reactions introduce non-linear effects;
- and
- (d) unsteady meteorological conditions require an explicit treatment of source to receptor transport.

Spatial homogeneity of emission reduction is seldom achieved in any real situation involving a stationary source emission control strategy. Simple linear rollback models are of questionable utility in these cases. Spatial homogeneity assumptions can be relaxed so that the effect of controlling geographically dissimilar source classes to different degrees of stringency may be deduced (provided that a long history of emissions and air quality data is available for model development; see Cass, 1975). However, as model complexity increases, the effort involved in constructing an empirical emissions-air quality model can quickly approach that required for a deterministic representation of the problem based on solution of the atmospheric diffusion equation.

### 3.2.2 Models Based on a Description of Atmospheric Transport and Chemistry

Deterministic emissions to air quality models are distinguished into two types based on the coordinate system employed: Lagrangian or Eulerian. In the Lagrangian approach, air pollutant dispersion is represented by the trajectories of representative fluid particles. The underlying coordinate system is tied to the moving fluid particle. Pollutant concentrations at downwind receptor locations are determined by the probability that a pollutant-laden fluid parcel emitted at a known time,  $t'$ , and place,  $x'$ , will occupy a given location,  $x$ , in the airshed at later time  $t$ .

A generalized expression for most Lagrangian air quality models in current use is of the form:

$$\begin{aligned} \langle c(x,t) \rangle = & \int_{-\infty}^{\infty} \int_{-\infty}^{\infty} \int_{-\infty}^{\infty} Q(x,t|x_0,t_0) \langle c(x_0,t_0) \rangle R(t,t_0) dx_0 \\ & + \int_{-\infty}^{\infty} \int_{-\infty}^{\infty} \int_{-\infty}^{\infty} \int_{t_0}^t Q(x,t|x',t') S(x',t') R(t,t') dt' dx' \quad (3.1) \end{aligned}$$

where

$\langle c(x,t) \rangle$  is the ensemble mean pollutant concentration at point  $x$  at time  $t$ .

$Q(x,t|x',t')$  is the transition probability density that a fluid particle at location  $x'$  at time  $t'$  will undergo a displacement to location  $x$  at time  $t$ .

$R(t,t')$  is the probability that a fluid particle will retain its chemical identity at time  $t'$  until time  $t$ .

$S(x',t')$  is the spatial-temporal distribution of emission sources, in mass per location per unit time.

$x_0$  and  $t_0$  establish initial conditions for location and time within the airshed.

The form in which equation (3.1) is expressed is largely as developed for air quality modeling by Lamb (see Lamb and Neiburger, 1971; Lamb, 1971; Lamb and Seinfeld, 1973).

The first integral term on the right hand side of equation (3.1) maps initial pollutant concentration in the airshed into its effect on air quality at time  $t$ . The second term on the right hand side of equation (3.1) computes the effect of fresh emissions on air quality over the time interval  $t_0$  to  $t$ . The chemical reaction expressions  $R(t,t_0)$  and  $R(t,t')$  in equation (3.1) are valid for first-order chemistry. For first-order chemistry, each fluid particle's probability of undergoing chemical reaction is independent of the chemical conversion of other particles of that species elsewhere in the system. In that case, fluid transport and fluid chemistry are independent. The probability that the fluid particle is found at location  $x$ , at time  $t$  is thus simply the product of the transition probability  $Q(x,t|x',t')$  that air parcel transport to that location will occur, times the probability  $R(t,t')$  that the chemical status of that air parcel will not change in the interim.

Eulerian air quality models rely on a mass balance constructed for a volume element which is fixed in space. The instantaneous pollutant concentration for each species  $i$ ,  $c_i$ , within that volume element must satisfy the following continuity equation:

$$\frac{\partial c_i}{\partial t} + \frac{\partial u_j c_i}{\partial x_j} = D_i \frac{\partial^2 c_i}{\partial x_j \partial x_j} + R_i(c_1, \dots, c_N, T) + S_i(x, t) \quad (3.2)$$

$$i = 1, 2, \dots, N$$

$$j = 1, 2, 3$$

where

$u_j$  is the fluid velocity in the  $j^{\text{th}}$  coordinate direction at the location of interest.

$D_i$  is the molecular diffusivity of species  $i$  in the air within the control volume.

$R_i$  is the rate of formation of species  $i$  by chemical reaction (as a function of pollutant concentrations and temperature,  $T$ ).

$S_i$  is source strength for species  $i$  within the volume element.

$x$  is location, given as  $(x_1, x_2, x_3)$ .

$t$  is time.

From this fundamental mass balance, one can derive an approximate relationship for the mean concentration of a pollutant species (see Lamb and Seinfeld, 1973).

$$\frac{\partial \langle c_i \rangle}{\partial t} + \frac{\partial}{\partial x_j} (\bar{u}_j \langle c_i \rangle) = \frac{\partial}{\partial x_j} \left( \bar{K}_{jk} \frac{\partial \langle c_i \rangle}{\partial x_k} \right) + R_i(\langle c_1 \rangle, \dots, \langle c_N \rangle) + S_i(x, t) \quad (3.3)$$

$$i = 1, 2, \dots, N$$

$$j = 1, 2, 3$$

$$k = 1, 2, 3$$

where

$\bar{u}_j$  is the average wind velocity in the  $j^{\text{th}}$  coordinate direction.

$\bar{K}_{jk}$  is the atmospheric eddy diffusivity tensor.

Usually it is assumed for convenience that  $\bar{K}_{jk} = 0$  for  $j \neq k$ .

For a discussion of the theoretical relationship between the modeling approaches of equations (3.1) and (3.3), see Lamb and Seinfeld (1973). For a discussion of some of the implications of the assumptions needed to introduce those equations into practical urban air quality models, see Liu and Seinfeld (1975).

### 3.2.3 Application of Deterministic Air Quality Models to the Calculation of Long-Term Average Air Quality

There are two methods in current use for modeling long-run average air pollutant concentrations. A dynamic model for short-term concentration predictions could be developed based on equations (3.1) or (3.3). Then the very large number of nearly instantaneous concentration predictions that result could be averaged. However, when a fully determined short-term urban air quality simulation is run over a period of several years, the computing resources required become enormous if the simulation is at all realistic. For that reason, long-term average air pollutant levels are usually calculated using pseudo-steady state models.

Pseudo-steady state air quality models are derived from a Lagrangian formulation of the atmospheric diffusion equation, such as given in (3.1). The objective of these models is to directly calculate a

long-term average concentration as a function of location within the airshed:

$$\overline{\langle c(X) \rangle} = \frac{1}{T} \int_0^T \langle c(X,t) \rangle dt \quad (3.4)$$

where  $T$ , in our case, is a month or a year in duration.

Long-term average air quality models in current use view meteorological behavior as a sequence of steady state conditions. Steady meteorological conditions exist when constant wind speed, wind direction, and atmospheric stability persist for time periods longer than the characteristic time for which an air pollutant parcel's contribution to observed air quality remains significant. That time period would correspond to the shorter of either the characteristic time for advection to beyond the boundaries of the air basin, or the time needed for dilution to reduce pollutant concentration to insignificance. One can see that many locations affected by light and variable winds may not often encounter meteorological circumstances which satisfy this steady state definition. Therefore, for the sake of discussion, Seinfeld (1975) defines two meteorological domains.

$\Omega_s$  = the collection of all time intervals during the long time period  $(0,T)$  in which wind speed exceeds a defined minimum value, and the meteorology is steady.

$\Omega_u$  = the collection of all time intervals during the long time period  $(0,T)$  in which either the wind speed does not exceed a defined threshold (stagnation conditions) or the meteorology is unsteady.

For the simple case of an inert pollutant with  $\langle c(X,t_0) \rangle = 0$  and  $t_0 = 0$ , substitution of equation (3.1) into (3.4) plus a separation

of meteorological conditions into domains  $\Omega_s$  and  $\Omega_u$ , Seinfeld (1975) obtains an expression for long-term average pollutant concentration against which virtually all long-run average emissions-air quality models may be judged.

$$\begin{aligned} \overline{\langle c(x) \rangle} &= \int_{-\infty}^{\infty} \int_{-\infty}^{\infty} \int_{-\infty}^{\infty} \sum_{m=1}^M \sum_{i=1}^{N_1} \sum_{j=1}^{N_2} f_{ijm} g(x, x', U_i, \theta_j, \sigma(t_{ijm})) S(x', t_{ijm}) \Delta t_{ijm} dx' \\ &+ \int_{-\infty}^{\infty} \int_{-\infty}^{\infty} \int_{-\infty}^{\infty} \int_{\Omega_u} \bar{Q}(x, x', t'; T) S(x', t') dt' dx' \end{aligned} \quad (3.5)$$

where the newly introduced terms are:

$f_{ijm}$  the joint frequency distribution of wind speed, wind direction, and atmospheric stability class during the  $m$  periods of steady meteorology which make up domain  $\Omega_s$ .

$g(x, x', U_i, \theta_j, \sigma(t_{ijm}))$

a diffusion kernel which gives the response at location  $x$  to a unit source at location  $x'$  which began emitting at time  $t'$  under *steady* meteorological conditions. Usually the form of  $g(x, x', U_i, \theta_j, \sigma(t_{ijm}))$  is obtained from a Gaussian plume formula (see Turner, 1969).

$U_i$  scalar wind speed, expressed within speed class intervals  $i = 1, \dots, N_1$ .

$\theta_j$  wind direction blowing into sector  $j$ .

$\sigma(t_{ijm})$  the standard deviation of plume spread about its centerline as a function of travel time.

$\Delta t_{ijm}$  the length of the  $m^{\text{th}}$  steady meteorological time interval (with wind speed in class  $i$  and wind direction into sector  $j$ ).

$\bar{Q}(x, x', t'; T)$  an averaged source to receptor transport probability equal to

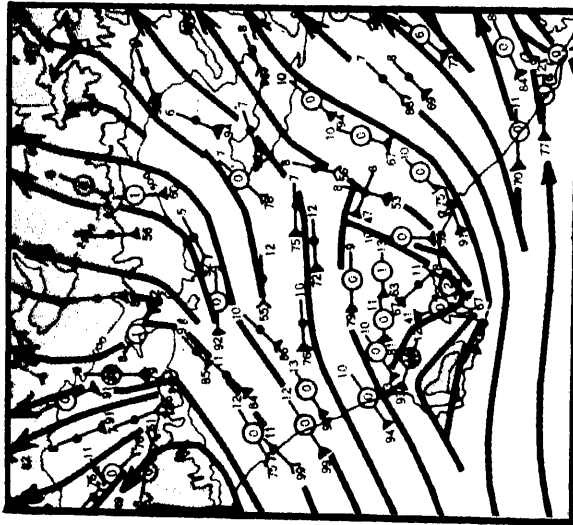
$$\frac{1}{T} \int_{t'}^T Q(x, t | x', t') dt .$$

Equation (3.5) is the complete expression for the long-run average concentration of an inert pollutant. Existing long-term average air quality models, however, commonly evaluate only the steady state joint Gaussian term [i.e. the first term on the right hand side of equation (3.5)]. Popular long-run average models which do not treat unsteady meteorological conditions include those of Martin and Tikvart (1968), Calder (1971) and Gifford and Hanna (1970). Seinfeld (1975) notes that the neglect of the unsteady meteorological domain  $\Omega_u$  can be a serious problem with typical long-run average air quality models:

"Because the form of  $\bar{Q}$  under dynamic or stagnant conditions is very difficult to determine, most steady-state models based on (3.5) neglect the contribution to  $\langle c(X) \rangle$  from  $\Omega_u$ . Unfortunately, during stagnation periods the contribution to the overall long-term average concentration  $\langle c(X) \rangle$  is the most important. Thus, steady-state models based on  $\Omega_s$  may underestimate the long-term average concentration."

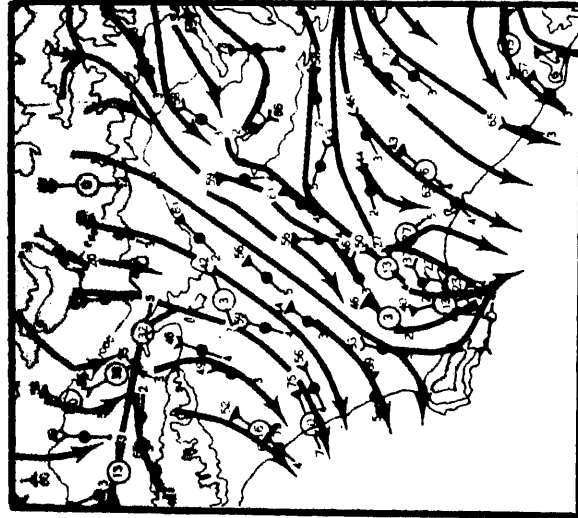
### 3.3 A Long-Term Average Model for Sulfate Air Quality Under Unsteady Meteorological Conditions

Examination of Los Angeles meteorology indicates that the steady state assumptions inherent in conventional long-term average air quality models are regularly violated in this locale. The Los Angeles Basin is influenced by coastal meteorology characterized by a daily land breeze/ sea breeze wind reversal. Differential solar heating of land and sea surfaces leads to a daytime wind pattern with transport inland across the coastline as shown in Figure 3.1. At night, the characteristic transport pattern reverses. Slow drainage winds and land breeze conditions cause flow out to sea, as shown in Figure 3.2. Early morning



Typical Afternoon Onshore Flow Pattern  
July 12:00-18:00 Hours PST

FIGURE 3.1



Typical Late Night  
Offshore Flow Pattern  
October 00:00-07:00 Hours PST

FIGURE 3.2

(from DeMarrais, Holzworth and Hosler, 1965)

and early evening wind stagnation periods occur as transition from one transport direction to another takes place.

Secondly, there is a strong diurnal variation in inversion base behavior over the Los Angeles Basin. Solar heating of the land surface causes the base of low overnight inversions to be eroded by warming of air from below during the day. Superimposed on this is a sinking motion induced by the Pacific Anticyclone which causes the inversion base to descend again at night after the strong solar input has ceased. Thus maximum air parcel dilution in the vertical direction changes drastically as a function of time during air parcel transport across the basin. This too violates steady state assumptions.

A pseudo-steady state model for ground level area source emission of a conserved pollutant might still function reasonably well in Los Angeles. That would be the case if relative pollutant dilution were so rapid as to shorten the time,  $\Delta t_m$ , over which steady state conditions had to be maintained in order to reasonably reproduce observed air quality. For carbon monoxide emissions from automotive traffic, observed air quality is often dominated by emissions from the immediate neighborhood of the receptor point. A succession of steady state conditions might still be used to represent transport over such short travel distances.

However, sulfate air quality is the result of atmospheric chemical reactions in which sulfates are formed with travel distance downwind. Dilution is not sufficiently rapid to overwhelm sulfate formation rates. For that reason, the time interval,  $\Delta t_m$ , over which steady state

transport conditions would have to be maintained in order to model sulfate concentrations is limited by the time necessary for an air parcel to clear the airshed. In Los Angeles, the characteristic times for wind reversal, inversion base change, and air stagnation periods are shorter than transport times out of the air basin. An air parcel may wander in the basin for more than a day until a high speed wind event clears it from the airshed. For that reason, a long-term average air quality model for sulfate formation in Los Angeles will have to cope with unsteady meteorological conditions.

Lamb and Seinfeld (1973) suggest that the only feasible way of determining source to receptor transport probabilities under unsteady meteorological conditions is by means of a simulation model. Analytical solutions are unavailable. Lamb (1971) has used Deardorff's (1970) planetary boundary layer model to explore such a simulation for a single point source release into an atmosphere with a steady wind but inhomogeneous non-stationary turbulence. In the following sections of this chapter, we will describe the formulation of a multiple source urban simulation model for long-term average sulfate concentrations. The model uses a Lagrangian marked particle technique to compute source to receptor transport and reaction probabilities in accordance with the time sequence of meteorological events. The model is derived for a geographic region characterized by unsteady meteorological conditions and an idealized persistent temperature inversion aloft. First order chemical reactions and pollutant dry deposition are incorporated.

At first, the progress of a single representative fluid particle containing sulfur oxides will be tracked through the airshed. Then by integrating over all such particles in the airshed, general expressions will be written for the average concentration of sulfur dioxide and sulfates within a ground level receptor cell. Finally, the meteorological data available for Los Angeles will be examined and the general approach to tracking fluid particle location and chemical status will be reduced to a specific computational procedure. Long-run average pollutant concentrations may then be resolved by simulating release of sulfur oxides-laden fluid particles from a multiplicity of urban source classes.

### 3.3.1 Single Particle Transport and Reaction Probabilities

Consider the history of a fluid particle containing a sulfur oxide molecule which was emitted from location  $x'$  at time  $t_0$ . The fluid particle has several important attributes which determine its future importance to observed sulfate air quality. These attributes include:

- (a) a time history of its trajectory across the air basin in the horizontal plane
- (b) its position over time in the vertical dimension
- (c) its initial chemical composition
- (d) its chance of being absorbed by reaction with the earth's surface, and
- (e) its chance of undergoing atmospheric chemical reactions.

We wish to know the likelihood that this representative fluid particle will be present as a sulfate molecule within the ground level air volume surrounding location  $x(x_1, x_2, 0)$  at future time  $t = (t_0 + n\Delta t)$ .

The trajectory and chemical history of each fluid particle is determined by a sequence of meteorological events, and by the air parcel's retention time in the airshed. Let the fluid particle's history be broken down into  $n$  short time steps of  $\Delta t$  in duration, each short enough that meteorological conditions were unchanging over the span of one time step. Since these time steps may be arbitrarily small, even unsteady meteorological conditions, as defined previously, may be represented easily.

A set of physical rules will be specified which allows one to calculate the air parcel's likely chemical status and location at the end of a single time step,  $n_j$ , given its initial starting conditions and its status at the end of the  $n_{j-1}^{\text{th}}$  time step. Then the fluid particle's probable location over time can be modeled as the result of a stochastic chain of events.

The transition probabilities linking this chain of events are functions of meteorological conditions and chemical reaction paths. In order to specify one form of those functions, our air quality model will be derived for air pollution problems which may be approximated by the following idealized meteorological and chemical conditions:

- (1) *The important chemical reactions and pollutant removal paths to be considered are confined to pseudo-first order reactions and ground level dry deposition.*

- (2) *The geographic region of interest is characterized as having an idealized persistent temperature inversion. An idealized temperature inversion is defined as a multi-layered system, with unstable air from ground level to height  $h(x',t')$ , and a stable layer of air from height  $h(x',t')$  upward. The function  $h(x',t')$  will be referred to as the inversion base height.*
- (3) *The case will be considered in which inversion base height above ground level may be taken as independent of location in the horizontal plane at any single time. Inversion base height, however, varies with time throughout the airshed;  $h(x',t')$  equals  $h(t')$  alone.*
- (4) *Vertical mixing of air parcels within the unstable layer next to the ground is assumed to be quasi-instantaneous. By that, we mean that the time scales used to integrate the transport equations may be made long compared to the time scales for vertical mixing.*
- (5) *Vertical diffusion will be neglected for air parcels located within the stable portion of the elevated temperature inversion.*
- (6) *Vertical exchange between air parcels embedded within the inversion and those below the inversion base takes place as the inversion base height changes with time. Air parcels located above the inversion base are fumigated downward as the inversion base height,  $h(t)$ , rises during the day to intercept a previously stable air mass at height  $H$  within the inversion. At night the inversion base descends. Some of the*

air parcels which were previously located in the mixed layer next to the ground are now trapped above the new lowered inversion base and are stabilized to prevent further vertical motion or contact with the ground. Air parcels remaining below the overnight inversion base are still free to mix vertically and maintain a uniform distribution between ground level and inversion base in the presence of ground level removal processes. The inversion thus described acts much like a diode in an electric circuit. It insures vertical transport and mixing as the inversion base rises but does not reconcentrate previously diluted pollutants as the inversion base is lowered.

The idealized physical setting hypothesized above will not necessarily be found in any particular airshed. The degree to which an air pollution problem in a given geographic region corresponds to that description of course can be tested on a case by case basis.<sup>1</sup>

Factors affecting vertical dilution within our idealized airshed are specified independently of air parcel location in the horizontal plane at any single time. In that case we find it convenient to separate calculation of horizontal source-to-receptor transport probability from vertical transport. The chemical status of each air parcel

---

<sup>1</sup>For example, the assumption of direct modulation of ground level sulfate concentrations by inversion base location is supported in the Los Angeles basin by the strong correlation between inversion base height and sulfate levels shown in the analysis of Cass (1975) presented in Chapter 2 of this study. (See correlation matrices of Appendix B8).

will depend on ground level deposition of sulfur oxides, which in turn depends on whether the fluid particle's likely vertical location is above or below the inversion base. Thus vertical motion and pollutant chemistry must be combined.

\*

### 3.3.2 Vertical Motion and Pollutant Chemistry

We wish to construct a set of rules by which we may calculate the probability that a given fluid particle containing a sulfur oxides molecule is both in communication with ground level (i.e. below the inversion base within the fully-mixed layer) and is present as sulfates (rather than  $\text{SO}_2$ ). These are the two obvious conditions which must be met if the pollutant emission is to contribute to ground level sulfate air quality. First the initial conditions present after parcel insertion into the atmosphere will be considered.

The following terms are defined:

$U_a(\phi)$  = a unit step function

$$U_a(\phi) = \begin{cases} 0 & \text{when } \phi \leq a \\ 1 & \text{when } \phi > a \end{cases}$$

$P_{\text{SO}_{2a}}(t|t_o, i)$  = the probability that a fluid particle is above the inversion base at time  $t$ , and that its chemical identity is as  $\text{SO}_2$ , given that it was emitted from source class  $i$  at time  $t_o$ .

$P_{\text{SO}_{4a}}(t|t_o, i)$  = the probability that a fluid particle is above the inversion base at time  $t$ , and that its chemical identity is as  $\text{SO}_4$ , given that it was emitted from source class  $i$  at time  $t_o$ .

$P_{\text{SO}_{2b}}(t|t_o, i)$  = the probability that a fluid particle is below the inversion base at time  $t$ , and that its chemical identity is as  $\text{SO}_2$ , given that it was emitted from source class  $i$  at time  $t_o$ .

$P_{SO_4b}(t|t_o, i)$  = the probability that a fluid particle is below the inversion base at time  $t$ , and that its chemical identity is as  $SO_4^{=}$ , given that it was emitted from source class  $i$  at time  $t_o$ .

$P_{SO_2d}(t|t_o, i)$  = the probability that a fluid particle emitted from source class  $i$  which resided below the inversion as  $SO_2$  has deposited at the ground between time  $t$  and time  $t_o$ .

$P_{SO_4d}(t|t_o, i)$  = the probability that a fluid particle emitted from source class  $i$  which resided below the inversion as  $SO_4^{=}$  has deposited at the ground between time  $t$  and time  $t_o$ .

At the time of fluid particle release,  $t_o$ , from source class  $i$  at effective stack height  $H(t_o, i)$  the initial probability of finding the fluid particle in a given compartment depends only on exhaust gas composition and height of insertion into the atmosphere:

$$P_{SO_{2a}}(t_o, i) = u_{h(t_o)}(H(t_o, i)) \cdot [1 - f_{s_o}(i)] \quad (3.6)$$

$$P_{SO_{4a}}(t_o, i) = u_{h(t_o)}(H(t_o, i)) \cdot f_{s_o}(i) \quad (3.7)$$

$$P_{SO_{2b}}(t_o, i) = [1 - u_{h(t_o)}(H(t_o, i))] \cdot [1 - f_{s_o}(i)] \quad (3.8)$$

$$P_{SO_{4b}}(t_o, i) = [1 - u_{h(t_o)}(H(t_o, i))] \cdot f_{s_o}(i) \quad (3.9)$$

$$P_{SO_{2d}}(t_o, i) = 0 \quad (3.10)$$

$$P_{SO_{4d}}(t_o, i) = 0 \quad (3.11)$$

where

$f_{s_o}(i)$  is the initial fraction of the sulfur oxides from source class  $i$  which are present in the particulate phase (e.g. as sulfates or sulfuric acid mist).

Examining the arguments of the unit step functions in equations (3.6) through (3.11) we note that

$$\begin{aligned} P_{SO_{2a}}(t_o, i) + P_{SO_{4a}}(t_o, i) + P_{SO_{2b}}(t_o, i) + P_{SO_{4b}}(t_o, i) \\ + P_{SO_{2d}}(t_o, i) + P_{SO_{4d}}(t_o, i) = 1 \end{aligned} \quad (3.12)$$

Schematically, we have two possible initial conditions as shown in Figure 3.3. The first case represents pollutant insertion below the inversion base with rapid vertical mixing. In the second case, the plume is inserted into the stable layer aloft and no fluid particles are found initially in the mixed layer below the inversion base.

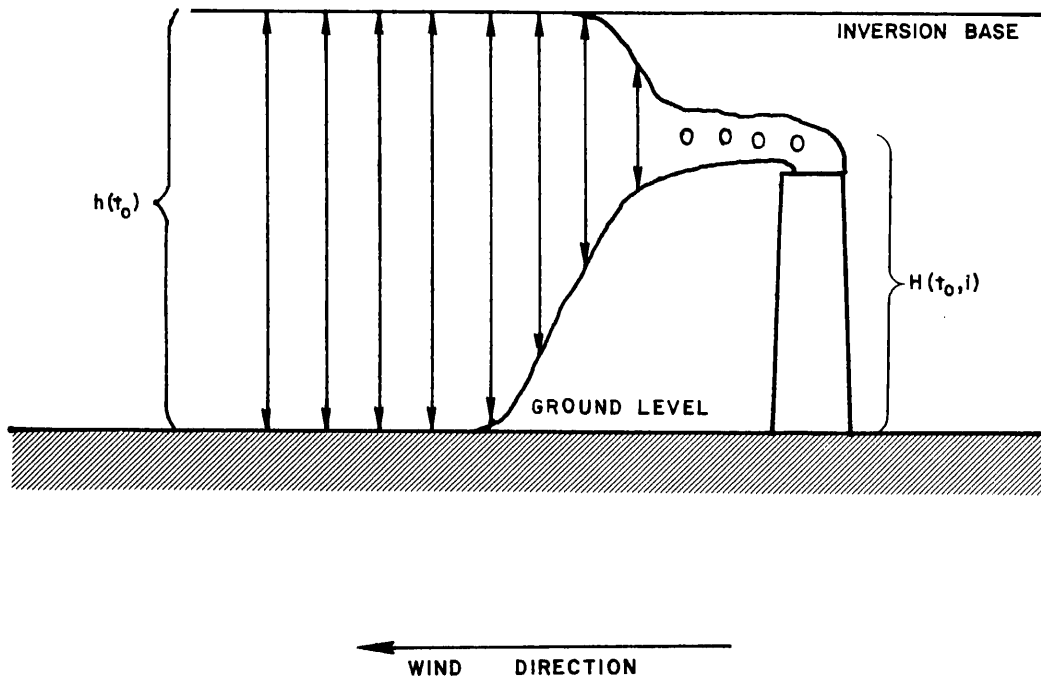
Next, we must define a set of rules which will propagate the air parcel's probable status from that initial condition through each successive time step. First consider atmospheric chemistry and pollutant dry deposition.

Atmospheric chemical reactions compete with dry deposition for the removal of  $SO_2$  molecules from the gas phase within the mixed layer. In Chapter 2, it was decided that chemical conversion of  $SO_2$  to form sulfates would be modeled as a pseudo-first order chemical reaction.  $SO_2$  dry deposition may also be represented as a simple first order process. Within our fully mixed layer next to the ground, a differential equation for  $SO_2$  removal from the gas phase would be:

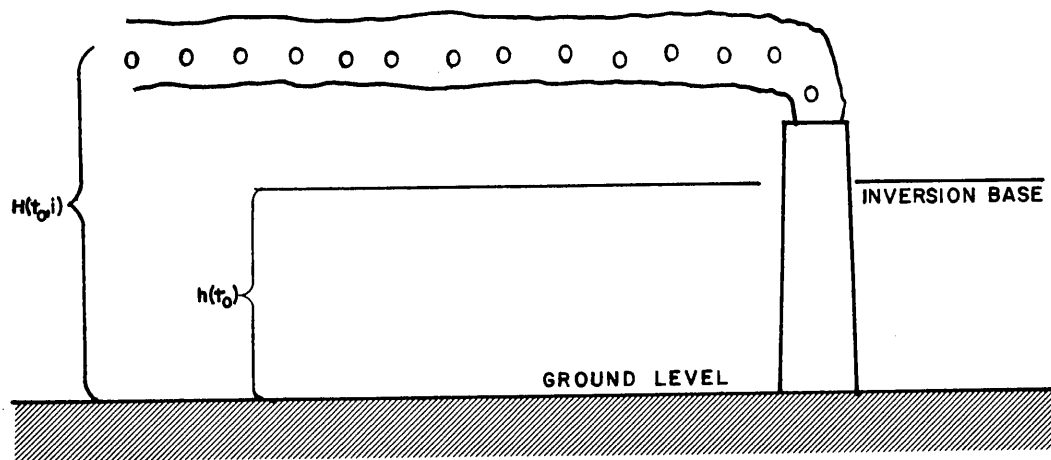
$$\frac{d S_{SO_{2b}}}{dt} = -k S_{SO_{2b}} - \frac{v_g}{h} S_{SO_{2b}} \quad (3.13)$$

FIGURE 3.3  
Air Parcel Insertion into the Atmosphere

## CASE 1



## CASE 2



where

- $S_{SO_{2b}}$  denotes sulfur atoms present as sulfur dioxide below the inversion base.
- $k$  is the pseudo-first order rate constant for oxidation of  $SO_2$  to form sulfates by all competing chemical paths.
- $V_g$  is the "deposition velocity" for  $SO_2$ . This is not actually a settling velocity, but rather the ratio between pollutant flux to the ground and atmospheric concentration.

Solving this expression for  $SO_2$  removal from the gas phase over a time interval  $t$  to  $(t+\Delta t)$  which is short enough that  $h(t) \approx h(t+\Delta t) \approx h$ , we get

$$S_{SO_{2b}}(t+\Delta t) = S_{SO_{2b}}(t) \exp\left\{-\left[k + \frac{V_g}{h}\right]\Delta t\right\} \quad (3.14)$$

The term  $\exp\{-[k + V_g/h]\Delta t\}$  takes the form of a transition probability that an  $SO_2$  molecule in the gas phase within the mixed layer will still be present in that state at the end of a time step of  $\Delta t$  in duration.

The sulfur dioxide removed from the gas phase within the mixed layer appears as either sulfates or deposited material at the ground. Changes in sulfate concentration are affected by formation of new material out of the gas phase and by depletion of sulfates by dry deposition at the ground.

$$\frac{d S_{SO_{4b}}}{dt} = k S_{SO_{2b}} - \frac{V_p}{h} S_{SO_{4b}} \quad (3.15)$$

where

- $V_p$  is the deposition velocity for particulate sulfur oxides.

Ground level deposition of  $\text{SO}_2$  and sulfates is represented by

$$\frac{d S_{\text{SO}_2\text{d}}}{dt} = \frac{v_g}{h} S_{\text{SO}_2\text{b}} \quad (3.16)$$

and

$$\frac{d S_{\text{SO}_4\text{d}}}{dt} = \frac{v_p}{h} S_{\text{SO}_4\text{b}} \quad (3.17)$$

Solving equation (3.15) over the time interval  $t$  to  $(t+\Delta t)$  in light of the  $\text{SO}_2$  time history given in equation (3.14) we get

$$S_{\text{SO}_4\text{b}}(t+\Delta t) = S_{\text{SO}_4\text{b}}(t) \exp\left\{-\frac{v_p}{h} \Delta t\right\} + \frac{k S_{\text{SO}_2\text{b}}(t)}{k + \frac{v_g}{h} - \frac{v_p}{h}} \cdot \left\{ \exp\left\{-\frac{v_p}{h} \Delta t\right\} - \exp\left\{-\left[k + \frac{v_g}{h}\right] \Delta t\right\} \right\} \quad (3.18)$$

Substituting the  $\text{SO}_2$  time history into equation (3.16) and integrating we get

$$S_{\text{SO}_2\text{d}}(t+\Delta t) = S_{\text{SO}_2\text{d}}(t) + \frac{\frac{v_g}{h}}{k + \frac{v_g}{h}} \cdot \left\{ 1 - \exp\left\{-\left[k + \frac{v_g}{h}\right] \Delta t\right\} \right\} S_{\text{SO}_2\text{b}}(t) \quad (3.19)$$

Substituting atmospheric concentrations for both  $\text{SO}_2$  and sulfates into equation (3.17) and solving

$$\begin{aligned}
S_{SO_{4d}}(t+\Delta t) &= S_{SO_{4d}}(t) + S_{SO_{4b}}(t) \left\{ 1 - \exp\{-[V_p/h]\Delta t\} \right\} \\
&+ \frac{k S_{SO_{2b}}(t)}{k + \frac{g}{h} - \frac{p}{h}} \left\{ \left[ 1 - \exp\{-[V_p/h]\Delta t\} \right] \right. \\
&\quad \left. - \left[ \frac{(V_p/h)}{k + (V_g/h)} \right] \cdot \left[ 1 - \exp\{-[k + \frac{V_g}{h}]\Delta t\} \right] \right\}
\end{aligned} \tag{3.20}$$

The terms such as  $\frac{[V_g/h]}{k + [V_g/h]} \left\{ 1 - \exp\{-[k + \frac{V_g}{h}]\Delta t\} \right\}$  in equation (3.19) can also be thought of as transition probabilities which determine the likely disposition of the  $SO_2$  removed from the gas phase.

Above the mixed layer, the pollutants are stably stratified and are not in communication with the ground. Dry deposition does not affect such elevated air parcels. The transition probabilities affecting air parcels above the inversion base are due to chemical reaction alone.

$$S_{SO_{2a}}(t+\Delta t) = S_{SO_{2a}}(t) \exp\{-k\Delta t\} \tag{3.21}$$

$$S_{SO_{4a}}(t+\Delta t) = S_{SO_{4a}}(t) + S_{SO_{2a}}(t) [1 - \exp\{-k\Delta t\}] \tag{3.22}$$

Combining transport probabilities in the vertical direction with chemical reaction and deposition terms we see that the chain of coupled vertical transport and chemical reaction events is propagated by the following series of equations:

$$P_{SO_{2a}}(t+\Delta t | t_o, i) = \left\{ P_{SO_{2a}}(t | t_o, i) \cdot [1-r(t+\Delta t | t_o, i)] + P_{SO_{2b}}(t | t_o, i) \cdot [d(t+\Delta t | t_o, i)] \right\} \cdot e^{-k\Delta t} \quad (3.23)$$

$$P_{SO_{4a}}(t+\Delta t | t_o, i) = \left\{ P_{SO_{4a}}(t | t_o, i) \cdot [1-r(t+\Delta t | t_o, i)] + P_{SO_{4b}}(t | t_o, i) \cdot [d(t+\Delta t | t_o, i)] \right\} \\ + \left\{ P_{SO_{2a}}(t | t_o, i) \cdot [1-r(t+\Delta t | t_o, i)] + P_{SO_{2b}}(t | t_o, i) \cdot [d(t+\Delta t | t_o, i)] \right\} \cdot \{1 - e^{-k\Delta t}\} \quad (3.24)$$

$$P_{SO_{2b}}(t+\Delta t | t_o, i) = \left\{ P_{SO_{2a}}(t | t_o, i) \cdot [r(t+\Delta t | t_o, i)] + P_{SO_{2b}}(t | t_o, i) \cdot [1-d(t+\Delta t | t_o, i)] \right\} \\ \cdot \exp\left\{-\left[k + \frac{V}{h(t+\Delta t)}\right]\Delta t\right\} \quad (3.25)$$

$$P_{SO_{2d}}(t+\Delta t | t_o, i) = P_{SO_{2d}}(t | t_o, i) + \left\{ P_{SO_{2a}}(t | t_o, i) \cdot [r(t+\Delta t | t_o, i)] + P_{SO_{2b}}(t | t_o, i) \cdot [1-d(t+\Delta t | t_o, i)] \right\} \\ \cdot \left\{ \frac{\frac{V}{h(t+\Delta t)}}{\frac{V}{h(t+\Delta t)} + k} \left[ 1 - \exp\left\{-\left[k + \frac{V}{h(t+\Delta t)}\right]\Delta t\right\} \right] \right\} \quad (3.26)$$

$$\begin{aligned}
P_{SO_{4b}}(t+\Delta t | t_o, i) &= \left\{ P_{SO_{4a}}(t | t_o, i) \cdot [r(t+\Delta t | t_o, i)] + P_{SO_{4b}}(t | t_o, i) \cdot [1-d(t+\Delta t | t_o, i)] \right\} \cdot \exp\left\{-\frac{V}{h(t+\Delta t)} \Delta t\right\} \\
&+ \left\{ P_{SO_{2a}}(t | t_o, i) \cdot [r(t+\Delta t | t_o, i)] + P_{SO_{2b}}(t | t_o, i) \cdot [1-d(t+\Delta t | t_o, i)] \right\} \\
&\cdot \left\{ \frac{k}{k + \frac{V}{h(t+\Delta t)} - \frac{V}{h(t+\Delta t)}} \left[ \exp\left\{-\frac{V}{h(t+\Delta t)} \Delta t\right\} - \exp\left\{-\left[k + \frac{V}{h(t+\Delta t)}\right] \Delta t\right\} \right] \right\}
\end{aligned} \tag{3.27}$$

$$\begin{aligned}
P_{SO_{4d}}(t+\Delta t | t_o, i) &= P_{SO_{4d}}(t | t_o, i) + \left\{ P_{SO_{4a}}(t | t_o, i) \cdot [r(t+\Delta t | t_o, i)] + P_{SO_{4b}}(t | t_o, i) \cdot [1-d(t+\Delta t | t_o, i)] \right\} \\
&\cdot \left\{ 1 - \exp\left\{-\frac{V}{h(t+\Delta t)} \Delta t\right\} \right\} + \left\{ P_{SO_{2a}}(t | t_o, i) \cdot [r(t+\Delta t | t_o, i)] + P_{SO_{2b}}(t | t_o, i) \cdot [1-d(t+\Delta t | t_o, i)] \right\} \\
&\cdot \left\{ \frac{k}{k + \frac{V}{h(t+\Delta t)} - \frac{V}{h(t+\Delta t)}} \left[ 1 - \exp\left\{-\frac{V}{h(t+\Delta t)} \Delta t\right\} \right] - \left[ \frac{\frac{V}{h(t+\Delta t)}}{k + \frac{V}{h(t+\Delta t)}} \right] \cdot \left[ 1 - \exp\left\{-\left[k + \frac{V}{h(t+\Delta t)}\right] \Delta t\right\} \right] \right\}
\end{aligned} \tag{3.28}$$

where the newly introduced functions  $r$  and  $d$  are defined as follows:

$r(t+\Delta t|t_0, i)$  is the probability that the inversion base is rising and that a representative fluid particle emitted from source class  $i$  at time  $t_0$  will be transferred from above the mixed layer to below the inversion base during the time interval  $t$  to  $t+\Delta t$ .

$d(t+\Delta t|t_0, i)$  is the probability that the inversion base is descending and that a representative fluid particle emitted from source class  $i$  at time  $t_0$  will be transferred from below the inversion base to above the mixed layer during the time interval  $t$  to  $t+\Delta t$ .

Obviously, the inversion base cannot be both rising and descending at the same time in our spatially homogeneous system, so  $r$  and  $d$  never take on non-zero values simultaneously.

Stated simply, equation (3.23) says that the probability of finding an  $\text{SO}_2$  molecule above the mixed layer at time  $(t+\Delta t)$ , given that it was emitted from source class  $i$  at time  $t_0$ , is equal to

- (a) the probability that it was above the mixed layer at the start of the time step and was not mixed downward; plus
- (b) the probability that it was below the inversion base at the start of the time interval and was mixed upward; both multiplied by
- (c) the probability that it did not lose its chemical identity as  $\text{SO}_2$  during the time interval.

The other expressions above have analogous meanings. Once the forms of the functions  $r$  and  $d$  have been specified, equations (3.23) through (3.28) form a series of recursion formulae which can be embedded in a simulation model. A means of estimating the upward and downward mixing

probabilities  $r(t+\Delta t|t_o, i)$  and  $d(t+\Delta t|t_o, i)$  from available meteorological data will be considered in section 3.4.1 of this chapter.

It should be noted that the scheme of equations (3.23) through (3.28) implies that transport precedes chemical reaction. The two processes could be considered simultaneously, but that would require input of new material into the chemical reactions as inversion base height changed within the course of a single time step. As will be seen in section 3.4 of this chapter, inversion base motion is not known accurately enough to justify such detail. Instead, time steps will be chosen which are short compared to the time scales of the chemical reactions and also short enough that inversion base height is known no better than to a single value over that time step. A further important feature of this scheme for propagating pollutant status between time steps is that it absolutely conserves sulfur mass.

$$\begin{aligned}
 & P_{SO_{2a}}(t+\Delta t|t_o, i) + P_{SO_{4a}}(t+\Delta t|t_o, i) + P_{SO_{2b}}(t+\Delta t|t_o, i) \\
 & \quad + P_{SO_{4b}}(t+\Delta t|t_o, i) + P_{SO_{2d}}(t+\Delta t|t_o, i) + P_{SO_{4d}}(t+\Delta t|t_o, i) \\
 = & P_{SO_{2a}}(t|t_o, i) + P_{SO_{4a}}(t|t_o, i) + P_{SO_{2b}}(t|t_o, i) + P_{SO_{4b}}(t|t_o, i) \\
 & \quad + P_{SO_{2d}}(t|t_o, i) + P_{SO_{4d}}(t|t_o, i) \\
 = & 1.0 \tag{3.29}
 \end{aligned}$$

### 3.3.3 Transport Probabilities in the Horizontal Plane

Having specified a chain of events which tracks both the vertical location and chemical composition of a single fluid particle over time, we now turn to advection in the horizontal plane. Particle motion in the horizontal plane is determined by all scales of atmospheric turbulence acting together. Large scale features of the atmospheric circulation are resolvable by hourly average measurements of wind speed and direction. Wind measurements along the air parcel's path can be integrated to yield an air parcel trajectory. In addition to the trajectory of the particle computed from hourly wind fields, small scale features of the atmospheric turbulence with period less than about one half hour act to randomize particle location beyond that computed from gross wind behavior alone. The cumulative effect of this small scale turbulence is usually referred to as eddy diffusion. It is seen, however, that separation of transport and diffusion into two categories merely reflects the observer's frame of reference. A single particle in the fluid is simply transported from one location to another by a variety of scales of motion in the atmosphere. Therefore, without loss of generality, we may write

$$x''(t|x_0, t_0) = \int_{t_0}^t U(x''(t'|x_0, t_0)) dt' + x_0 \quad (3.30)$$

where

$x''(t|x_0, t_0)$  is fluid particle location at time  $t$  given starting location,  $x_0$ , and starting time,  $t_0$ .

$U(x''(t'|x_0, t_0))$  is instantaneous fluid velocity along the path followed by the particle.

The integration above is performed along the path of the particle.

If the above integration were performed exactly, then the probability of finding the particle within a given volume element  $x_i - \frac{\Delta x_i}{2} < x_i < x_i + \frac{\Delta x_i}{2}$ ,  $i = 1, 2, 3$ , surrounding location  $x$  at time  $t$ , given that the particle originated at location  $x_0$  at time  $t_0$  would be

$$P(x, t | x_0, t_0) = \lambda(x'' - x) \quad (3.31)$$

where

$P(x, t | x_0, t_0)$  is the probability of finding the particle in the volume element surrounding location  $x$  at time  $t$ , given that it was emitted at location  $x_0$  at time  $t_0$ .

$\lambda(x'' - x)$  is a proximity function

$$\lambda(x'' - x) = \begin{cases} 1 & \text{if } |(x_i'' - x_i)| < \frac{\Delta x_i}{2} \text{ for all } i = 1, 2, 3 \\ 0 & \text{otherwise} \end{cases}$$

Now take the following step: equations (3.30) and (3.31) are integrated over all possible locations in the vertical dimension (direction  $x_3$ ).

The above expressions may be rewritten as

$$\tilde{x}''(t | \tilde{x}_0, t_0) = \int_{t_0}^t \tilde{U}(\tilde{x}''(t' | \tilde{x}_0, t_0)) dt' + \tilde{x}_0 \quad (3.32)$$

and

$$\tilde{P}(\tilde{x}, t | \tilde{x}_0, t_0) = \tilde{\lambda}(\tilde{x}'' - \tilde{x}) \quad (3.33)$$

where all terms have the same meaning as before, except that the underbar ( $\tilde{\phantom{x}}$ ) refers to their projection on the  $\tilde{x} = (x_1, x_2)$  horizontal plane only. For example,  $\tilde{P}(\tilde{x}, t | \tilde{x}_0, t_0)$  now denotes the probability of finding the particle of interest in the airspace over the surface area element

$$x_1 - \frac{\Delta x_1}{2} < x_1 < x_1 + \frac{\Delta x_1}{2} \quad \text{by} \quad x_2 - \frac{\Delta x_2}{2} < x_2 < x_2 + \frac{\Delta x_2}{2} .$$

Combining that transport probability in the horizontal plane with the vertical transport and chemical reaction expressions of equations (3.25) and (3.27), plus the ongoing assumption that the air mass next to ground level is vertically well mixed, we may write:

$$P_{SO_4}(\tilde{x}, t | \tilde{x}_o, t_o, i) = P(\tilde{x}, t | \tilde{x}_o, t_o) \cdot P_{SO_{4b}}(t | t_o, i) \cdot \frac{\Delta x_3}{h(t)} \quad (3.34)$$

and

$$P_{SO_2}(\tilde{x}, t | \tilde{x}_o, t_o, i) = P(\tilde{x}, t | \tilde{x}_o, t_o) \cdot P_{SO_{2b}}(t | t_o, i) \cdot \frac{\Delta x_3}{h(t)} \quad (3.35)$$

where the left sides of these expressions have the following definition:

$P_{SO_4}(\tilde{x}, t | \tilde{x}_o, t_o, i)$  is the probability that a sulfur oxide molecule emitted from source class  $i$  at location  $\tilde{x}$  at time  $t_o$  resides as sulfate in the ground level volume element

$$x_i - \frac{\Delta x_i}{2} < x_i < x_i + \frac{\Delta x_i}{2} ; i = 1, 2$$

by  $0 < x_3 < \Delta x_3$  at later time  $t$ .

$P_{SO_2}(\tilde{x}, t | \tilde{x}_o, t_o, i)$  is the probability that a sulfur oxide molecule emitted from source class  $i$  at location  $\tilde{x}$  at time  $t_o$  resides as sulfur dioxide in the ground level volume element

$$x_i - \frac{\Delta x_i}{2} < x_i < x_i + \frac{\Delta x_i}{2} ; i = 1, 2$$

by  $0 < x_3 < \Delta x_3$  at later time  $t$ .

and  $\Delta x_3/h(t)$  is the probability that a sulfur oxide molecule known to be within the mixed layer at time  $t$  will be found within the thin ground level layer of height  $\Delta x_3$ .

Recall that the initial vertical location of the air parcel,  $x_{3_o}$ , enters these expressions through the effective stack height  $x_{3_o} = H(t_o, i)$  for the  $i^{\text{th}}$  source class.

### 3.3.4 Ground Level Pollutant Concentrations

As stated so far,  $P_{SO_4}(x, t | x_o, t_o, i)$  is a transition probability representing transport and reaction of a single sulfur oxide molecule.

If one now defines a source strength function over the airshed and integrates over all source classes and starting times, we acquire

$$\langle c_{SO_4}(x, t) \rangle = \frac{1}{\Delta x_1 \Delta x_2 \Delta x_3} \sum_{i=1}^{N_4} \int_{-\infty}^{\infty} \int_{-\infty}^{\infty} \int_{-\infty}^t P_{SO_4}(x, t | x_o, t_o, i) S(x_o, t_o, i) dt_o dx_o \quad (3.36)$$

and

$$\langle c_{SO_2}(x, t) \rangle = \frac{1}{\Delta x_1 \Delta x_2 \Delta x_3} \sum_{i=1}^{N_4} \int_{-\infty}^{\infty} \int_{-\infty}^{\infty} \int_{-\infty}^t P_{SO_2}(x, t | x_o, t_o, i) S(x_o, t_o, i) dt_o dx_o \quad (3.37)$$

where

$\langle c_{SO_4}(x, t) \rangle$  is total sulfur concentration existing as sulfates in the ground level element of volume  $\Delta x_1 \Delta x_2 \Delta x_3$  surrounding location  $(x_1, x_2, 0)$  at time  $t$ .

$\langle c_{SO_2}(x, t) \rangle$  is total sulfur concentration existing as sulfur dioxide in the ground level element of volume  $\Delta x_1 \Delta x_2 \Delta x_3$  surrounding location  $(x_1, x_2, 0)$  at time  $t$ .

$S(x_o, t_o, i)$  is the source strength for sulfur oxides molecules from source class  $i$  at horizontal location  $x_o$  at release time  $t_o$ .

Equations (3.36) and (3.37) anticipate summation over a discrete number of source classes,  $i$ , within the airshed of interest.

As structured above,  $\langle c_{SO_4}(x, t) \rangle$  is computed by a Lagrangian marked particle technique. The source strength function,  $S$ , counts the number of sulfur oxide "particles" released from each source class and location. The transition probabilities  $P_{SO_4}$  and  $P_{SO_2}$  mark each particle

with a likelihood that it will appear as sulfate or as  $\text{SO}_2$  within a given volume element at a later time. The concentration within that volume element is computed by adding up the probable number of particles with the desired chemical status in the volume element at time  $t$ , and then dividing by the volume of the cell.

### 3.3.5 Long-Term Average Sulfate and Sulfur Dioxide Air Quality

The concentration predictions of the model of equations (3.36) and (3.37) are instantaneous representations at time  $t$ . For long-term average sulfate concentrations at ground level over horizontal location  $\underline{x}$  we wish to obtain

$$\overline{\langle c_{\text{SO}_4}(\underline{x}; T, t_s) \rangle} = \frac{1}{T} \int_{t_s}^{T+t_s} \langle c_{\text{SO}_4}(\underline{x}, t) \rangle dt \quad (3.38)$$

and

$$\overline{\langle c_{\text{SO}_2}(\underline{x}; T, t_s) \rangle} = \frac{1}{T} \int_{t_s}^{T+t_s} \langle c_{\text{SO}_2}(\underline{x}, t) \rangle dt \quad (3.39)$$

where

$\overline{\langle c_{\text{SO}_4}(\underline{x}; T, t_s) \rangle}$  is the long-term average total sulfur concentration existing as sulfate at ground level at horizontal location  $\underline{x}$  over the time interval  $(t_s, T+t_s)$ .

$\overline{\langle c_{\text{SO}_2}(\underline{x}; T, t_s) \rangle}$  is the long-term average total sulfur concentration existing as sulfur dioxide at ground level at horizontal location  $\underline{x}$  over the time interval  $(t_s, T+t_s)$ .

$T$  is, for example, the length of a given month or year.

$t_s$  is the beginning of the time interval of interest.

Next, consider the case where the individual emission sources within a given source class have a common diurnal periodicity. An

example would be the diurnal pattern imposed by daily rush-hour traffic peaks, or the daily cycling of power plants between afternoon peak demand and late night off-peak periods. Then a point source distribution might be represented as

$$S(\tilde{x}_o, t_o, i) = \bar{S}(\tilde{x}_o, i) \omega(t_o, i) \quad (3.40)$$

where

$\bar{S}(\tilde{x}_o, i)$  = average emission source strength for sources of class  $i$  as a function of location in the horizontal plane of the air basin

$\omega(t_o, i)$  = a diurnal source strength cycle for sources of class  $i$ .

Two obvious properties of  $\omega(t_o, i)$  are that

$$\bar{\omega} = \frac{1}{24} \text{ hrs} \int_{t_s}^{t_s + 24 \text{ hours}} \omega(t_o, i) dt_o = 1$$

and

$$\omega(t, i) = \omega(t+24 \text{ hours}, i).$$

Introduce the change of variable  $t_o = t - \tau$ . Then substituting equations (3.40), (3.36) and (3.37) into equations (3.38) and (3.39), and performing the indicated integrations over time, we get

$$\overline{\langle c_{SO_4}(x; T, t_s) \rangle} = \sum_{i=1}^{N_4} \int_{-\infty}^{\infty} \int_{-\infty}^{\infty} \bar{Q}_{SO_4}(x | \tilde{x}_o, i; T, t_s) \bar{S}(\tilde{x}_o, i) d\tilde{x}_o \quad (3.41)$$

and

$$\overline{\langle c_{SO_2}(x; T, t_s) \rangle} = \sum_{i=1}^{N_4} \int_{-\infty}^{\infty} \int_{-\infty}^{\infty} \bar{Q}_{SO_2}(x | \tilde{x}_o, i; T, t_s) \bar{S}(\tilde{x}_o, i) d\tilde{x}_o \quad (3.42)$$

where

$$\bar{Q}_{SO_4}(x|x_o, i; T, t_s) = \frac{1}{T\Delta x_1 \Delta x_2 \Delta x_3} \int_{t_s}^{T+t_s} \int_0^{\infty} P_{SO_4}(x, t | x_o, t-\tau, i) \omega(t-\tau, i) d\tau dt$$

$$\bar{Q}_{SO_2}(x|x_o, i; T, t_s) = \frac{1}{T\Delta x_1 \Delta x_2 \Delta x_3} \int_{t_s}^{T+t_s} \int_0^{\infty} P_{SO_2}(x, t | x_o, t-\tau, i) \omega(t-\tau, i) d\tau dt$$

In practice, one need not integrate air parcel starting times over all past history. Integration over  $\tau$  from  $\tau = 0$  to  $\tau = \tau_c$  should be sufficient, where  $\tau_c$  is the longest time for retention of an air parcel within the airshed of interest. When  $T \gg \tau_c$ , the outer integral determines the length of the computation required.

Up to this point, we have discussed a general approach to calculating sulfate and sulfur dioxide concentrations in a region characterized as having an idealized persistent temperature inversion. A means for direct estimation of  $\bar{Q}_{SO_4}$  and  $\bar{Q}_{SO_2}$  from meteorological measurements made in a particular airshed now will be developed.

### 3.4 A Computational Procedure for Simulating Los Angeles Sulfate Air Quality

Analytical solutions for the source to receptor transition probabilities appearing in equations (3.41) and (3.42) are unlikely to be obtained for an arbitrary sequence of unsteady meteorological events. But the stochastic chain of events pictured in equations (3.23) through (3.28) plus trajectory equations (3.32) and (3.33) is ideally suited for inclusion in a numerical simulation model. The only additions to these equations needed to simulate the fate of representative fluid particles are a means of calculating the upward and downward mixing

probabilities  $d(t+\Delta t|t_0, i)$  and  $r(t+\Delta t|t_0, i)$ , plus a means of obtaining particle trajectories,  $X''(t|x_0, t_0)$ , in the horizontal plane. By simulating the fate of a large number of representative fluid particles, and then averaging over their ultimate dispositions, one can estimate the desired source to receptor transition probability densities.

#### 3.4.1 Calculating Exchange Between the Stable Inversion and the Mixed Layer Below from Available Monitoring Data

Historic data on inversion base movement have been regularly compiled by the Los Angeles Air Pollution Control District (LAAPCD) for many years. But while the extent of the data base is great, the detail is rather coarse. Each day's data base contains an early morning inversion base height sounding at a coastal location, nominally taken at Los Angeles International Airport at 6:00 am. Secondly, each afternoon's maximum mixing depth,  $h_{\max}$ , is calculated from earlier soundings plus temperature conditions observed at downtown Los Angeles. Additional data on inversion base motion might be acquired from military installations on the fringes of the South Coast Air Basin or from an acoustic sounder operated at the California Air Resources Board laboratory in El Monte. However, only the LAAPCD meteorological records are available in a uniform format extending throughout our years of interest. For the long-term study that we intend to pursue, only the LAAPCD data are in a form suitable for practical use.

Inversion base motion must still be defined as a function of space and time if air parcel progress is to be tracked. In light of having only two point estimates of maximum and minimum inversion base height

daily, some further assumptions must be made. Regarding the spatial distribution of mixing depths above ground level at a given time, the assumption made is that inversion base height *above ground level* is spatially homogeneous at any single time over the central flatlands of the Los Angeles Basin. This approximation can be checked against the average cross-sectional inversion height diagram shown in Figure 3.4. Figure 3.4 was adapted from Neiburger, Beer and Leopold (1945) after having sketched a ground elevation profile. A second set of nearly instantaneous cross-sections through the air basin prepared by Edinger (1973) is shown in Figure 3.5. Over a long-term average (Figure 3.4), the mixing depth between the inversion base and ground level is roughly constant throughout the cross-section shown, while at any single time the assumption of a spatially homogeneous mixing depth holds only approximately. Note that Figure 3.5 shows ozone concentrations from aloft being fumigated downward as inversion base height rises into a previously stable layer, as would be modeled for sulfates by our vertical transport scheme.<sup>2</sup>

Mixing depth is thus taken as independent of location over the central portion of the air basin. The function  $h(x',t')$  is roughly equal to  $h(t')$  alone, and thus is compatible with our earlier model derivation.

Specification of short term temporal fluctuations in inversion base height must proceed by means of an interpolation scheme. Since the

---

<sup>2</sup>Ozone is not expected to be fully mixed in the vertical at all times (see Figure 3.5 c'). One reason is that strong spatial gradients exist in pollutant species (like NO) which scavenge ozone.

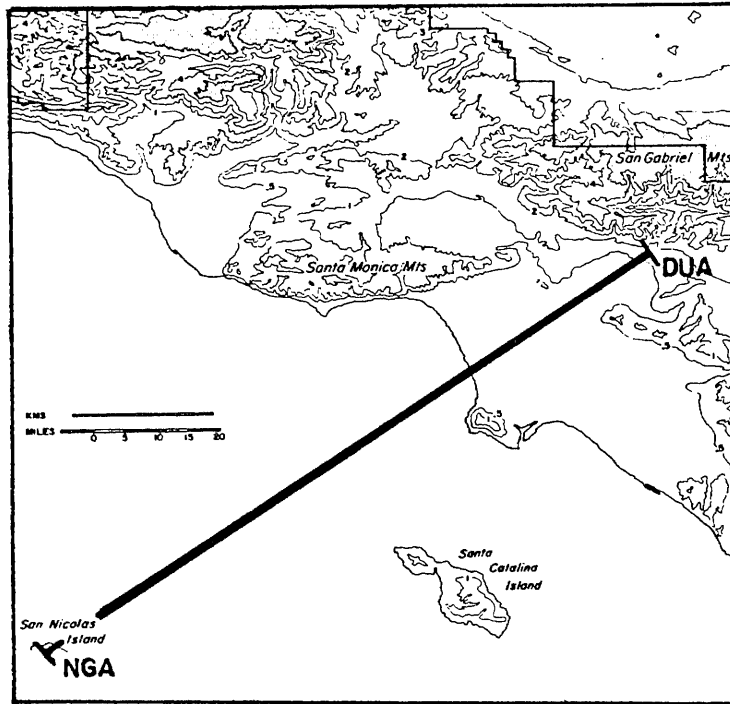
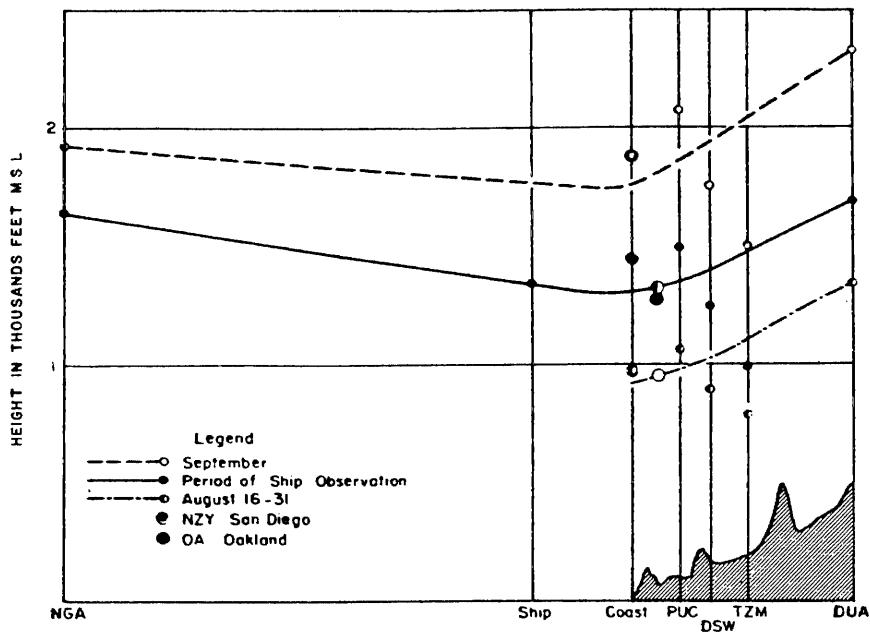
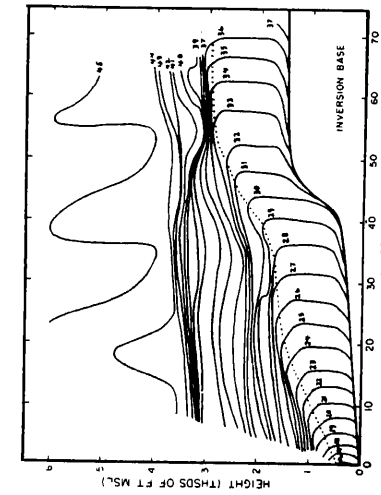


FIGURE 3.4

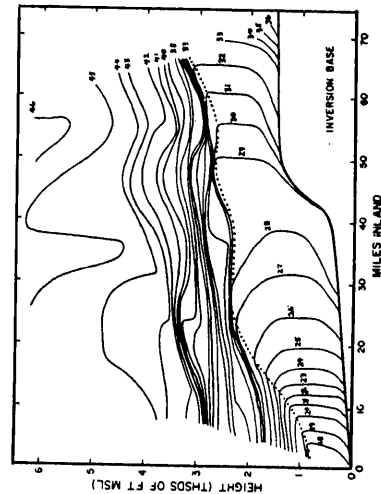


AVERAGE CROSS SECTION OF INVERSION BASE  
NORMAL TO COAST  
STATIONS ARE ARRANGED ACCORDING TO DISTANCE FROM SHORE  
INDEPENDENTLY OF POSITION ALONG IT

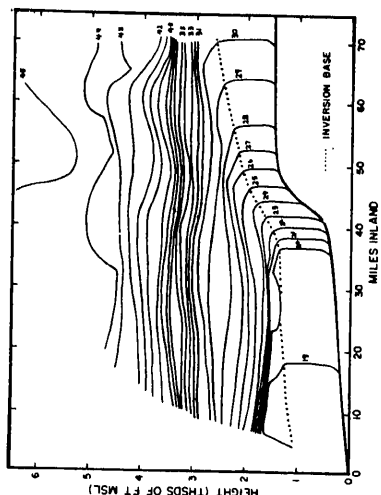
Reference: Neiburger, Beer and Leopold (1945)



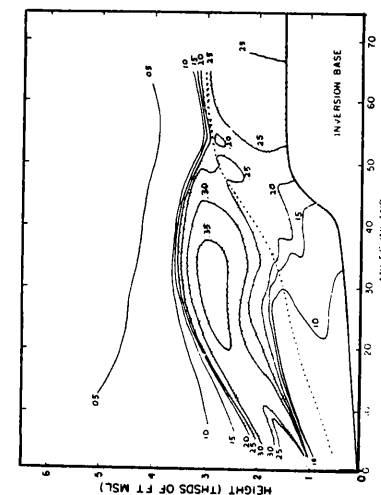
(a) Field of potential temperature ( $^{\circ}\text{C}$ ) in the vertical cross section from Santa Monica to Rialto-Miro, 9:00 am, June 20, 1970



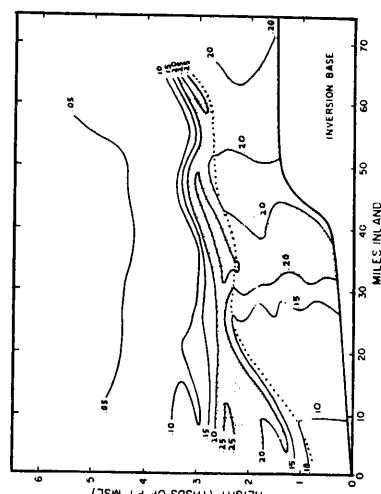
(b) Field of potential temperature ( $^{\circ}\text{C}$ ) in the vertical cross section from Santa Monica to Rialto-Miro, 12:00 noon, June 20, 1970



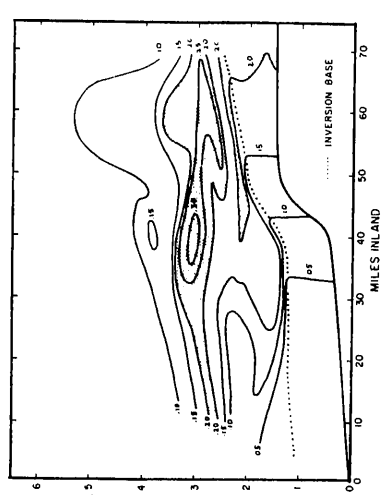
(c) Field of potential temperature ( $^{\circ}\text{C}$ ) in the vertical cross section from Santa Monica to Rialto-Miro, 4:30 pm, June 20, 1970



(a') Field of oxidant concentrations (ppm) in the vertical cross section from Santa Monica to Rialto-Miro, 9:00 am, June 20, 1970



(b') Field of oxidant concentrations (ppm) in the vertical cross section from Santa Monica to Rialto-Miro, 12:00 noon, June 20, 1970



(c') Field of oxidant concentrations (ppm) in the vertical cross section from Santa Monica to Rialto-Miro, 4:30 pm, June 20, 1970

source: Edinger, 1973

FIGURE 3.5

Vertical Temperature Structure and Inversion Base Location in the Los Angeles Atmosphere at Three Times of the Day - June 20, 1970.

data only represent daily peaks and troughs, it is hard to argue about the merits of different ways to specify intermediate behavior. All interpolation schemes will substantially exceed the available data. The method chosen here is similar to that suggested by Goodin (1976). Overnight mixing depth above ground level is set equal to the mixing depth reported for Los Angeles International Airport (LAX) at 6:00 am according to the records of the LAAPCD. If a surface-based inversion existed, it was recorded by the LAAPCD as a mixing depth of 30.48 m (100 ft). At sunrise, ground level heating causes the base of the inversion to begin to lift. A linear rate of inversion base rise is maintained until the LAAPCD's reported maximum mixing depth over downtown Los Angeles for that day is achieved at solar noon. Substantial inland transport of cooler marine air in the afternoon halts further rise in inversion base height. The inversion base is held constant at the maximum mixing depth achieved until sunset. Then at sunset, stable layers begin to reform in the atmosphere beneath the level of that day's maximum mixing depth. The lowest of these new stable layers becomes the next overnight inversion base height. Thus at sunset, the mixing depth adjacent to ground level is set equal to the next measured overnight value at LAX and remains there until sunrise the following day.

As stated so far, the form of the downward and upward transport probabilities,  $r$  and  $d$ , is quite general. Let us consider a hypothetical time history of an inert individual fluid particle and note some of the possible interactions between it and the inversion base which could affect upward and downward transport. In Figure 3.6, a fluid particle

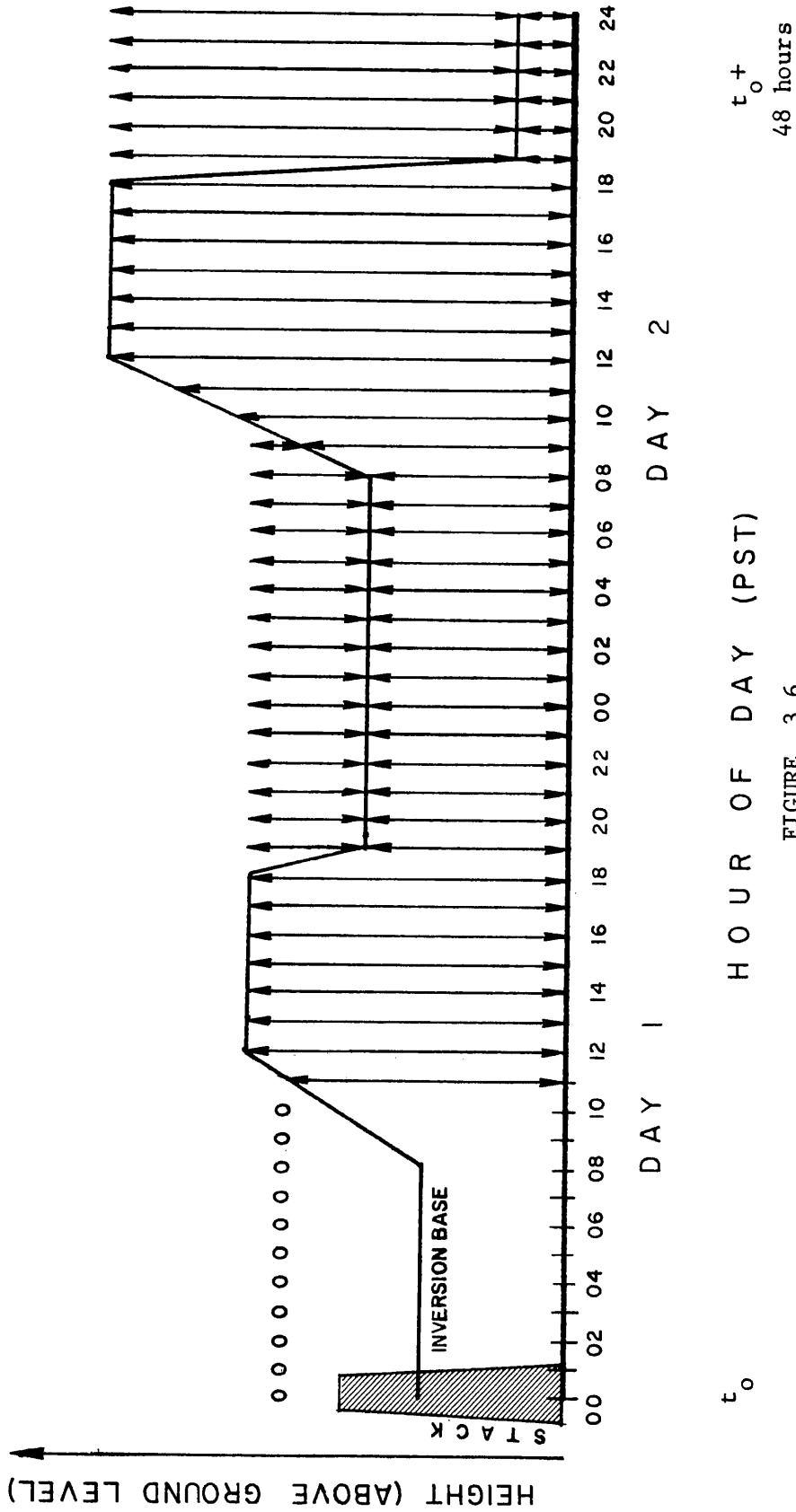


FIGURE 3.6  
Hypothetical Time History of Interaction Between the  
Inversion Base and a Fluid Particle Released at Time  $t_0$

is emitted from a source belonging to class  $i$  and enters the atmosphere at  $t_0$  equals midnight at effective stack height  $H(t_0, i)$ . The height of emission is within the stable inversion and no vertical motion occurs. The early morning proceeds by time steps of  $\Delta t$  equal to one hour, but nothing happens immediately to alter air parcel vertical location. By sunrise that morning, the inversion base begins to rise at a constant rate from its overnight low toward its maximum mixing height for the day. The fluid particle is still within what remains of the stable layer until 11:00 am. At that point, the inversion has passed the height of insertion of the particle into the stable layer and down-mixing occurs. The particle now has a uniform probability of being found anywhere within the unstable mixed layer.

The vertical space over which the particle is free to travel expands until the day's maximum mixing height is reached at solar noon. Then as the sun goes down, the inversion reforms and establishes itself at its overnight base height. A segment of the vertical space in which the particle might have resided previously is now found above the new inversion base. With some probability, the particle is either above or below the new overnight inversion base. If it is below the inversion base overnight, it is exposed to the possibility of undergoing deposition at the ground. Above the inversion base, the probability of finding the particle in any given vertical space remains unchanged overnight due to the extreme stability of the atmosphere within the inversion. Then as the inversion base rises the next day, this uniformly mixed layer aloft is progressively destabilized and entrained

downward, carrying with it some probability that the particle has been returned to the mixed layer below the inversion base.

Given the type of inversion base behavior pictured in Figure 3.6, two relatively simple algebraic expressions for the upward and downward transport transition probabilities are proposed:

$$r(t+\Delta t|t_0, i) = \frac{h(t+\Delta t) - h(t)}{\ell(t+\Delta t|t_0) - h(t)} \cdot u_{h(t)}(h(t+\Delta t)) \cdot u_{H(t_0, i)}(\ell(t+\Delta t|t_0)) \quad (3.43)$$

and

$$d(t+\Delta t|t_0, i) = \frac{h(t) - h(t+\Delta t)}{h(t)} \cdot u_{h(t+\Delta t)}(h(t)) \cdot u_{H(t_0, i)}(\ell(t+\Delta t|t_0)) \quad (3.44)$$

where the newly introduced function

$\ell(t+\Delta t|t_0)$  is a marker which tracks the maximum vertical dilution experienced by an air parcel located below the inversion base between time  $t_0$  and time  $(t+\Delta t)$ . In our vertically mixed system,  $\ell(t+\Delta t|t_0)$  tracks maximum mixing depth achieved over the life<sup>o</sup> history of the particle:

$$\ell(t+\Delta t|t_0) = h(t+\Delta t) \cdot u_{\ell(t|t_0)}(h(t+\Delta t)) + \ell(t|t_0) \cdot [1 - u_{\ell(t|t_0)}(h(t+\Delta t))] \quad (3.45)$$

Equation (3.45) merely says that the maximum mixing depth seen by an air parcel is the maximum depth seen in the past history of the air parcel or the current inversion base height, whichever is greater.

Initial conditions for propagation of  $\ell$  would be

$$\ell(t_0|t_0) = h(t_0) \quad (3.46)$$

Consider how the expression for  $r(t+\Delta t|t_0, i)$  responds to the various interrelationships between air parcel location and a rising inversion base as shown in Figure 3.6. At hours prior to 11:00 am on the first day of travel,  $H(t_0, i) > \ell(t+\Delta t|t_0)$  and the unit step function

on the right side of equation (3.43) yields zero probability of down-mixing. Between 11:00 am and noon on the first day  $h(t+\Delta t) = \ell(t+\Delta t | t_0)$ , the inversion base is rising, and  $\ell(t+\Delta t | t_0) > H(t_0, i)$ , giving unit probability that an air parcel above the mixed layer would be mixed downward. For the period just following noon, the inversion base is not moving,  $u_{h(t)}(h(t+\Delta t))$  takes on value zero, and no vertical transport occurs. Until the inversion begins to reform near the ground at sunset, the function  $d(t+\Delta t | t_0, i)$  has taken only zero values. As the inversion base height is lowered, a pollutant particle traveling within the mixed layer at time  $t$  has probability  $d(t+\Delta t | t_0, i) = [h(t) - h(t+\Delta t)]/h(t)$  of being caught above the new inversion base height, and probability  $[1 - d(t+\Delta t | t_0, i)]$  of being caught below the overnight inversion base. Then as the inversion base rises on the second day, a particle which was caught above the inversion base is likely to be fumigated downward into the mixed layer with probability  $r(t+\Delta t | t_0, i) = [h(t+\Delta t) - h(t)]/[\ell(t+\Delta t | t_0) - h(t)]$  in proportion to the fraction of the stable polluted layer aloft which has been mixed downward at each time step.

These simple expressions for  $r$  and  $d$  will not hold exactly for indefinitely long transport chains. In particular if an air parcel were mixed to a high altitude  $h_{\max_1}$ , on the first day, then a second day followed with  $h_{\max_2} < h_{\max_1}$ , by the morning of the third day, the inversion base would be rising into a stable inversion which contained a non-uniform vertical distribution of the probability of finding the particle at a given altitude within the inversion. In that case, the probability of down-mixing of the particle would depend on the maximum

mixing depth achieved on both of the prior days, and the form of  $r(t+\Delta t|t_0,i)$  becomes more complex. However, this problem is not of major concern in the application which we have in mind. The probability of finding the particle in the mixed layer is calculated as correctly as possible for more than a day and a half. By that time, the air parcel will typically have exited the study area surrounding the Los Angeles coastal plains and San Gabriel and San Fernando Valleys. If the particle has not yet been deposited at the ground or advected out of the study area, then its probable composition is likely to be as sulfate after over a day and a half of reaction time. Sulfates behave as a nearly inert pollutant in our model. Inversion base motion acts only in the direction toward reestablishing a uniform pollutant concentration in the vertical both above and below the inversion base for an inert pollutant. Any significant non-uniform distribution of  $P_{SO_4}(t|t_0,i)$  with altitude is transitory when it does occur. Since this situation will be transitory by nature and will occur only under a special series of meteorological circumstances involving at least one day of relatively high dilution, (and thus low ground level impact in any case), modification of the form of  $r(t+\Delta t|t_0,i)$  to cover this special case is not felt to be necessary for the application that we have in mind.

The form adopted for  $r(t+\Delta t|t_0,i)$  and for  $d(t+\Delta t|t_0,i)$  may be inserted into equations (3.23) through (3.28). Given the available ambient monitoring data, a time series of inversion base motion like that of Figure 3.6 can be constructed for any time period of interest in the Los Angeles Basin over the past decade. Thus the probability

that any representative fluid particle containing sulfur oxides is at ground level in a given chemical state can be estimated from ambient monitoring data, given that its initial chemical status, location, and time of origin were known.

### 3.4.2 Calculating Trajectories in the Horizontal Plane

Equation (3.32) calls for particle trajectories to be constructed by integration of the wind vector apparent along the path of each particle. Unfortunately, wind data are not available along such trajectories. Rather, wind speed and direction is measured by a network of Eulerian wind stations which are fixed to the earth's surface.

A variety of means may be used to compute particle trajectories from a network of Eulerian measurements. Perhaps the most realistic approach would be to interpolate wind data from the thirty or so available wind stations in the Los Angeles Basin to form a mass-consistent wind field at a closely spaced network of grid points. If data were available on winds aloft, then a vertical wind speed and direction profile reflecting the effects of wind shear could be included. A random number generator could be used to perturb particle position between time steps and thus simulate those scales of atmospheric motion which were too small to be resolved by conventional wind measurements. Then the fluid particle could be passed through a sequence of transport steps by a self-propagating stochastic chain similar in concept to the chains developed for vertical motion and pollutant chemistry.

Our air quality model derivation is compatible with a sophisticated trajectory calculation procedure. However, the application that we intend to pursue involves simulation of sulfate air quality over months covering a three year test period. The computer time needed to construct highly accurate wind fields hourly for three years is simply beyond our budget. It therefore becomes necessary to consider the merits of testing this model using an approximate trajectory calculation scheme. Since our interest lies in a particular air quality problem in Los Angeles, the following discussion will be placed in the context of that air basin.

The two main parameters of our sulfate air quality model which depend on horizontal trajectory calculations are air parcel retention time in the air basin, and the lateral location of various concentration peaks. From the standpoint of making most sulfate air quality control strategy decisions, a correct computation of air parcel retention time is probably the more critical of the two. That is because the retention time allowed for chemical reactions to proceed determines the total amount of sulfate formed within the study area. An air parcel trajectory calculation which differentiates between seaward and landward transport regimes and which distinguishes stagnation periods from times of high winds will probably track those features most important to determining air parcel retention time in Los Angeles.

Correct computation of the horizontal path of an air mass in the Los Angeles Basin is made difficult by complex terrain. Fluid flow lines are diverted around the obstructions posed by many hills and valleys.

If these obstructions are ignored, the calculated lateral location of air masses far downwind will be distorted. The main effect of ignoring streamline diversion around terrain features within the context of a sulfate model for the Los Angeles Basin is to sacrifice some information on exactly who is exposed to a peak pollutant concentration. Most air quality standards are aimed at protecting the general public from pollutant exposures above certain levels regardless of where they might live. Therefore a little uncertainty in the location of a predicted concentration peak can usually be tolerated in most practical decision-making processes.

Therefore, the following approximation is made: horizontal motion in the atmosphere over the Los Angeles Basin will be represented as if it were in uniform parallel flow at any single time. That approximation is certainly untrue for near stagnant conditions over the scale of a given time step. Over a long averaging time the approximation may not be too bad. That is because most net transport occurs during higher wind speed events at which time flow over the basin is quite organized. Returning to Figures 3.1 and 3.2 we note that the predominant wind flow directions during daytime and nighttime transport by and large do follow parallel paths to within the  $22.5^\circ$  of arc which are included within each sector of the 16 point compass into which wind direction measurements are resolved. Two exceptions to this behavior are apparent. There is a flow diversion around the Palos Verdes Hills at the center of the Los Angeles County coastline. That diversion however seems to pose only a local problem. Secondly, there is a distinct turning of

the wind flow at the entrance to the San Fernando Valley. As a result, calculation of pollutant transport into the San Fernando Valley definitely requires the use of a detailed windfield. Use of a parallel flow approximation in this locale at least restricts the validity of air quality model calculations to the central flatlands of the Los Angeles Basin and the adjoining San Gabriel Valley. Fortunately, the area over which model calculations still should perform well is substantially the same area identified in Chapter 2 as having air quality data sufficient to verify model predictions.

If the air mass over the basin were actually in uniform parallel flow, wind speed and direction at any location in the air basin should be represented well by observations at a single wind station. However, since this type of flow regime is only an approximation in our case, a representative wind station should be chosen carefully. To minimize discrepancies between the generally higher wind speeds at the coast versus the slower wind speeds in inland valleys, a wind station in the center of the air basin will be chosen. Secondly, to partially account for higher wind speeds aloft at the height of elevated sources, a wind station with a relatively high measurement height should be chosen. Finally, if average trajectories are to be calculated, then a LAAPCD wind station which reports integrated wind speed and direction over each hourly interval should be picked rather than a U.S. Weather Service airport wind station which reports only point measurements at a single instant once per hour. A wind station is available which satisfies these criteria at the downtown Los Angeles headquarters

monitoring site of the LAAPCD. It is located in the center of our study area on a mast above the top of a six story building with relatively unobstructed exposure. Its strip chart record is reduced to hourly average speed and direction. And because of its proximity to agency staff, its equipment probably receives superior maintenance.

Having selected a given wind station, trajectory calculation in the horizontal plane is straightforward. Breaking equation (3.32) into components in the  $x_1$  and  $x_2$  directions, we get

$$x_1''(t|x_{1_0}, t_0) = \int_{t_0}^t U_1(t') dt' + x_{1_0} \quad (3.47)$$

$$x_2''(t|x_{2_0}, t_0) = \int_{t_0}^t U_2(t') dt' + x_{2_0} \quad (3.48)$$

If wind measurements reduced from each hour's strip chart recording have previously been integrated over that hour, we may obtain the expected value of particle location at the end of each time step of the chemical chain of the previous section of this chapter by summing wind components in each coordinate direction.

$$x_1''(t|x_{1_0}, t_0) = \sum_{n=0}^{N_5-1} U_1(t_0 + n\Delta t) \Delta t + x_{1_0} \quad (3.49)$$

$$x_2''(t|x_{2_0}, t_0) = \sum_{n=0}^{N_5-1} U_2(t_0 + n\Delta t) \Delta t + x_{2_0} \quad (3.50)$$

where  $N_5 = \frac{(t - t_0)}{\Delta t}$ .

If wind direction were known accurately, our trajectory integration procedure would be nearly complete. But reported wind direction measurements at downtown Los Angeles are resolved only to within the  $22.5^\circ$  of arc which make up the sectors of a 16 point compass. As far as can be discerned from available monitoring data, a given particle trajectory for an hour could have followed any path consistent with the compass sector and wind speed reported. In order to construct a specific trajectory at each hour from the family of wind directions within each sector, our calculations will employ several random number generators. In order to pick the mean wind direction used at each hour, a specific bearing is drawn from a uniform distribution of the possible directions contained within the sector of interest. The resulting mean wind vectors will be integrated in time series as in equations (3.49) and (3.50). But in addition to this mean displacement over time, small scale atmospheric fluctuations (measurable in terms of the standard deviation of the wind direction about its mean) impart small diffusive displacements to individual fluid particles. This process of eddy diffusion will be simulated by means of a two dimensional Gaussian random number generator. The standard deviation of fluid particle displacements from mean trajectory paths dispersing over urban areas can be estimated as a function of travel time downwind from experimental data available for Los Angeles and elsewhere (Drivas and Shair, 1975; Shair, 1977; McElroy and Pooler, 1968). Then mean trajectory end points can be perturbed by adding a pair of displacements,  $\delta x_1$  and  $\delta x_2$ , drawn at random from the family of displacements having a

two dimensional normal distribution with mean zero and variance  $(\sigma_1^2(t - t_o), \sigma_2^2(t - t_o))$ .

At this point, it becomes evident why the instantaneous parallel flow assumption leads to large gains in computational efficiency which make it attractive in spite of certain limitations as to accuracy. First, given that assumption, the displacement of a particle from its release point  $(x_1'' - x_{1o}'')$  is only a function of  $t$  and  $t_o$  plus randomness. A single set of trajectories represents source to receptor transport from all starting locations in the airshed. Separate trajectory integrations for hundreds or thousands of possible source locations can be collapsed into one source to receptor transfer calculation which may then be adapted to any starting location,  $x_o$ , merely by subtracting starting location from all trajectory end points of interest. The useful result is that

$$P_{SO_4}(\tilde{x}, t | \tilde{x}_o, t-\tau, i) = P_{SO_4}(\tilde{x} - \tilde{x}_o, t, t-\tau, i) \quad (3.51)$$

$$P_{SO_2}(\tilde{x}, t | \tilde{x}_o, t-\tau, i) = P_{SO_2}(\tilde{x} - \tilde{x}_o, t, t-\tau, i) \quad (3.52)$$

and

$$\bar{Q}_{SO_4}(\tilde{x} | \tilde{x}_o, i; T, t_s) = \bar{Q}_{SO_4}(\tilde{x} - \tilde{x}_o, i; T, t_s) \quad (3.53)$$

$$\bar{Q}_{SO_2}(\tilde{x} | \tilde{x}_o, i; T, t_s) = \bar{Q}_{SO_2}(\tilde{x} - \tilde{x}_o, i; T, t_s) \quad (3.54)$$

### 3.4.3 Calculation of Monthly Average Pollutant Levels

Given the foregoing methods for calculating probable chemical status and air parcel location over time, a simulation may be conducted to evaluate  $\bar{Q}_{SO_4}$  and  $\bar{Q}_{SO_2}$  for a given month. The procedure adopted is to order the necessary integrations so that a monthly average of pollutant concentrations apparent at given times of the day is first computed for each source class of interest. Then the average concentrations at  $n = \left( \frac{24 \text{ hours}}{\Delta t} \right)$  times of the day will be pooled to obtain total monthly average concentration estimates for each source class. Finally, the source classes will be superimposed to form the total air quality impact due to local sources. This concentration estimate is then added to background air quality levels to obtain a total pollutant concentration estimate over the airshed of interest. A step by step description of one means of carrying out this numerical integration follows.

First we wish to calculate the chemical status and vertical dilution of all air parcels present in the airshed at a known time of day on each day of the month. Consider a simplified case. Let  $\Delta t$  equal one hour. Attention is focussed on the first source class. An initial time of day is chosen, for example 0:00 hrs (midnight) at the start of each of the  $\eta$  days of the month. Then the wind and inversion base data are repacked into  $\eta$  sequences of  $\tau_c$  consecutive hours of data each, starting with the  $\tau_c^{\text{th}}$  hour preceeding midnight of each day of the month, for example. At each hour represented in each string of

meteorological data, a marker particle is released with an associated magnitude  $\omega(t_o, i)$  at a height  $H(t_o, i)$ . The probable chemical status and vertical progress of each particle is tracked by the methods outlined previously from its time of release until the midnight hour at the end of its parent data string. The first particle released for each of the  $\eta$  data strings travels for  $\tau_c$  hours the second particle for  $\tau_c - 1$  hours, and so forth. This process is illustrated in Figure 3.7. After  $P_{SO_{4b}}$  and  $P_{SO_{2b}}$  have been evaluated for each particle at the final hour of each data string, the probabilities  $P_{SO_{2b}}$  and  $P_{SO_{4b}}$  associated with each particle are stored in a location tagged with their initial starting time.

Next the  $\eta$  sets of wind data of  $\tau_c$  hours each are integrated backwards by time steps of  $\Delta t$  from the ending midnight of interest. This generates a set of streaklines which contain the horizontal displacement at the hour of initiation of the backward integration (i.e. at the  $\eta$  midnights of interest) of all of the individual particles for which  $P_{SO_{4b}}$  and  $P_{SO_{2b}}$  were just calculated. This cuts the number of operations required for trajectory integration substantially.<sup>3</sup> The point is illustrated schematically for  $\tau_c$  equals 5 hours in Figure 3.8.

Streaklines ending at all "midnights" for the month are superimposed. Then the horizontal displacement of each particle is paired

---

<sup>3</sup>The suggestion that wind vectors be integrated backward in order to increase computational efficiency is due to R.C.Y. Koh.

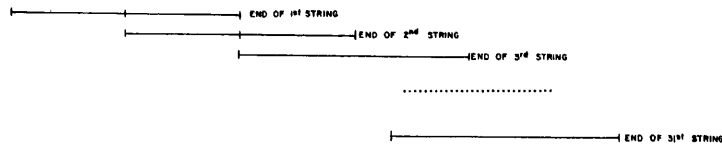
FIGURE 3.7

OBJECTIVE: TO CALCULATE THE CHEMICAL STATUS AND VERTICAL DILUTION OF AIR PARCELS PRESENT IN THE AIRSHED AT A KNOWN TIME OF DAY ON EACH DAY OF A MONTH.

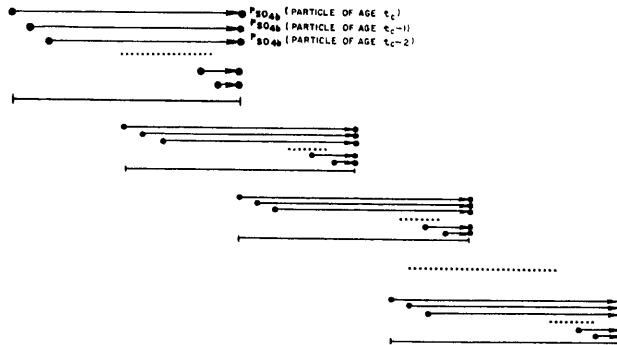
STEP 1: FOCUS ON A TIME OF DAY, FOR INSTANCE, MIDNIGHT AT THE START OF EACH DAY OF THE MONTH.



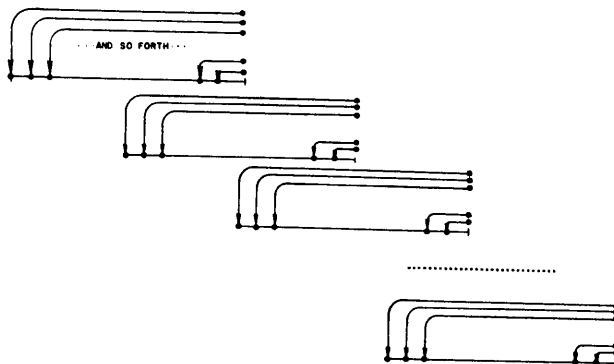
STEP 2: REPACK DATA INTO 31 STRINGS OF  $t_c$  HOURS, EACH ENDING AT THE TIME OF DAY AT WHICH WE WISH TO COMPUTE AIR PARCEL STATUS.



STEP 3: RELEASE ONE FLUID PARTICLE AT EACH TIME STEP SHOWN IN EACH DATA STRING. TRACK EACH PARTICLE'S CHEMICAL PROGRESS AND VERTICAL DILUTION UNTIL THE LAST HOUR APPEARING IN ITS PARENT DATA STRING.



STEP 4: STORE RESULTS IN A LOCATION ASSOCIATED WITH EACH FLUID PARTICLE'S ORIGINAL RELEASE TIME.

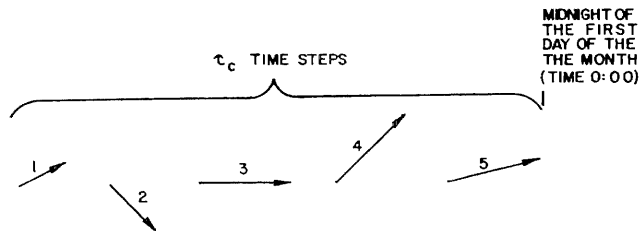


RESULT: THE CHEMICAL STATUS AND VERTICAL DILUTION OF REPRESENTATIVE AIR PARCELS OF ALL AGES PRESENT AT ALL MIDNIGHTS OF THE MONTH HAS BEEN DETERMINED. THE RESULTS ARE STORED IN A MANNER IN WHICH THEY ARE EASILY ASSOCIATED WITH TRAJECTORIES CALCULATED IN THE HORIZONTAL PLANE AND WITH THE DIURNAL SOURCE STRENGTH EVALUATED AT EACH PARTICLE'S TIME OF RELEASE.

FIGURE 3.8

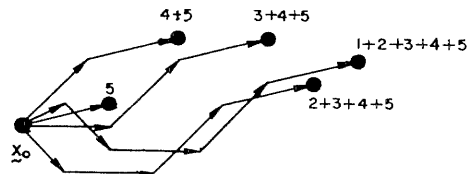
OBJECTIVE: TO CALCULATE THE HORIZONTAL DISPLACEMENT FROM LOCATION  $X_0$  AT A GIVEN MIDNIGHT FOR ALL PARTICLES RELEASED PRIOR TO THAT TIME.

STEP 1: TAKE A SERIES OF  $\tau_c$  WIND VECTORS.

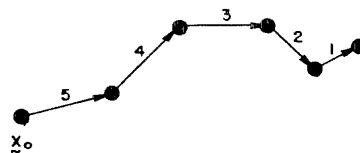


STEP 2: TO GET DISPLACEMENT FROM LOCATION  $X_0$  AT TIME 0:00 FOR ALL PARTICLES RELEASED PREVIOUSLY:

(a) CALCULATE  $\tau_c$  FORWARD TRAJECTORIES,



(b) OR ONE BACKWARD STREAKLINE INTEGRATION.



THINK OF THIS AS A SNAPSHOT OF A CROOKED PLUME PHOTOGRAPHED AT MIDNIGHT

STEP 3: PERFORM STREAKLINE TRAJECTORY INTEGRATION ON THE SEQUENCE OF WIND VECTORS PRESENT IN EACH DATA STRING SHOWN IN FIGURE 3.7. THESE PARTICLE DISPLACEMENTS ARE THEN TO BE MATCHED WITH THE CHEMICAL STATUS OF EACH PARTICLE, PARTICLE VERTICAL DILUTION, AND THE DIURNAL SOURCE STRENGTH FUNCTION APPROPRIATE TO THE TIME OF PARTICLE RELEASE.

with the particle's probable chemical status and weighted by its diurnal source strength. The resulting magnitudes are accumulated to a matrix of receptor cells by summing magnitudes for all particles having displacements falling within the same receptor cell. Totals are accumulated separately for  $\text{SO}_2$  and for sulfates. We divide the elements of these accumulation matrices by the size of the receptor cell and the number of "midnights" being superimposed. One quickly obtains a rough estimate of the spatial distribution of average  $\text{SO}_2$  or sulfate concentrations appearing in the air at midnight due to a unit source of  $\text{SO}_x$  of source class  $i$  located at the origin of our coordinate system. That averaging process is illustrated schematically in Figure 3.9.

Next, advance the starting time from midnight by increments of  $\Delta t$  through the remainder of a day, repeating the above procedure and then averaging the set of source-receptor transfer relationships obtained. We finally arrive at the desired estimates of  $\bar{Q}_{\text{SO}_4}$  and  $\bar{Q}_{\text{SO}_2}$  in the form of matrices which were constructed from information on all trajectory starting and ending times for the month. Figure 3.10 shows this superposition of source to receptor transport matrices calculated at different trajectory ending times for the month.

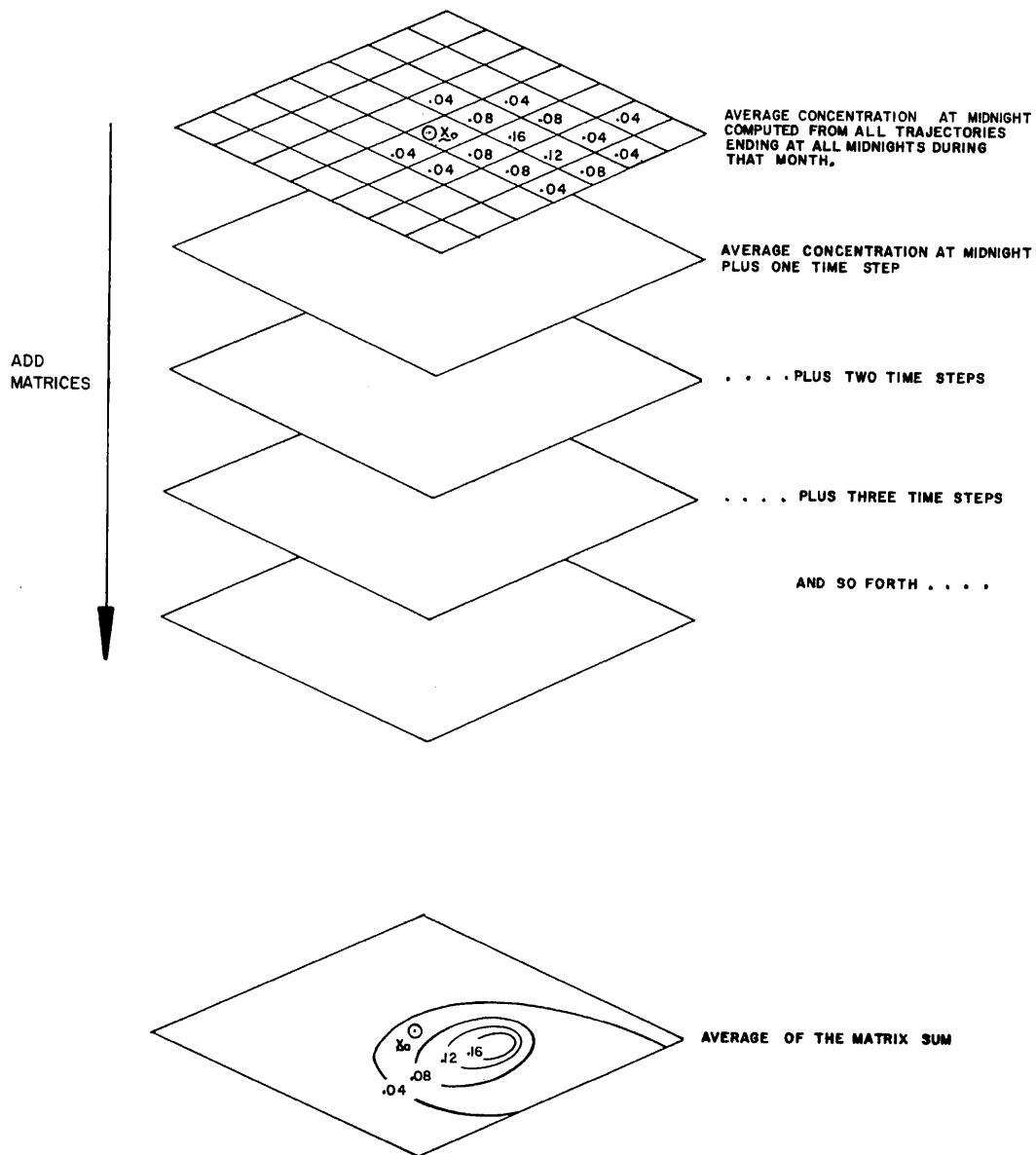
If average source emission strength  $\bar{S}(x_o, i)$  is given for each source location in class  $i$  as if the source were located in the center of a grid cell with the same spacing as the receptor cells, then the source to receptor transport probability matrices  $\bar{Q}_{\text{SO}_2}$  and  $\bar{Q}_{\text{SO}_4}$  just calculated may be used to map emissions into air quality by a process



FIGURE 3.10

OBJECTIVE: TO CALCULATE THE MONTHLY AVERAGE SOURCE  
TO RECEPTOR TRANSFER RELATIONSHIP

PROCEDURE: SUPERIMPOSE THE RELATIONSHIPS CALCULATED FROM  
TRAJECTORIES ENDING AT EACH TIME OF DAY FOR  
THAT MONTH.



of superposition. The appropriate influence matrices  $\bar{Q}_{SO_2}$  and  $\bar{Q}_{SO_4}$  are merely centered on the origin of the source of interest and the emissions are scaled to incremental air quality impact at surrounding receptor sites.

The matrix of air quality increments defined at each receptor site due to emissions from the first source class is stored for future reference. Next the integration over fluid particle release, reaction and transport is repeated for each remaining source class of interest. Then all incremental impacts from all source classes are added to form a total air quality impact at each receptor point due to local pollution sources. Background air quality is added to the air quality impact predicted for local sources. The monthly average air quality calculations are now complete.

Superposition is permitted because the entire model is linear in  $SO_x$  emissions. A multiple source urban air quality model for sulfate formation and dispersion is thus achieved which shows the contribution of each source class to air quality observed at each receptor site. That knowledge of source class influence is very valuable when searching for efficient emission control strategies. Control strategies can be aimed at source classes with the greatest air pollution impact per dollar spent on control.

Of course the order of integration could be changed in the above description. There is no necessity for accumulating intermediate concentration estimates at twenty-four hourly trajectory ending times per month. Source emission strength could be associated with individual

particles before the magnitudes of each particle are accumulated at each receptor site. No matter what the order of integration, evaluation of  $\overline{c_{SO_4}}$  and  $\overline{c_{SO_2}}$  by the equations presented previously simply results in estimation of long-run average pollutant concentrations from a distribution of sources by release of representative marker particles at intervals of  $\Delta t$  followed by indexing of accumulating registers within each receptor cell at the end of each time step  $\Delta t$ .

### 3.5 Summary and Discussion

A simulation model has been described for calculating long-run average sulfate air quality levels in a multiple source urban setting. The model computes pollutant concentrations by a long-run average Lagrangian marked particle technique. First order chemical reactions and ground level dry deposition are incorporated. The model is capable of handling unsteady meteorological conditions in a region characterized as having an idealized persistent temperature inversion. This atmospheric temperature structure results in a well-mixed layer near ground level capped by a stable air mass aloft.

The *long-term average* air quality model thus formed has many of the merits and faults commonly associated with *short-term average* air quality models based on air parcel trajectory calculations. Potential sources of error in many of the most advanced trajectory models in use today include (Liu and Seinfeld, 1975):

1. neglect of horizontal diffusion (not neglected in our case)
2. neglect of the vertical component of the wind
3. neglect of wind shear.

Of these problems, neglect of wind shear and return flows aloft is probably the most serious. Due to a lack of wind data aloft, the wind shear problem would remain in practice in our intended application even if the computational procedure were designed to handle wind shear explicitly. Each of the above mentioned difficulties can be overcome in our marked particle simulation model given appropriate meteorological data and more computing resources.

In addition to these problems common to nearly all trajectory-based models, a series of approximations has been made in order to adapt a quite general concept for use in a particular application: sulfate air quality prediction in Los Angeles. The available meteorological data for Los Angeles were discussed. Then the following approximations were made which permit rapid calculation of the elements of the simulation model from existing monitoring records:

1. that inversion base height above ground level over the central Los Angeles Basin is spatially homogeneous at any given time
2. that inversion base motion over time may be represented by a stylized diurnal cycle which passes through the known daily maximum and minimum inversion base heights
3. that at any single time, the wind field over the Los Angeles Basin may be approximated as a uniform parallel flow.

Each of these approximations was made as a practical consideration aimed at conserving available computing resources, and not out of theoretical necessity. The accuracy of this air quality simulation depends on meteorological resolution, chemical resolution, and resolution obtained

by defining source class behavior more accurately. Within a fixed computing budget, contributions to model accuracy from treatment of each of these degrees of freedom must be balanced. Approximations (1) and (3) above permit isolation of chemical calculations and trajectory calculations from detailed dependence on a given starting location in the airshed. This results in a huge savings in computing time versus that which would be needed if either of these approximations were relaxed. That computational savings is necessary in our case if a reasonable number of source classes are to be defined. In short, a compromise has been struck between meteorological elegance and the number of separate source classes which may be entered into the model within a fixed computing budget.

Several of the particular merits of this simulation model also bear discussion at this point. First, the long-run average Lagrangian marked particle model need not compute pollutant concentrations as a real-time sequence of events. The order of integration over air parcel release and transport may be arranged to minimize computing time and intermediate data storage requirements. Secondly, the calculations required are very simple. The computational algorithm is completely stable over time. There are no artificial numerical diffusion problems associated with mixing a particle into a cell and then forgetting where it was located before mixing occurred. Pollutant mass is absolutely conserved.

The model builds its own initial conditions by integrating backward to connect all locally-emitted air parcels in the airshed at a given

time to their source. This is very important for solving our sulfate problem because instantaneous sulfate concentration data representing initial conditions at any time are completely unavailable. Even if measurements on pollutant initial conditions were available, one would prefer the chosen method because it permits deduction of the sources responsible for creating those initial conditions.

The chosen computational method also has advantages in the way that it treats behavior at the edges of the receptor grid. The model does not require that boundary conditions be specified at the edges of the grid system. Air parcels advected beyond the borders of the receptor grid are not lost to the model. Their position is remembered but their magnitudes are not accumulated to a receptor grid cell unless the air parcels are advected back into the region of the receptor grid. Receptor cells may thus be specified only over those areas where concentration estimates are desired without compromising model accuracy.

In the above discussion, the proposed long-term average air quality simulation has been discussed in light of features often sought in a dynamic model for short-term average air quality prediction. In a comparison with the pseudo-steady state models routinely used to predict *long-term average* air quality, the simulation model proposed here fares quite well. Pseudo-steady state models which employ a joint frequency distribution of wind speed, wind direction and atmospheric stability have no hope of correctly computing air parcel retention time in an air basin because they do not contain any information about the serial correlation of wind vectors. Without utilizing wind data in

time sequence to compute air parcel retention time, conventional pseudo-steady state air quality models cannot hope to track slow chemical reactions occurring in a recirculating air mass over the Los Angeles Basin.

## CHAPTER 4

AN ENERGY AND SULFUR BALANCE  
ON THE SOUTH COAST AIR BASIN4.1 Introduction

The most outstanding feature of sulfur oxides emissions in the Los Angeles area is that virtually all of the anthropogenic sulfur in this community's atmosphere originally entered the air basin in a barrel of crude oil. The questions of air pollutant emissions and energy use in Los Angeles are inseparably related.

In order to place the Los Angeles sulfur management problem in perspective, the origin of the sulfur itself will be sought. The sources of supply for crude oil used in the air basin in 1973 will be characterized by origin, quantity and sulfur content. *Potential* sulfur oxides emissions which could occur if all of that sulfur were released to the atmosphere during combustion will then become apparent.

The second problem at hand is to identify the sources from which sulfur oxides air pollutant emissions actually are released to the atmosphere within the Los Angeles area. Our immediate need is for the emissions data required as input to an air quality simulation model for sulfate formation in the Los Angeles atmosphere. But a broader goal is to achieve an understanding of the underlying demand for energy in various forms which brings with it the processing and combustion of sulfur-containing fuels. This understanding is important if one wishes

to control pollutant emissions to some desired level while at the same time meeting the fundamental demands for energy to run the economy of Southern California. Since our ultimate objective is to study possible air pollutant emissions control strategies, the effort needed to pursue this broader outlook is well justified.

The traditional approach to preparing emission inventories for Los Angeles is to locate the several hundred largest emission sources, measure their emissions, and then accumulate their emissions to form a total "from the bottom up". Examples of this sort of inventory have been compiled from time to time for Los Angeles sulfur oxides emissions by air pollution control agencies and by engineering consulting firms (Environmental Protection Agency, 1974; Trijonis, et al., 1975; Hunter and Helgeson, 1976; Southern California Air Pollution Control District, 1976b). In this report we will first collect and compile an inventory of stationary and mobile source  $SO_x$  emissions for each month of the years 1972 through 1974. This inventory is based on a comparative appraisal of individual source emission estimates made possible by cooperation from the Southern California Air Pollution Control District, the California Air Resources Board, KVB Incorporated (a state ARB contractor), the Southern California Gas Company, the Southern California Edison Company, the California Department of Transportation, and conversations with a number of industrial source owners. Information will be presented on the spatial distribution of sources across the air basin, the seasonal and diurnal variation of source strength, the effective height of injection of emissions into the atmosphere, and

the distribution of emissions between gaseous and particulate sulfur oxides species. This data base will be specifically designed to meet the needs of an air quality modeling effort for monthly average sulfate concentrations.

Sulfur flows entering the air basin in crude oil then will be compared to estimates of atmospheric  $\text{SO}_x$  emissions. It quickly becomes apparent that only a small fraction of the basin's sulfur supply is becoming airborne. In order to confirm that observation and to explain its occurrence, both mass balance and energy balance calculations will be performed on the flows of energy resources containing sulfur across a control surface drawn around the perimeter of the air basin. Petroleum resources will be tracked through the Los Angeles refinery complex, subdivided into refinery products, refinery fuel, recovered elemental sulfur and sulfuric acid. Then refinery products will be assigned to the consuming sectors of the air basin's economy, and to out-of-basin export markets. Natural gas and liquified petroleum gas use within the air basin will be detailed, as will be the importation of electric energy from outside the basin, and the generation of electricity within the airshed.

Sulfur flows accompanying each energy flow will be estimated. Points within the Los Angeles energy economy at which sulfur oxides emissions to the atmosphere occur thus will be identified.

In the following sections of this study, the crude oil supply characterization, the spatially resolved emission inventory and the energy and sulfur balance will be briefly introduced. Findings will

be summarized and discussed. The detailed basis for those discussions is described in a series of appendices which accompany this report.

#### 4.2 The Quantity and Sulfur Content of Crude Oil Supplied to the South Coast Air Basin in 1973

In Appendix A1, the methods used to trace crude oil from its source to the South Coast Air Basin are described. The purpose of this study was to assure that the amount of sulfur entering the air basin via crude oil was fully determined. Therefore, a serious attempt was made to find the sulfur content as well as the quantity of the oil delivered. This survey was nominally conducted for the year 1973, although some of the data employed came from other recent years. In the following paragraphs, a brief description of the approach used in this study will be given.

##### 4.2.1 Crude Oil Characterization -- Approach and Methods

Crude oil quality varies widely from one oil field to another. In order to obtain a quantitative description of crude oil properties entering the South Coast Air Basin, the oil must be tracked to its source. Oil-producing regions of the world were subdivided into three basic categories: California oil fields, other domestic sources, and foreign crude oil supplies. These categories are convenient because different data sources are needed to assess crude oil properties from each of these three producing territories.

Smaller geographic regions within each producing category were then defined. California oil fields were subdivided into five

producing regions based on geographic terrain and access to common transportation links. Previously reported surveys of California oil use (Nehring, 1975) showed that the only non-California domestic oil producing regions important to California oil consumption were in Alaska and the Four Corners area between Utah and New Mexico. Foreign crude oils first were considered by country of origin, and then grouped into ten major geographic zones (e.g. South Pacific, Persian Gulf, etc.).

Total oil production in each major field in each producing district was determined for a base year of interest. Then sulfur content information for crude oil from each field was used to compute the total quantity of associated sulfur produced along with the oil. Sulfur and oil production data were next pooled for all fields within the producing district of interest. The distribution of crude oil production within sulfur content intervals was determined. The fraction of oil production with a sulfur content between 0.26% and 0.50% sulfur, for example, was then apparent in any producing district. Finally, a weighted average sulfur content of crude oil was determined for each sulfur content interval in each producing district. In that manner, oil supplies at the wellhead around the world were organized and stratified by sulfur content.

Next, oil shipments to the South Coast Air Basin were estimated by investigating available transportation links. California crude oil shipments to the South Coast Air Basin were estimated from local production within the Los Angeles Basin, plus waterborne commerce data and pipeline capacities.

Crude oil transfers to the entire state of California from out-of-state domestic sources and from major foreign countries were obtained by producing district of origin for 1973. Total receipts of non-California crude oil at local harbors were determined. Unfortunately, the local harbor crude oil receipts are not resolved by state or by country of origin. Therefore the assumption was made that the distribution of crude oil by country of origin arriving at South Coast Air Basin ports was directly proportional to that estimated for all foreign and out-of-state domestic oils received by ship in California.

By combining crude oils from California fields, out-of-state domestic sources and foreign imports, both the total quantity of crude oil and the distribution of that oil between high sulfur and low sulfur crude oils was estimated. The details of this crude oil characterization study are given in Appendix A1. A discussion of this survey's implications for control of sulfur oxides emissions by manipulation of crude oil entering the South Coast Air Basin will now be presented.

#### 4.2.2 Crude Oil Characterization -- Summary and Discussion

Table 4.1 and Figure 4.1 summarize the estimated crude oil and associated sulfur receipts by South Coast Air Basin customers in 1973. The result is that just over one million barrels of crude oil were received daily containing 3821 thousand pounds of sulfur per day. These crude oil receipts almost exactly match 1973 South Coast Air Basin refinery capacity of 1,006,200 bbls per stream day (Cantrell,

TABLE 4.1  
 Summary of 1973 South Coast Air Basin  
 Crude Oil Receipts plus Associated Sulfur Content

Origin of Crude Oil	Average % Sulfur by Weight	1973	1973
		Estimated Quantity Received in SCAB (1000's barrels/yr)	Approximate Quantity of Sulfur Contained (1000's lbs/year)
Los Angeles Basin	1.49	128,207.9 <sup>a</sup>	613,878.5
Ventura and Federal Offshore	1.36	41,172.8 <sup>a</sup>	176,503.9
Central California Coast	3.35	8,648.9	99,808.8
San Joaquin Valley	0.81	39,055.4	102,912.4
California subtotal	1.42	217,085.0	993,103.6
Alaska	0.08	26,950.5	6,509.3
Utah	0.27	12,000.1	9,553.5
Domestic Import subtotal	0.14	38,950.6	16,062.8
Group 1 (Persian Gulf)	1.83	54,034.9	298,633.0
Group 2 (Remainder of Middle East)	1.64	644.1 <sup>b</sup>	3,243.3
Group 3 (Africa, north and west coast)	0.21	8,364.1 <sup>b</sup>	5,084.7
Group 4 (South Pacific)	0.14	30,357.0	12,633.5
Group 5 (South America, Caribbean Coast)	1.99	4,580.0	28,315.1
Group 6 (Western South America)	1.00	8,526.2 <sup>b</sup>	25,594.5
Group 7 (Europe)	1.38	454.6 <sup>b</sup>	1,887.6
Group 8 (Mexico)	2.56	762.3 <sup>b</sup>	6,099.0
Group 9 (Canada)	0.51	2,581.3 <sup>b</sup>	3,895.7
Group 10 (Japan & Taiwan)	0.13	24.6 <sup>b</sup>	9.6
Foreign Import subtotal	1.16	110,329.1	385,396.0
TOTAL	1.20	366,364.7	1,394,562.4

( = 3,821 thousand pounds  
per day)

- Notes: (a) Local production less estimated net exports from the basin.
- (b) Crude oil coming to the South Coast Air Basin from undesignated countries of origin was distributed amongst all producing regions whose exports to California were not known explicitly.

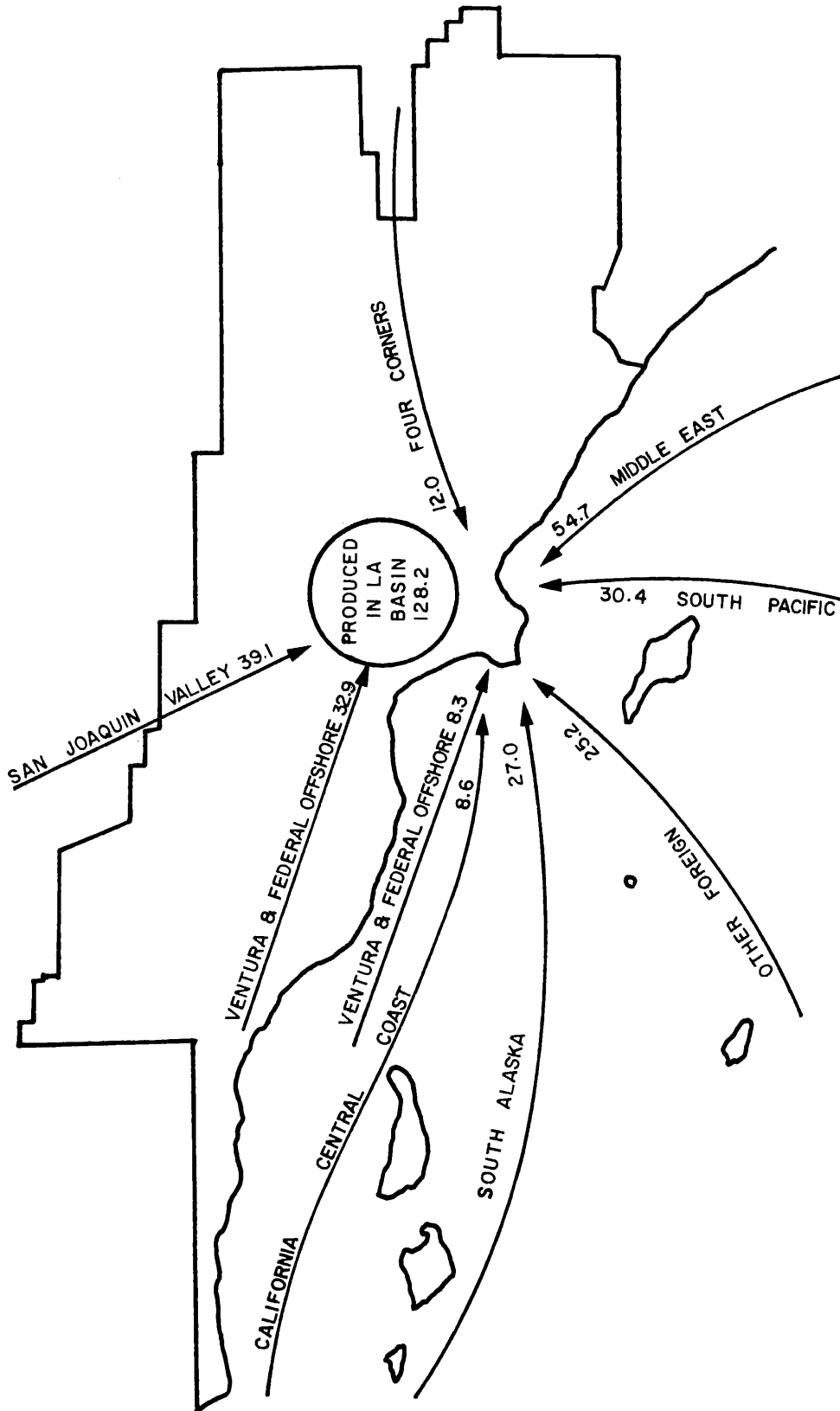


FIGURE 4.1

The Estimated Origin and Quantity of Crude Oils Received by South Coast Air Basin Customers in 1973. (Millions of Barrels per Year)

1973). Data on total 1973 crude oil sulfur intake by Los Angeles County refineries has been obtained by the Southern California Air Pollution Control District (1976a). Their data report that 3551.49 thousand pounds of sulfur arrived daily at Los Angeles County refineries in feedstocks (net of unfinished oils rerun) in that year. This agrees with our independent estimate to within about 7%. There are at least two small South Coast Air Basin refineries excluded from the APCD survey which, if included, would probably bring these two sulfur supply estimates into even closer agreement.

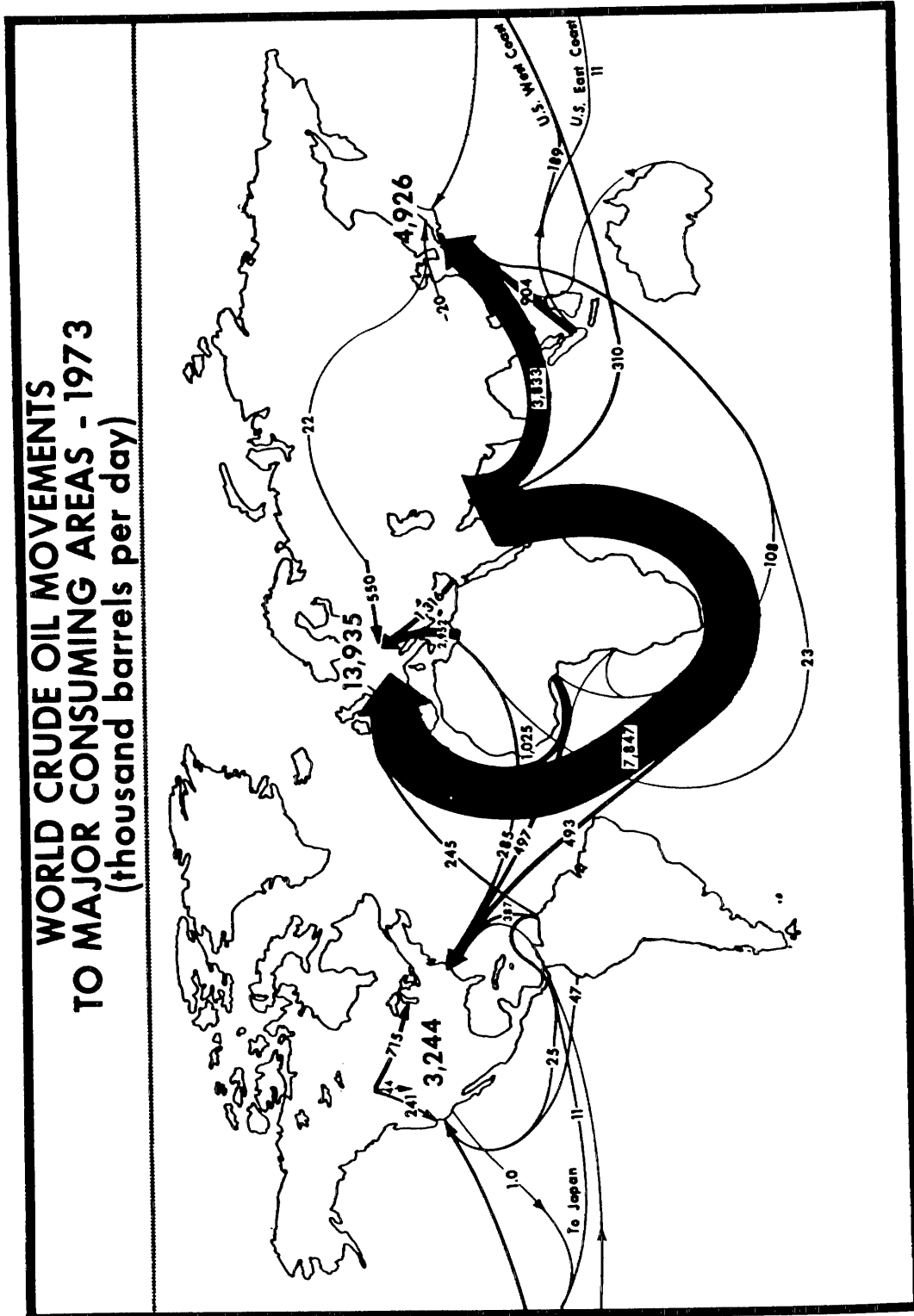
In spite of the high gasoline consumption in the Los Angeles area, the South Coast Air Basin uses only a very small portion of total world oil production. This fact is easily seen in Table 4.2. Most importantly, the basin uses but a small part of the very low sulfur (less than 0.25% S) crude oil produced in the world today. As seen in the trade maps of Figures 4.2 through 4.4, Japan is the major customer for South Pacific region (generally low sulfur) oil, buying more than ten times the amount delivered to the South Coast Air Basin from that producing region. An even smaller fraction of low sulfur African oils are imported to California. It is thus not physically impossible that sulfur input to the South Coast Air Basin could be sharply reduced by substitution of low sulfur crude oils for current high sulfur oil receipts.

However, the practical problems posed by such a fuel switching strategy look very formidable indeed. Figures 4.5 and 4.6 yield several important insights into the nature of the sulfur management

TABLE 4.2  
 Estimated South Coast Air Basin Crude Oil Receipts  
 As a Fraction of Oil Available at the Wellhead  
 in Various Producing Regions

Origin of Crude Oil	1973		Percent of total 1973 Production
	Average Percent Sulfur by Weight	Estimated Quantity Consumed in SCAB (1000's barrels/yr)	
Los Angeles Basin	1.49	128,207.9	97.0%
Ventura and Federal Offshore	1.36	41,172.8	87.4
Central California Coast	3.35	8,648.9	29.2
San Joaquin Valley	<u>0.81</u>	<u>39,055.4</u>	<u>30.8</u>
California subtotal	1.42	217,085.0	64.7%
Alaska (southern)	0.08	26,950.5	36.9
Utah	<u>0.27</u>	<u>12,000.1</u>	<u>46.2</u>
Domestic Import subtotal	0.14	38,950.6	
Group 1 (Persian Gulf)	1.83	54,034.9	0.7
Group 2 (Remainder of Middle East)	1.64	644.1	0.4 <sup>a</sup>
Group 3 (Africa, north and west coasts)	0.21	8,364.1	0.4 <sup>a</sup>
Group 4 (South Pacific)	0.14	30,357.0	3.7
Group 5 (South America, Caribbean Coast)	1.99	4,580.0	0.3
Group 6 (Western South America)	1.00	8,526.2	3.0
Group 7 (Europe)	1.38	454.6	0.4 <sup>a</sup>
Group 8 (Mexico)	2.56	762.3	0.4 <sup>a</sup>
Group 9 (Canada)	0.51	2,581.3	0.4 <sup>a</sup>
Group 10 (Japan & Taiwan)	<u>0.13</u>	<u>24.6</u>	<u>0.4<sup>a</sup></u>
Foreign Import subtotal	1.16	110,329.1	
TOTAL	1.20	366,364.7	

Note: (a) Crude oil coming to the South Coast Air Basin from undesignated countries of origin was distributed amongst all producing regions whose exports to California were not known explicitly.



Source: Bureau of Mines (1975)

FIGURE 4.2

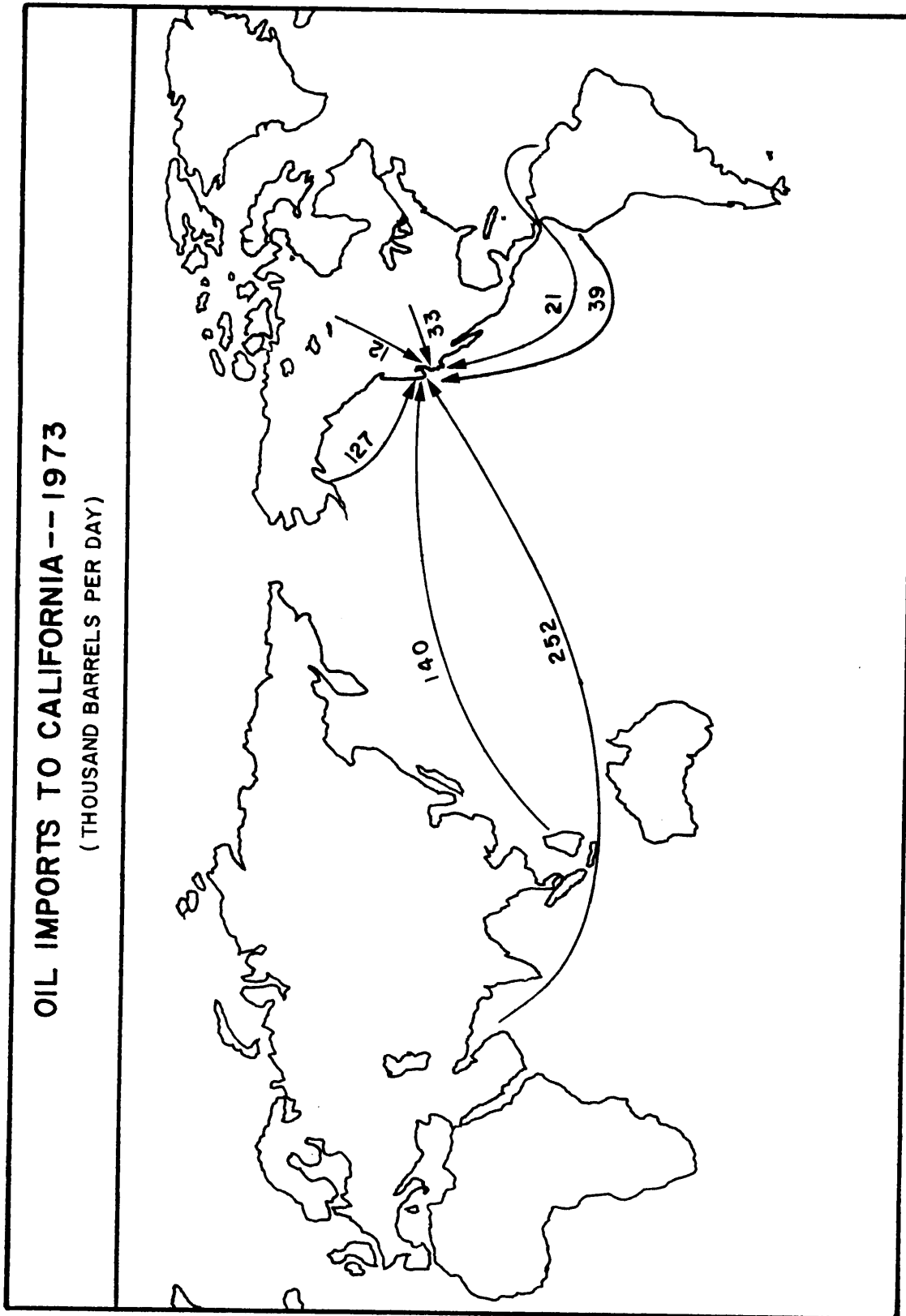


FIGURE 4.3

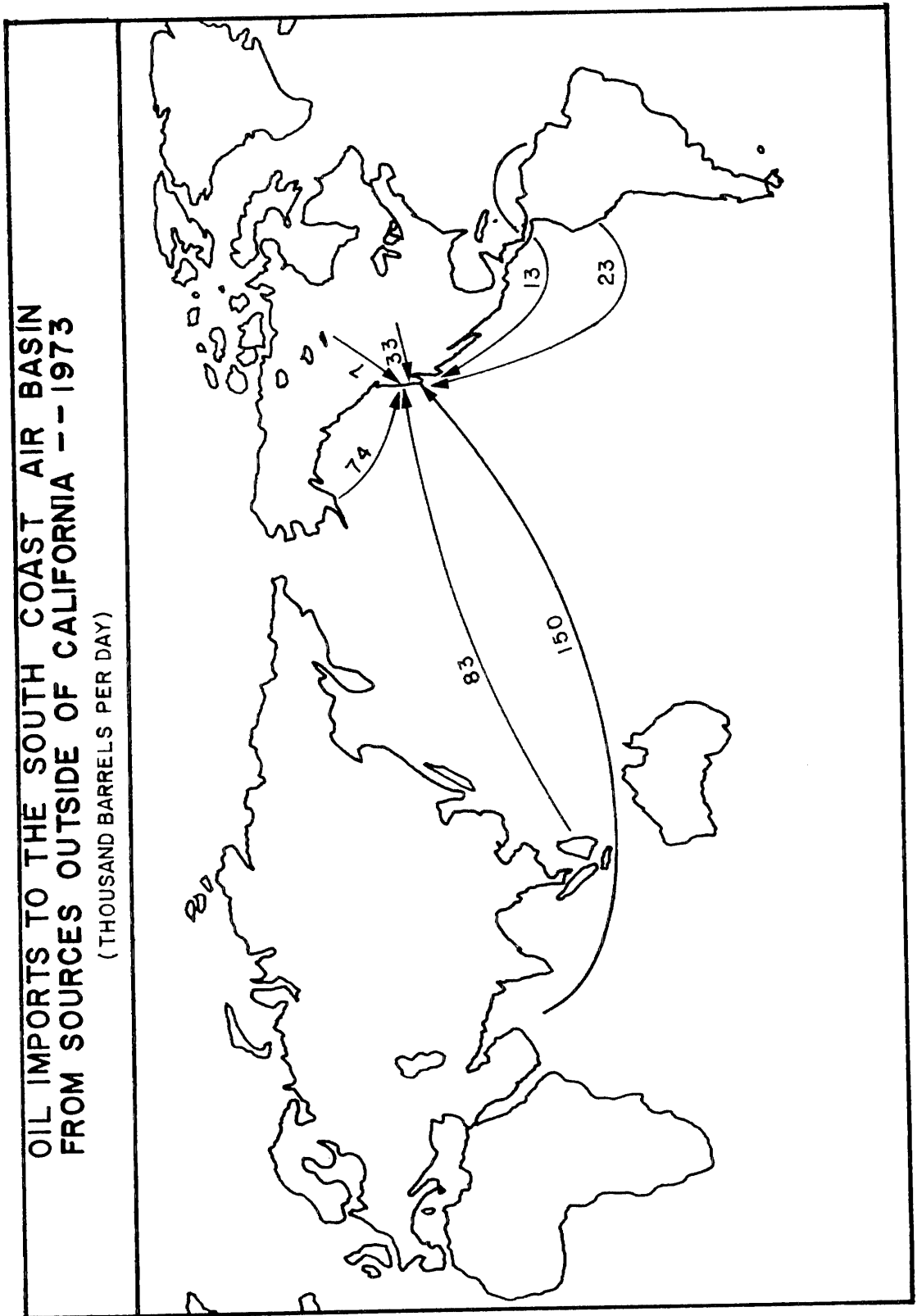


FIGURE 4.4

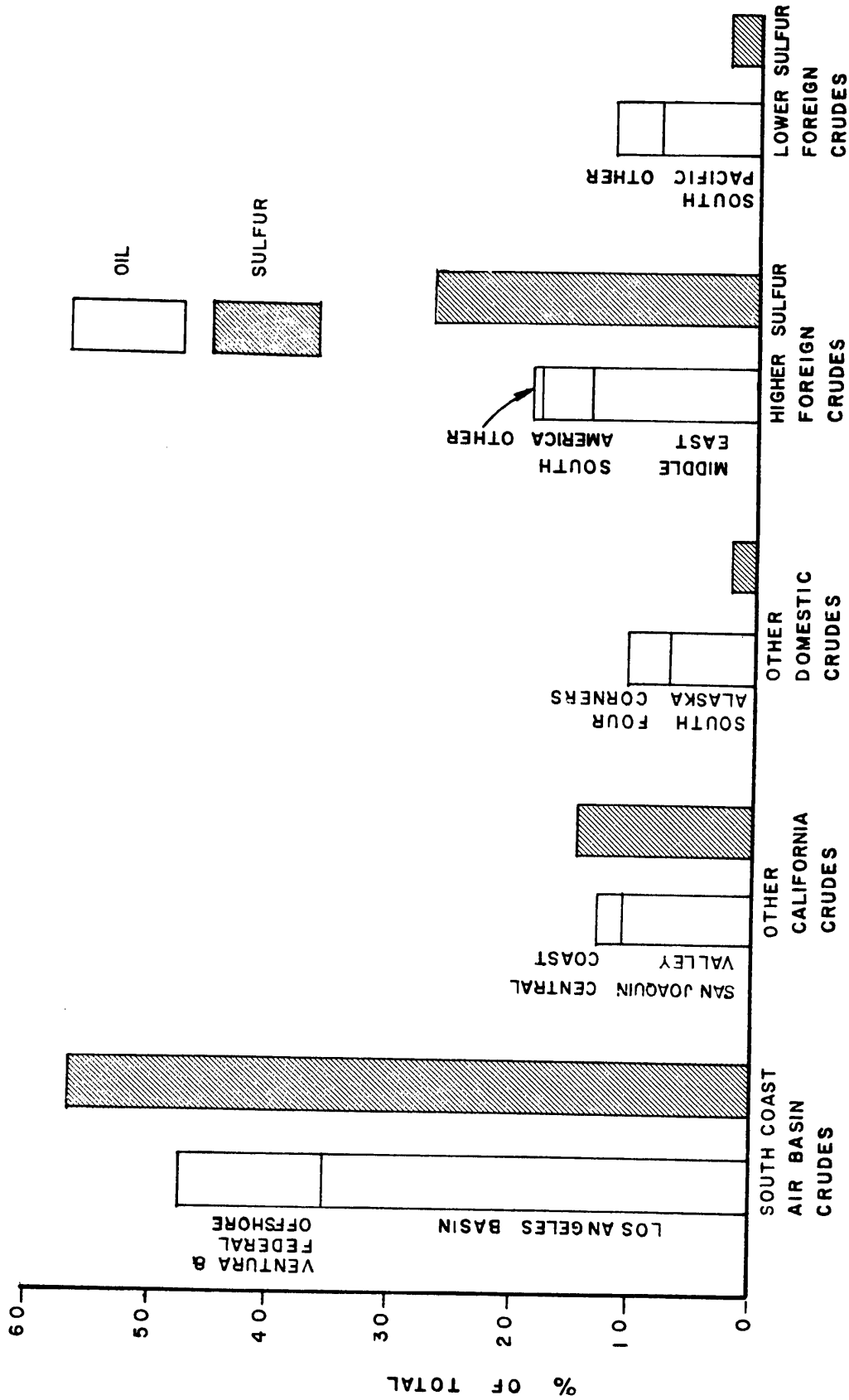


FIGURE 4.5

The Fraction of Crude Oil and Sulfur Received in the South Coast Air Basin from Various Producing Regions of the World - 1973.

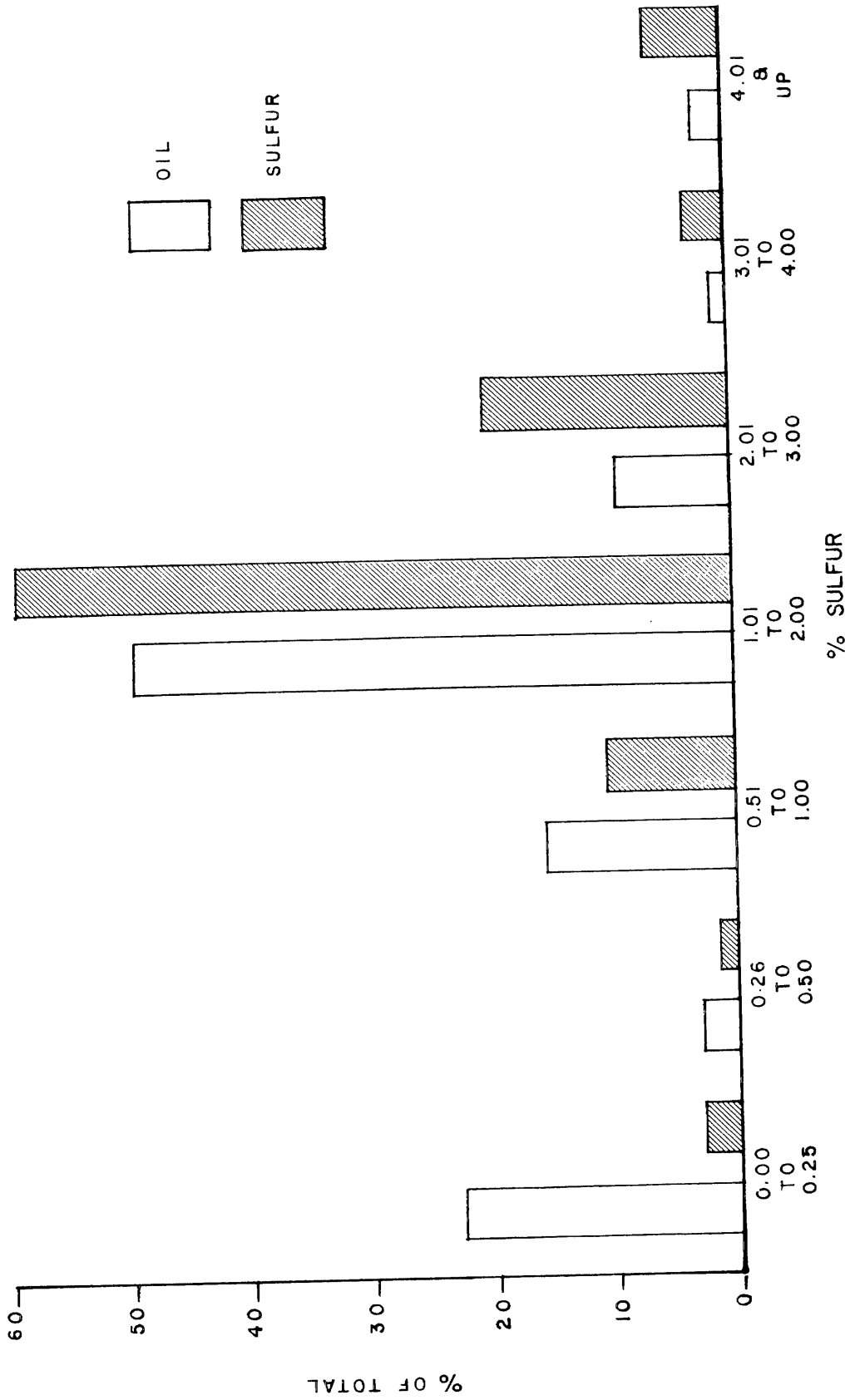


FIGURE 4.6

The Distribution of Crude Oils by Sulfur Content Received in the South Coast Air Basin in 1973.

problems facing Los Angeles area refineries. In the lowest sulfur category ( $< 0.25\%$  S), 22% of the total oil contributes only 2% to the total sulfur burden on basin oil refineries, while in the 2.01% and higher sulfur categories, 12% of the total oil contributes 28.5% of the sulfur. Even so, the major portion of sulfur supply to the air basin comes from the 1.01 to 2.00% sulfur category where 49% of the total oil contributes 59% of the total sulfur. That 1.01% to 2.00% sulfur category is dominated by local crude oils produced in the Los Angeles and Ventura oil fields. One cannot easily divert this source of supply to other ports because the supply is already landed ashore. Substantial alteration of transfer and storage facilities would be needed if that oil were to be sold elsewhere. Thus, locally produced crude oil would be difficult to displace by importation of alternate low-sulfur oils. The South Coast Air Basin is apparently saddled with a sulfur management problem that is not likely to be exported elsewhere as long as local crude oils are processed in local refineries.

If converted completely into sulfur oxides air pollutant emissions, 3551 to 3821 thousand pounds of sulfur entering local refineries daily in feedstocks would result in 3551 to 3821 tons per day of  $\text{SO}_x$  emissions (stated as  $\text{SO}_2$ ). Actual atmospheric emissions within the South Coast Air Basin are thought to be far less than that, as explained in the following sections of this study.

#### 4.3 A Spatially Resolved Sulfur Oxides Emission Inventory: 1972 Through 1974

In Figure 4.7, a square area 50 miles on each edge is shown superimposed over the central portion of the South Coast Air Basin. That square has been subdivided into a system of grid cells with a two mile spacing between adjacent cell boundaries. This grid system is suitable for use in displaying sulfate air quality model results since it substantially covers those areas of the air basin for which extensive air quality data are available for model validation. For historic reasons, the grid system is also convenient for compiling and displaying a detailed sulfur oxides source emission inventory. Each two mile by two mile grid cell corresponds to a combination of four one square mile areas used by the Southern California APCD to identify point source locations. Secondly, this grid system closely matches that used by Roth, et al. (1974) to display baseline traffic counts for Los Angeles for the year 1969 which are widely used by other air quality modeling groups. An attempt will be made here to develop inventory information which may assist the on-going efforts of these other investigators. The grid system employed does not cover the outlying areas of the airshed. An air quality model constructed to use this inventory should thus be capable of handling the few major off-grid sources that will be detailed later in this report.

##### 4.3.1 Emission Inventory Methods and Approach

Appendix A2 describes the assembly of an inventory of sulfur oxides emissions for the central portion of the South Coast Air Basin.

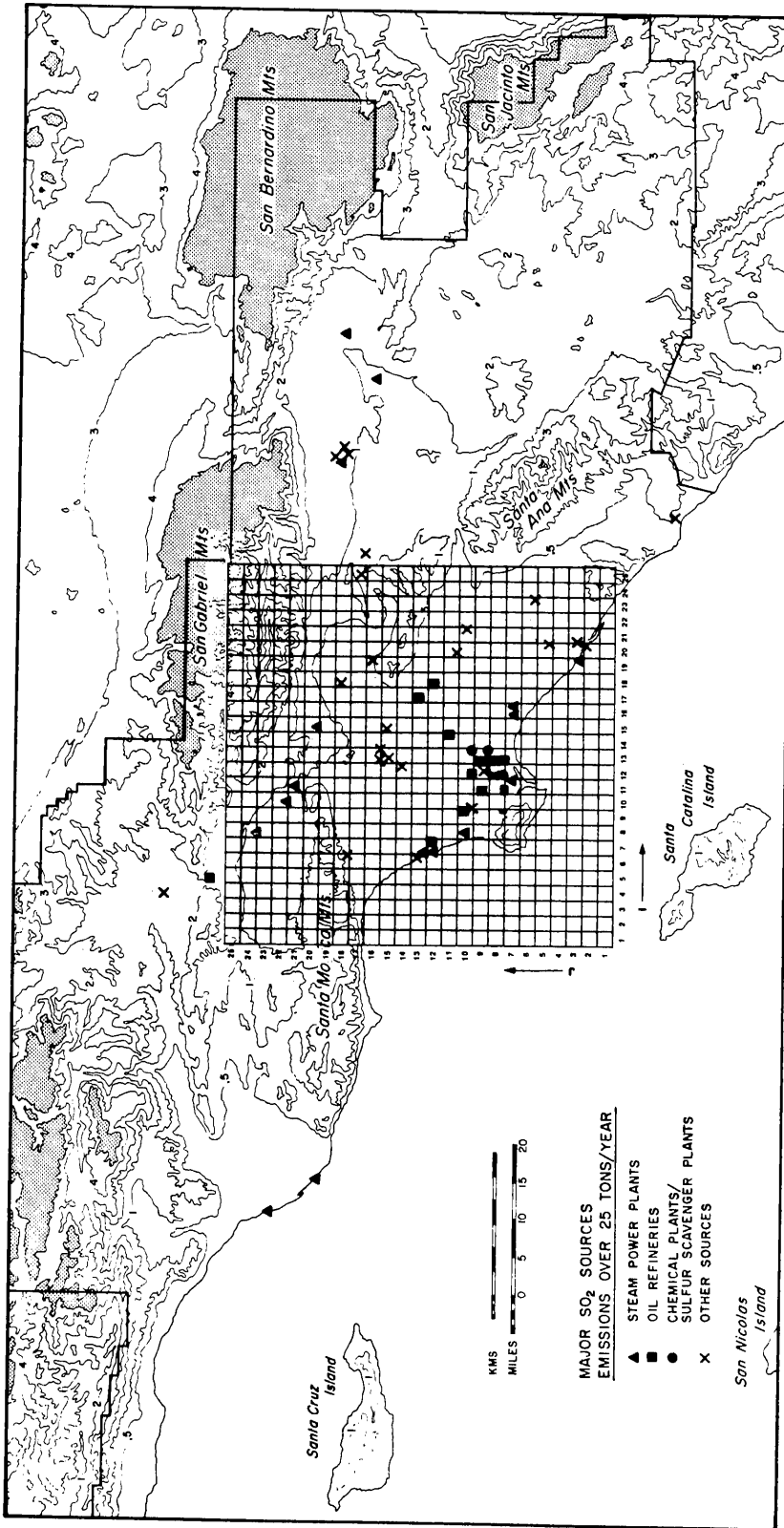


FIGURE 4.7  
The Central Portion of the South Coast Air Basin  
Showing the Grid System Used

Estimates were made of the emissions from over two thousand five hundred stationary sources and from seven classes of mobile sources for each month of the years 1972 through 1974. A general description of the approach used in assembling this inventory will be given here. Appendix A2 should be consulted for a detailed description of the emission estimation procedure for each source type.

Los Angeles Air Pollution Control District (1975) historical emission summaries were reviewed to obtain an idea of the relative magnitude of various classes of emission sources. The inventory was subdivided into mobile and stationary source categories, and the stationary sources were approached first. Los Angeles APCD permit files were consulted, and an APCD computerized data listing entitled "Emissions by ID Number" was selected for initial study. From this data base (hereafter referred to as the permit file) the location, ownership, equipment type and permit file emissions estimates were obtained for 2003 stationary source equipment items in Los Angeles County. Data on all equipment items listed as current sulfur oxides emitters were copied, as well as data on all boilers and all miscellaneous  $\text{NO}_x$  emissions sources at premises with  $\text{NO}_x$  emissions of greater than 50 pounds per week. Boilers and other  $\text{NO}_x$  emission sources were considered as *potential*  $\text{SO}_x$  emission sources in the event that their natural gas supply was curtailed.

While emission data were thus acquired for a large number of sources, it was quickly determined by conversation with APCD staff members that much of this permit file emission data was out-dated or

reflected source operation on only one type of fuel while fuel switching from oil to gas was known to be practiced on a seasonal basis. The permit file emission inventory is thus best suited to serve as an equipment list around which better emissions estimates might be organized.

The equipment list was therefore subdivided into fuel burning equipment, industrial process equipment, and incinerators. The permit file emissions data for fuel burning sources were discarded, and month by month emissions from fuel burning sources were estimated from actual fuel use data available for electric utilities, oil refineries, major industries and small natural gas users, as described in detail in Appendix A2. In the course of that investigation, several hundred additional fuel burning sources were located and added to the inventory.

Next, items of industrial process equipment emitting over one hundred pounds of  $SO_x$  per week were isolated, and APCD staff engineers responsible for overseeing those sources were interviewed. As a result of this interview procedure, additional emission sources were located that were not yet a part of the computerized permit files, and better estimates were made of emissions from chemical plants, oil refineries, coke calcining kilns, glass furnaces and secondary lead smelters.

With the core of the stationary source emission data established, survey efforts were expanded beyond Los Angeles County. The source survey and staff interview procedures were repeated at the offices of the Southern California APCD-Southern Zone (formerly the Orange County

APCD). Fuel burning data on power plants located outside of Los Angeles County were acquired from the Southern California Edison Company. Major off-grid sources in San Bernardino and Riverside Counties were reviewed with the help of Southern California APCD staff. The operators of some emissions sources were contacted in order to firm-up data needed to make emission estimates.

Shortly after these emissions data from stationary sources were compiled, a detailed stationary source  $SO_x$  emission inventory prepared independently by Hunter and Helgeson (1976) became available for 1974, one of our three years of interest. The two inventories were cross-checked for the year in which they overlap, with generally excellent agreement. Additions and corrections were made to our inventory to reflect certain cases in which Hunter and Helgeson's source test data were thought to present a more recent picture of source operation than was otherwise available. In most cases, however, the time sequence of emissions estimated from our fuel burning records and discussion with APCD staff were retained since they represented a longer historic period of observation, and were usually quite close to Hunter and Helgeson's estimates for the year in which both inventories overlap. Hunter and Helgeson's data for the fraction of each source's emissions evolved as  $SO_3$  were adopted to supplement the APCD data base.

Finally, mobile source emissions categories for autos and light trucks, heavy duty vehicles, ships, railroads and aircraft were established. Freeway traffic counts were performed for each year of the three year period 1972 through 1974. A surface street traffic

growth survey was used to update existing 1969 surface street traffic data to the years of interest. Then the traffic count data were used to estimate motor vehicle  $SO_x$  emissions for freeways and for surface streets on a spatially resolved basis. Shipping activities and railroad track mileage were assigned geographically to the grid system. Then fuel use by ships and railroads was scaled down to the grid system from the basin-wide fuel use data developed in the Energy and Sulfur Balance portion of this report (see Appendix A3). Aircraft emissions were estimated on the basis of the number of take-off and landing operations at each airport and military air base within our grid system.

#### 4.3.2 Emission Inventory Summary and Discussion

Figure 4.8 summarizes sulfur oxides emissions within the 50 by 50 mile square for the years 1972 through 1974. The general source classes shown have been arranged to correspond to the traditional classification system of the Los Angeles Air Pollution Control District so that the reader may compare these results to historic emission trends given in Table 4.3. Historic data in Table 4.3 are available only for Los Angeles County, while the 50 by 50 mile grid covers the populated portions of both Los Angeles and Orange Counties. As will be seen, however, most major industrial emissions sources are confined to Los Angeles County.

From Figure 4.8, we note that the majority of sulfur oxides emissions arise from combustion-related sources, both stationary and mobile. Electric utility fuel combustion was the largest single  $SO_x$

SULFUR OXIDES EMISSIONS WITHIN THE 50 BY 50 MILE SQUARE

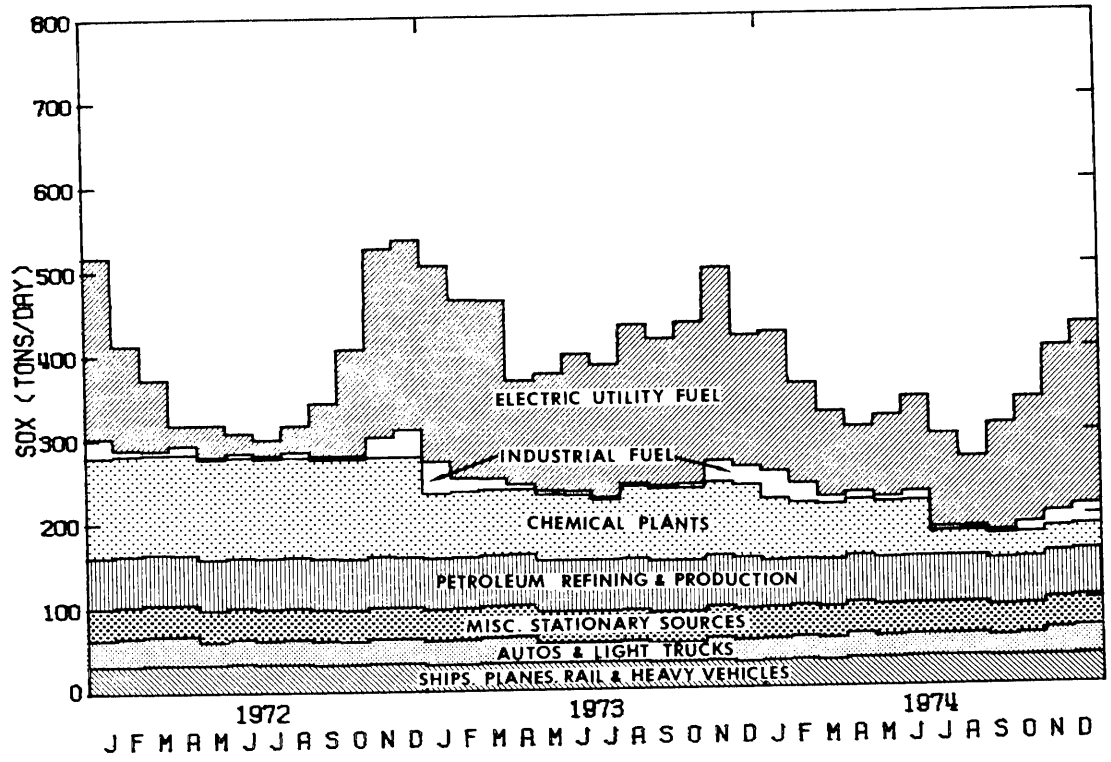


FIGURE 4.8

TABLE 4.3  
Emissions of Sulfur Dioxide  
in Los Angeles County  
(tons per average day)

Year	Steam Power Plants	Combustion of Fuels From Other Stationary Sources	Chemical Plants (a)	Petroleum Refining Producing and Marketing (b)	Misc. Sources	Gasoline Powered Vehicles	Aircraft, Ships, Railroads & Diesel Powered Vehicles	Total
1955	182(47) <sup>(c)</sup>	277	47	179	17	36	1	739
1956	187(47)					35		
1957	240(43)	150	46	50		35	14	545
1958	122(66)	183	47	50	1	35	15	453
1959	150(63)					30		
1960	153(65)	45	51	40	1	25	2	317
1961	132(71)	44	52	36	1	25	2	292
1962	120(75)					26		
1963	108(78)					25		
1964	116(77)	21	65	45	3	24	2	276
1965	136(76)					23		
1966	180(76)	33	65	35	3	25	2	343
1967	138(83)					26		
1968	90(83)	8	90	55	4	26	5	278
1969	57(79)					27		
1970	42(77)	11	116	49	7	27	5	257
1971	76(60)					28		
1972	83(58)					29		
1973	161(30)	14	60	55	30	30	15	365
1974	115(31)	15	20	60	20	30	15	275

(a) Includes emissions from sulfur recovery plants and sulfuric acid plants.

(b) Includes only those emissions from refining, producing and marketing operations. Does not include emissions from the combustion of fuels, i.e., from fired heaters, boilers, etc.

(c) Parentheses indicate percent level of service of natural gas.

Source: Los Angeles Air Pollution Control District (1975)

emission source category during 1974. This represents a substantial change since 1972 when sulfur recovery and sulfuric acid plants in the chemical plant category constituted the largest group of  $SO_x$  sources on an annual average basis. This shift in relative source contributions is attributed mainly to the installation of tail gas clean-up equipment at Los Angeles County chemical plants, combined with increased oil burning at power plants due to natural gas curtailment.

A second major shift in relative source contributions is seen to be seasonal in nature. Power plants historically have emitted greater quantities of  $SO_x$  during the winter months. From Figure 4.8 one might quickly assume that electricity demand is vastly higher in the winter months than in the summer, but that conclusion would be wrong. Energy use within the 50 by 50 mile square grid is detailed in Figure 4.9 from information gathered while compiling Appendices A2 and A3 to this study. Total monthly electricity use within that study area is fairly constant throughout the year. Instead, what has happened is that residential, commercial and light industrial demands for fossil fuel rise sharply during the winter. These customers have a higher priority for receiving "firm" service from the relatively fixed supply of natural gas available throughout the year than do the basin's electric utilities. The result is that the gas supply to utilities and large industries has been curtailed during winter months. The wintertime increase in  $SO_x$  emissions is due to substitution of sulfur-bearing fuel oil for natural gas by these curtailed gas customers. These major shifts in source emission strength from month to month will

ENERGY USE WITHIN THE 50 BY 50 MILE SQUARE

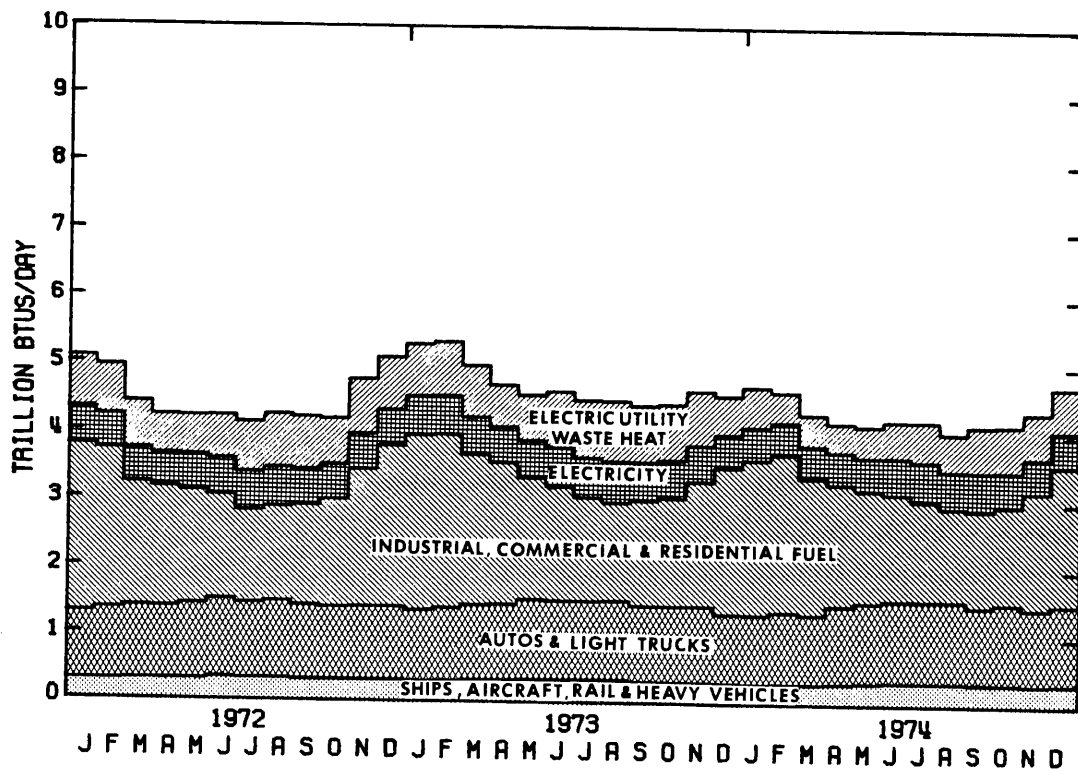


FIGURE 4.9

provide a tough test for any air quality model validation effort. This is particularly true for a sulfate air quality modeling study since sulfate concentration seasonal trends tend to buck the  $\text{SO}_x$  emissions history shown here: Los Angeles sulfate concentrations generally peak in the summer months (for example, see Chapter 2).

It would be tempting to refer to these emission patterns as winter emissions and summer emissions, respectively. That may be misleading however, since only the availability of natural gas during the summer has prevented the higher emission pattern from appearing in the summer season. In fact, as can be seen in Figure 4.8, total  $\text{SO}_x$  emissions for August 1973 were as high as any period of the winter 1973-74. By the year 1979 or 1980, natural gas supplies to electric utilities and large industries in Southern California are expected to be completely curtailed in all months of the year (1975 California Gas Report). The implication is that, in the absence of changes in 1974 emission control regulations, the summertime trough in electric utility  $\text{SO}_x$  emissions would be "filled-in" to about the level of past winter emissions peaks.  $\text{SO}_x$  emissions from industrial fuel burning would rise substantially.

Tables 4.4 through 4.6 show the monthly emissions history for individual source and equipment types within the general source categories of Figure 4.8. The emission inventory created for air quality model use contains spatially resolved source strength data defined on the 50 by 50 mile grid for each of the 26 source types shown in Tables 4.4 through 4.6 for each month of the years 1972

TABLE 4.4a

1972 Sulfur Oxides Emissions Within the 50 by 50 Mile Square Grid  
(in short tons per day as SO<sub>2</sub>)

STATIONARY SOURCES	JAN	FEB	MAR	APR	MAY	JUN	JUL	AUG	SEP	OCT	NOV	DEC	ANNUAL
<b>Fuel Combustion</b>													
Electric Utilities	214.86	123.46	83.56	23.90	38.33	23.98	18.54	32.22	62.40	126.81	223.96	225.17	99.81
Refinery Fuel	17.69	5.78	3.66	9.55	2.50	3.62	3.42	5.86	3.38	3.85	20.95	19.69	8.33
Other Interruptible Gas Customers	5.56	1.37	0.61	0.75	0.64	0.67	0.39	0.63	0.51	0.59	2.74	13.29	2.33
Firm Gas Customers	0.46	0.43	0.29	0.27	0.24	0.20	0.17	0.15	0.16	0.18	0.30	0.40	0.27
<b>Chemical Plants</b>													
Sulfur Recovery	93.53	93.53	93.53	93.53	93.53	93.53	93.53	93.53	93.53	93.53	93.53	93.53	93.53
Sulfuric Acid	25.00	25.00	25.00	25.00	25.00	25.00	25.00	25.00	25.00	25.00	25.00	25.00	25.00
Other Chemicals	0.09	0.09	0.09	0.09	0.09	0.09	0.09	0.09	0.09	0.09	0.09	0.09	0.09
<b>Petroleum Refining and Production</b>													
Fluid Catalytic Crackers	52.07	52.07	52.07	52.07	52.07	52.07	52.07	52.07	52.07	52.07	52.07	52.07	52.07
Sour Water Strippers	0.13	0.13	0.13	0.13	0.13	0.13	0.13	0.13	0.13	0.13	0.13	0.13	0.13
Delayed Cokers	2.28	2.28	2.28	2.28	2.28	2.28	2.28	2.28	2.28	2.28	2.28	2.28	2.28
Misc. Refinery Process	1.02	1.02	1.02	1.02	1.02	1.02	1.02	1.02	1.02	1.02	1.02	1.02	1.02
Oil Field Production	4.00	4.00	4.00	4.00	4.00	4.00	4.00	4.00	4.00	4.00	4.00	4.00	4.00
<b>Misc. Stationary Sources</b>													
Petroleum Coke Kilns	25.52	25.52	25.52	25.52	25.52	25.52	25.52	25.52	25.52	25.52	25.52	25.52	25.52
Glass Furnaces	2.00	2.00	2.00	2.00	2.00	2.00	2.00	2.00	2.00	2.00	2.00	2.00	2.00
Metals Industries	8.78	8.78	8.78	8.78	8.78	8.78	8.78	8.78	8.78	8.78	8.78	8.78	8.78
Mineral Products	0.00	0.00	0.00	0.00	0.00	0.00	0.00	0.00	0.00	0.00	0.00	0.00	0.00
Sewage Treatment Digesters	0.64	0.64	0.64	0.64	0.64	0.64	0.64	0.64	0.64	0.64	0.64	0.64	0.64
Other Industrial Processes	0.02	0.02	0.02	0.02	0.02	0.02	0.02	0.02	0.02	0.02	0.02	0.02	0.02
Permitted Incinerators	0.07	0.07	0.07	0.07	0.07	0.07	0.07	0.07	0.07	0.07	0.07	0.07	0.07
<b>MOBILE SOURCES</b>													
Autos and Lt. Trucks-Surface	19.43	20.25	21.14	20.98	17.04	18.00	17.27	17.81	16.97	16.70	18.07	17.93	18.46
Autos and Lt. Trucks-Freeway	12.21	12.72	13.28	13.18	10.70	11.31	10.85	11.91	10.66	10.49	11.35	11.26	11.60
Heavy Duty Vehicles-Surface	9.71	10.14	10.44	10.35	10.29	10.85	10.40	10.68	10.17	10.00	10.25	10.20	10.29
Heavy Duty Vehicles-Freeway	6.10	6.37	6.56	6.50	6.46	6.81	6.53	6.71	6.39	6.28	6.44	6.41	6.46
Airport Operations	1.15	1.15	1.15	1.15	1.15	1.15	1.15	1.15	1.15	1.15	1.15	1.15	1.15
Shipping Operations	11.89	11.89	11.89	11.89	11.89	11.89	11.89	11.89	11.89	11.89	11.89	11.89	11.89
Railroad Operations	3.39	3.39	3.39	3.39	3.39	3.39	3.39	3.39	3.39	3.39	3.39	3.39	3.39
<b>TOTAL</b>	517.60	412.10	371.12	317.06	317.78	307.02	299.15	317.55	342.22	406.48	525.64	535.93	389.13

TABLE 4.4b

Major Off-Grid Emission Sources Included within the 1972 South Coast Air Basin Sulfur Oxides Modeling Inventory  
(in short tons per day as SO<sub>2</sub>)

STATIONARY SOURCES	JAN	FEB	MAR	APR	MAY	JUN	JUL	AUG	SEP	OCT	NOV	DEC	ANNUAL
Fuel Combustion	55.74	24.32	16.79	6.75	9.99	6.01	9.52	10.52	19.56	29.19	58.04	63.68	25.89
Electric Utilities	---	---	---	---	---	---	---	---	---	---	---	---	---
Refinery Fuel	---	---	---	---	---	---	---	---	---	---	---	---	---
Other Interruptible Gas Customers	---	---	---	---	---	---	---	---	---	---	---	---	---
Firm Gas Customers	---	---	---	---	---	---	---	---	---	---	---	---	---
Chemical Plants	---	---	---	---	---	---	---	---	---	---	---	---	---
Sulfur Recovery	---	---	---	---	---	---	---	---	---	---	---	---	---
Sulfuric Acid	---	---	---	---	---	---	---	---	---	---	---	---	---
Other Chemicals	---	---	---	---	---	---	---	---	---	---	---	---	---
Petroleum Refining and Production	---	---	---	---	---	---	---	---	---	---	---	---	---
Fluid Catalytic Crackers	---	---	---	---	---	---	---	---	---	---	---	---	---
Sour Water Strippers	---	---	---	---	---	---	---	---	---	---	---	---	---
Delayed Cokers	---	---	---	---	---	---	---	---	---	---	---	---	---
Misc. Refinery Processes	---	---	---	---	---	---	---	---	---	---	---	---	---
Oil Field Production	---	---	---	---	---	---	---	---	---	---	---	---	---
Misc. Stationary Sources	---	---	---	---	---	---	---	---	---	---	---	---	---
Petroleum Coke Kilns	---	---	---	---	---	---	---	---	---	---	---	---	---
Glass Furnaces	0.23	0.23	0.23	0.23	0.23	0.23	0.23	0.23	0.23	0.23	0.23	0.23	0.23
Metals Industries	35.20	35.20	35.20	35.20	35.20	35.20	35.20	35.20	35.20	35.20	35.20	35.20	35.20
Mineral Products	2.30	2.30	2.30	2.30	2.30	2.30	2.30	2.30	2.30	2.30	2.30	2.30	2.30
Sewage Treatment Digesters	---	---	---	---	---	---	---	---	---	---	---	---	---
Other Industrial Processes	---	---	---	---	---	---	---	---	---	---	---	---	---
Permitted Incinerators	---	---	---	---	---	---	---	---	---	---	---	---	---
TOTAL	93.47	62.05	54.52	44.48	47.72	43.74	47.25	48.25	57.29	66.92	95.77	101.41	63.62

TABLE 4.5a  
1973 Sulfur Oxides Emissions Within the 50 by 50 Mile Square Grid  
(in short tons per day as SO<sub>2</sub>)

STATIONARY SOURCES	JAN	FEB	MAR	APR	MAY	JUN	JUL	AUG	SEP	OCT	NOV	DEC	ANNUAL
Fuel Combustion													
Electric Utilities	232.77	212.31	212.13	123.36	139.48	163.87	157.77	189.23	174.16	192.05	229.72	155.48	181.71
Refinery Fuel	25.07	13.50	10.61	4.26	3.99	3.73	2.91	2.14	2.37	4.01	21.69	18.96	9.42
Other Interruptible Gas Customers	12.78	2.24	2.07	0.98	0.81	0.39	0.39	0.40	0.43	0.76	3.58	2.57	2.29
Firm Gas Customers	0.46	0.46	0.37	0.33	0.26	0.21	0.17	0.16	0.19	0.20	0.26	0.36	0.29
Chemical Plants													
Sulfur Recovery	57.18	57.18	57.18	57.18	57.08	57.08	50.70	66.20	66.20	66.20	66.20	66.20	60.40
Sulfuric Acid	20.00	20.00	20.00	20.00	20.00	20.00	20.00	20.00	20.00	20.00	20.00	20.00	20.00
Other Chemicals	0.09	0.09	0.09	0.09	0.09	0.09	0.09	0.09	0.09	0.09	0.09	0.09	0.09
Petroleum Refining and Production													
Fluid Catalytic Crackers	52.07	52.07	52.07	52.07	52.07	52.07	52.07	52.07	52.07	52.07	52.07	52.07	52.07
Sour Water Strippers	0.13	0.13	0.13	0.13	0.13	0.13	0.13	0.13	0.13	0.13	0.13	0.13	0.13
Delayed Cokers	2.28	2.28	2.28	2.28	2.28	2.28	2.28	2.28	2.28	2.28	2.28	2.28	2.28
Misc. Refinery Process	1.02	1.02	1.02	1.02	1.02	1.02	1.02	1.02	1.02	1.02	1.02	1.02	1.02
Oil Field Production	4.50	4.50	4.50	4.50	4.50	4.50	4.50	4.50	4.50	4.50	4.50	4.50	4.50
Misc. Stationary Sources													
Petroleum Coke Kilns	25.52	25.52	25.52	25.52	25.52	25.52	25.52	25.52	25.52	25.52	25.52	25.52	25.52
Glass Furnaces	2.00	2.00	2.00	2.00	2.00	2.00	2.00	2.00	2.00	2.00	2.00	2.00	2.00
Metals Industries	8.78	8.78	8.78	8.78	8.78	8.78	8.78	8.78	8.78	8.78	8.78	8.78	8.78
Mineral Products	0.00	0.00	0.00	0.00	0.00	0.00	0.00	0.00	0.00	0.00	0.00	0.00	0.00
Sewage Treatment Digesters	0.64	0.64	0.64	0.64	0.64	0.64	0.64	0.64	0.64	0.64	0.64	0.64	0.64
Other Industrial Processes	0.02	0.02	0.02	0.02	0.02	0.02	0.02	0.02	0.02	0.02	0.02	0.02	0.02
Permitted Incinerators	0.07	0.07	0.07	0.07	0.07	0.07	0.07	0.07	0.07	0.07	0.07	0.07	0.07
MOBILE SOURCES													
Autos and Lt. Trucks-Surface	17.17	17.75	18.56	18.76	14.27	14.15	14.05	14.36	13.51	13.51	16.95	15.70	15.71
Autos and Lt. Trucks-Freeway	10.98	11.35	11.87	12.01	9.13	9.05	8.99	9.19	8.64	8.64	10.85	10.05	10.05
Heavy Duty Vehicles-Surface	10.18	10.50	10.94	11.05	10.99	10.88	10.80	10.99	10.35	10.34	10.71	9.90	10.64
Heavy Duty Vehicles-Freeway	6.51	6.72	7.00	7.07	7.03	6.96	6.91	7.03	6.62	6.61	6.85	6.33	6.80
Airport Operations	1.06	1.06	1.06	1.06	1.06	1.06	1.06	1.06	1.06	1.06	1.06	1.06	1.06
Shipping Operations	10.13	10.13	10.13	10.13	10.13	10.13	10.13	10.13	10.13	10.13	10.13	10.13	10.13
Railroad Operations	3.32	3.32	3.32	3.32	3.32	3.32	3.32	3.32	3.32	3.32	3.32	3.32	3.32
TOTAL	504.73	463.64	462.36	366.63	374.67	397.95	384.27	431.33	414.10	433.95	498.44	417.18	428.94

TABLE 4.5b

STATIONARY SOURCES	Major Off-Grid Emission Sources Included within the 1973 South Coast Air Basin Sulfur Oxides Modeling Inventory (in short tons per day as SO <sub>2</sub> )												ANNUAL
	JAN	FEB	MAR	APR	MAY	JUN	JUL	AUG	SEP	OCT	NOV	DEC	
Fuel Combustion	60.19	45.46	57.94	39.18	53.62	64.68	54.07	58.97	45.38	59.69	91.75	66.46	58.20
Electric Utilities	---	---	---	---	---	---	---	---	---	---	---	---	---
Refinery Fuel	---	---	---	---	---	---	---	---	---	---	---	---	---
Other Interruptible Gas Customers	---	---	---	---	---	---	---	---	---	---	---	---	---
Firm Gas Customers	---	---	---	---	---	---	---	---	---	---	---	---	---
Chemical Plants	---	---	---	---	---	---	---	---	---	---	---	---	---
Sulfur Recovery	---	---	---	---	---	---	---	---	---	---	---	---	---
Sulfuric Acid	---	---	---	---	---	---	---	---	---	---	---	---	---
Other Chemicals	---	---	---	---	---	---	---	---	---	---	---	---	---
Petroleum Refining and Production	---	---	---	---	---	---	---	---	---	---	---	---	---
Fluid Catalytic Crackers	---	---	---	---	---	---	---	---	---	---	---	---	---
Sour Water Strippers	---	---	---	---	---	---	---	---	---	---	---	---	---
Delayed Cokers	---	---	---	---	---	---	---	---	---	---	---	---	---
Misc. Refinery Processes	---	---	---	---	---	---	---	---	---	---	---	---	---
Oil Field Production	---	---	---	---	---	---	---	---	---	---	---	---	---
Misc. Stationary Sources	---	---	---	---	---	---	---	---	---	---	---	---	---
Petroleum Coke Kilns	0.23	0.23	0.23	0.23	0.23	0.23	0.23	0.23	0.23	0.23	0.23	0.23	0.23
Glass Furnaces	41.46	41.46	41.46	41.46	41.46	41.46	41.46	41.46	41.46	41.46	41.46	41.46	41.46
Metals Industries	1.90	1.90	1.90	1.90	1.90	1.90	1.90	1.90	1.90	1.90	1.90	1.90	1.90
Mineral Products	---	---	---	---	---	---	---	---	---	---	---	---	---
Sewage Treatment Digesters	---	---	---	---	---	---	---	---	---	---	---	---	---
Other Industrial Processes	---	---	---	---	---	---	---	---	---	---	---	---	---
Permitted Incinerators	---	---	---	---	---	---	---	---	---	---	---	---	---
TOTAL	103.78	89.05	101.53	82.77	97.21	108.27	97.66	102.56	88.97	103.28	135.34	110.05	101.79

TABLE 4.6a

1974 Sulfur Oxides Emissions Within the 50 by 50 Mile Square Grid  
(in short tons per day as SO<sub>2</sub>)

STATIONARY SOURCES	JAN	FEB	MAR	APR	MAY	JUN	JUL	AUG	SEP	OCT	NOV	DEC	ANNUAL
<b>Fuel Combustion</b>													
Electric Utilities	166.24	119.19	101.05	77.73	97.16	113.19	111.03	84.23	127.98	148.83	197.60	215.11	130.04
Refinery Fuel	23.69	20.91	7.61	7.59	5.18	9.27	4.35	3.22	3.78	10.44	15.53	20.32	10.93
Other Interruptible Gas													
Customers	8.30	1.61	0.94	0.71	0.69	1.05	0.64	0.59	0.54	1.12	2.04	3.72	1.84
Firm Gas Customers	0.41	0.41	0.35	0.27	0.23	0.21	0.17	0.15	0.16	0.17	0.25	0.35	0.26
<b>Chemical Plants</b>													
Sulfur Recovery	63.22	63.22	63.22	63.22	63.22	63.22	25.84	25.84	25.84	25.84	25.84	25.84	44.37
Sulfuric Acid	10.20	3.12	3.12	3.12	3.12	3.12	3.12	3.12	3.12	3.12	3.12	3.12	3.72
Other Chemicals	0.09	0.09	0.09	0.09	0.09	0.09	0.09	0.09	0.09	0.09	0.09	0.09	0.09
<b>Petroleum Refining and Production</b>													
Fluid Catalytic Crackers	45.48	45.48	45.48	45.48	45.48	45.48	45.48	45.48	45.48	45.48	45.48	45.48	45.48
Sour Water Strippers	1.03	1.03	1.03	1.03	1.03	1.03	1.03	1.03	1.03	1.03	1.03	1.03	1.03
Delayed Cokers	2.28	2.28	2.28	2.28	2.28	2.28	2.28	2.28	2.28	2.28	2.28	2.28	2.28
Misc. Refinery Processes	0.86	0.86	0.86	0.86	0.86	0.86	0.86	0.86	0.86	0.86	0.86	0.86	0.86
Oil Field Production	5.17	5.17	5.17	5.17	5.17	5.17	5.17	5.17	5.17	5.17	5.17	5.17	5.17
<b>Misc. Stationary Sources</b>													
Petroleum Coke Kilns	25.52	25.52	25.52	25.52	25.52	25.52	25.52	25.52	25.52	25.52	25.52	25.52	25.52
Glass Furnaces	2.00	2.00	2.00	2.00	2.00	2.00	2.00	2.00	2.00	2.00	2.00	2.00	2.00
Metals Industries	8.76	8.76	8.76	8.76	8.76	8.76	8.76	8.76	8.76	8.76	8.76	8.76	8.31
Mineral Products	0.00	0.00	0.00	0.00	0.00	0.00	0.00	0.00	0.00	0.00	0.00	0.00	0.00
Sewage Treatment Digesters	0.64	0.64	0.64	0.64	0.64	0.64	0.64	0.64	0.64	0.64	0.64	0.64	0.64
Other Industrial Processes	0.02	0.02	0.02	0.02	0.02	0.02	0.02	0.02	0.02	0.02	0.02	0.02	0.02
Permitted Incinerators	0.07	0.07	0.07	0.07	0.07	0.07	0.07	0.07	0.07	0.07	0.07	0.07	0.07
<b>MOBILE SOURCES</b>													
Autos and Lt. Trucks-Surface	15.84	16.84	15.88	17.71	15.63	15.94	16.00	15.86	15.02	15.44	19.65	20.50	16.66
Autos and Lt. Trucks-Freeway	9.88	10.27	9.91	11.05	9.75	9.94	9.98	9.89	9.37	9.63	12.26	12.79	10.39
Heavy Duty Vehicles-Surface	11.20	11.65	11.25	12.49	12.65	12.95	13.03	12.95	12.27	12.66	12.53	13.11	12.40
Heavy Duty Vehicles-Freeway	6.99	7.27	7.02	7.79	7.89	8.08	8.13	8.08	7.65	7.90	7.81	8.18	7.74
Airport Operations	1.17	1.17	1.17	1.17	1.17	1.17	1.17	1.17	1.17	1.17	1.17	1.17	1.17
Shipping Operations	9.38	9.38	9.38	9.38	9.38	9.38	9.38	9.38	9.38	9.38	9.38	9.38	9.38
Railroad Operations	2.87	2.87	2.87	2.87	2.87	2.87	2.87	2.87	2.87	2.87	2.87	2.87	2.87
<b>TOTAL</b>	421.31	359.83	325.69	307.02	320.86	342.31	297.63	269.27	309.71	339.13	400.61	427.02	343.24

TABLE 4.6b  
 Major Off-Grid Emission Sources Included within the 1974 South Coast Air Basin Sulfur Oxides  
 Modeling Inventory  
 (in short tons per day as SO<sub>2</sub>)

STATIONARY SOURCES	JAN	FEB	MAR	APR	MAY	JUN	JUL	AUG	SEP	OCT	NOV	DEC	ANNUAL
Fuel Combustion													
Electric Utilities	67.54	65.53	39.48	26.51	34.32	47.56	49.39	51.69	51.22	46.91	56.15	68.58	50.34
Refinery Fuel	---	---	---	---	---	---	---	---	---	---	---	---	---
Other Interruptible Gas Customers	---	---	---	---	---	---	---	---	---	---	---	---	---
Firm Gas Customers	---	---	---	---	---	---	---	---	---	---	---	---	---
Chemical Plants													
Sulfur Recovery	---	---	---	---	---	---	---	---	---	---	---	---	---
Sulfuric Acid	---	---	---	---	---	---	---	---	---	---	---	---	---
Other Chemicals	---	---	---	---	---	---	---	---	---	---	---	---	---
Petroleum Refining and Production													
Fluid Catalytic Crackers	---	---	---	---	---	---	---	---	---	---	---	---	---
Sour Water Strippers	---	---	---	---	---	---	---	---	---	---	---	---	---
Delayed Cokers	---	---	---	---	---	---	---	---	---	---	---	---	---
Misc. Refinery Processes	---	---	---	---	---	---	---	---	---	---	---	---	---
Oil Field Production	---	---	---	---	---	---	---	---	---	---	---	---	---
Misc. Stationary Sources													
Petroleum Coke Kilns	---	---	---	---	---	---	---	---	---	---	---	---	---
Glass Furnaces	0.23	0.23	0.23	0.23	0.23	0.23	0.23	0.23	0.23	0.23	0.23	0.23	0.23
Metals Industries	38.12	38.12	38.12	38.12	38.12	38.12	38.12	38.12	38.12	38.12	38.12	38.12	38.12
Mineral Products	1.90	1.90	1.90	1.90	1.90	1.90	1.90	1.90	1.90	1.90	1.90	1.90	1.90
Sewage Treatment Digesters	---	---	---	---	---	---	---	---	---	---	---	---	---
Other Industrial Processes	---	---	---	---	---	---	---	---	---	---	---	---	---
Permitted Incinerators	---	---	---	---	---	---	---	---	---	---	---	---	---
TOTAL	107.79	105.78	79.73	67.76	74.57	87.81	89.64	91.94	91.47	87.16	96.40	108.83	90.59

through 1974. An itemization of large off-grid sources is also included. Details of the emission estimation procedures for each source type and further information on the spatial distribution of emissions from individual source classes are given in Appendix A2.

In order to introduce the emission inventory of Appendix A2 into an air quality model for sulfate formation and dispersion, additional information is needed. One needs to know the fraction of the emissions from each source type which originate as particulate sulfur oxides rather than  $\text{SO}_2$ . The diurnal variation of source emission strength is also important.

Table 4.7 lists a compilation of data on  $f_{\text{SO}}$ , the fraction of total sulfur oxides emissions from various source classes which originate as sulfates or sulfuric acid mist rather than as gaseous  $\text{SO}_2$ . Using these data, a sulfur trioxide or "sulfates" emission inventory can be estimated from Tables 4.4 through 4.6 for each month of the years 1972 through 1974. An example  $\text{SO}_4^-$  inventory for 1973 is presented in Table 4.7. On an emissions-weighted average basis, about 2.7% of the  $\text{SO}_x$  emissions in the basin are evolved directly from their sources as  $\text{SO}_3$  or sulfates. The principal source of direct sulfate or sulfuric acid mist emissions in the basin is seen to be the electric utility industry, followed by petroleum coke calcining kilns, refinery fluid catalytic crackers and an off-grid steel mill.

Daily average emission strength is often modulated by a strong diurnal variation in source utilization patterns. Two of the strongest diurnal source fluctuations affect power plants and motor

TABLE 4.7  
 Particulate Sulfur Oxides as a Fraction  
 of Total SO<sub>x</sub> Emissions from Each Source Class

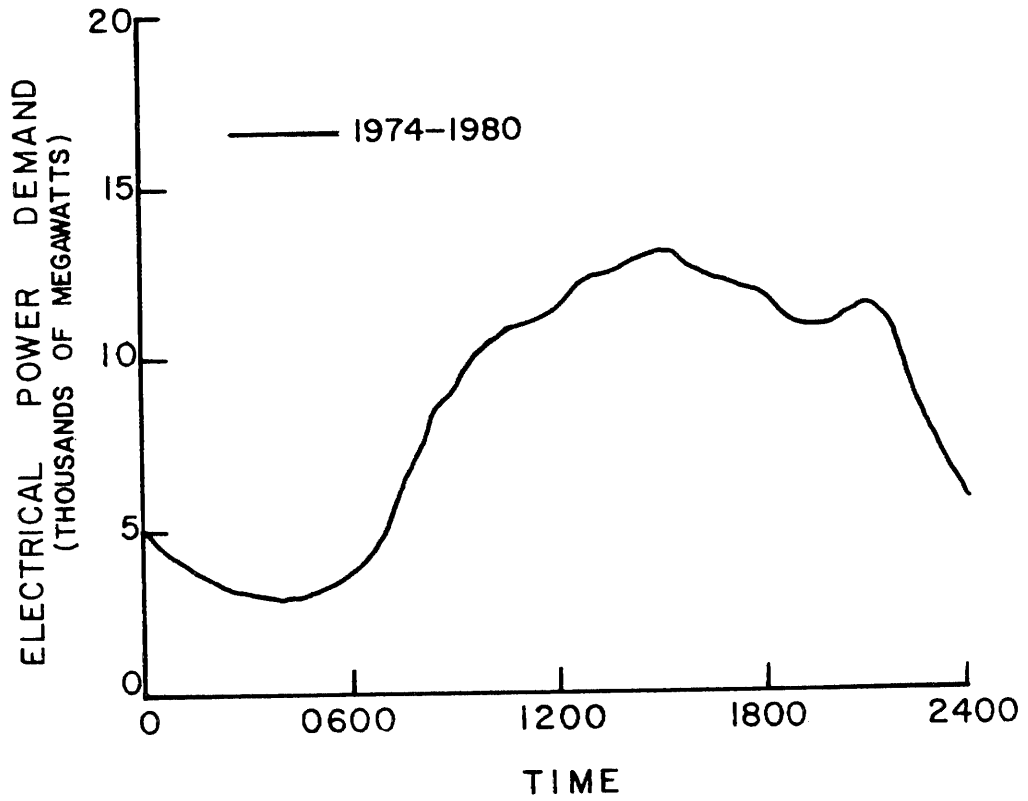
Stationary Sources	Fraction Sulfates in Exhaust			1973 Sulfate Emissions (Tons/day as SO <sub>4</sub> <sup>m</sup> )		Fraction Sulfates for Major Source Class Groups (1973 Emissions Weighted Average)	
	Range of Test Results (% S atoms as SO <sub>3</sub> or SO <sub>4</sub> <sup>m</sup> )	Value Adopted for 1972-1974 Base Period (% S atoms as SO <sub>3</sub> or SO <sub>4</sub> <sup>m</sup> )	Reference	On-Grid Sources	Off-Grid Sources	On-Grid Sources	Off-Grid Sources
<b>Fuel Combustion</b>		(h)					
Electric Utilities	<1.0% - 4.0%	3.0%	(a)	8.18	2.62	3.0%	3.0%
Refinery Fuel Burning		3.0%	(d)	0.42	----		
Other Interruptible Gas Customers		3.0%	(d)	0.10	----	3.0%	
Firm Gas Customers		3.0%	(d)	0.01	----		
<b>Chemical Plants</b>							
Sulfur Recovery Plants {Without Tail Gas Units}	0.2%	0.4% <sup>(i)</sup>	(a)	0.40	----		
Sulfur Recovery Plants {With Tail Gas Units}	2.8% - 29.1%	0.9%	(a)	0.27	----	0.55%	
Sulfuric Acid Plants	0.2% - 1.2%	1.0%	(e)	0.00	----		
Other Chemicals							
<b>Petroleum Refining and Production</b>							
Fluid Catalytic Crackers	0.0% - 7.9%	2.8%	(a)	2.19	----	2.8%	
Sour Water Strippers		1.0%	(e)	0.00	----		
Delayed Cokers		4.3%	(f)	0.15	----		
Miscellaneous Refinery Processes		1.0%	(e)	0.02	----		
Oil Field Production	1.7% - 1.8%	1.8%	(a)	0.12	----		
<b>Miscellaneous Stationary Sources</b>							
Petroleum Coke Calcining Kilns	5.4% - 9.7%	8.4%	(a)	3.22	----	8.4%	
Glass Furnaces	3.0% - 29.5%	18.0%	(a)	0.54	0.06	18.0%	18.0%
Secondary Metals Industries (On-Grid)	0.6% - 1.4%	1.0%	(a)	0.13	----	1.0%	
Primary Metals (off-Grid Steel Mill)	0.0% - 5.5%	2.5%	(a)	----	1.55	----	2.5%
Minerals Products		2.8%	(a)	----	0.08		
Sewage Treatment Digesters		3.0%	(d)	0.03	----		
Other Industrial Processes		3.0%	(e)	0.00	----	2.8%	
Permitted Incinerators		3.0%	(d)	0.00	----		
<b>Mobile Sources</b>							
Autos and Lt. Trucks - Surface		0.3%	(c)	0.07	----	0.3%	
Autos and Lt. Trucks - Freeway		0.3%	(c)	0.05	----		
Heavy Duty Vehicles - Surface	2.0% - 3.0%	2.3%	(b), (c)	0.37	----	2.5%	
Heavy Duty Vehicles - Freeway	2.0% - 3.0%	2.3%	(b), (c)	0.23	----		
Airport Operations		3.0%	(d)	0.05	----		
Shipping Operations		3.0%	(d)	0.46	----		
Railroad Operations		2.3%	(g)	0.11	----		
<b>TOTAL SO<sub>4</sub><sup>m</sup> EMISSIONS</b>				<b>17.12</b>	<b>4.31</b>		

## Key to References and Notes

- (a) Hunter and Helgeson (1976)  
 (b) Pierson and Brachaczek (1976)  
 (c) Personal Communication, Pierson (1977)  
 (d) Assumed for all other fuel combustion sources as was done by Hunter and Helgeson (1976)  
 (e) No data; value assumed.  
 (f) Taken from Hunter and Helgeson's (1976) refinery flare (odor incinerator) source test.  
 (g) Exhaust % sulfate assumed similar to highway diesel engines.  
 (h) For 0.5% sulfur oil.  
 (i) Most SO<sub>x</sub> emissions from this source class during the years 1972-1974 were from sulfur plants without tail gas units. Once tail gas units are applied to source, total SO<sub>x</sub> levels become so low that the higher SO<sub>3</sub>/SO<sub>x</sub> ratio does not affect the source class average very much.

vehicle traffic. As shown in Figure 4.10, South Coast Air Basin power plants typically reach peak load in the late afternoon. Motor vehicle traffic peaks twice daily (at morning and afternoon rush hours), as shown in Figure 4.11. From discussions with APCD personnel and from information presented by Hunter and Helgeson (1976), it is estimated that most large industrial process sources of  $SO_x$  in the South Coast Air Basin operate at a constant level throughout the day (although not always at full capacity). In view of the extremely small contribution to local  $SO_x$  emissions made by light industry and commercial establishments, no attempt will be made to modify emission rates to reflect a typical work day, or a five day per week work schedule. All sources other than power plants and motor vehicles will be assumed to contribute their  $SO_x$  emissions at an average rate independent of time of day. The fraction of daily emissions from power plants and motor vehicles assigned to each hour of the day by Figures 4.10 and 4.11 has been summarized in Table 4.8.

One principal reason for compiling emissions on a source by source basis is to be able to display the spatial distribution of  $SO_x$  emission strength. Figures 4.12 through 4.14 show annual average  $SO_x$  emissions density for the years 1972, 1973 and 1974 respectively. It is seen that the largest  $SO_x$  emission source densities are located in a narrow strip along the coastline stretching from Los Angeles International Airport (near Lennox) on the north to Huntington Beach (opposite Santa Ana) on the south.



Projected Baseline Diurnal Power Demand on Oil Fired Power Plants in the South Coast Air Basin (From Sjøvold, 1973).

FIGURE 4.10

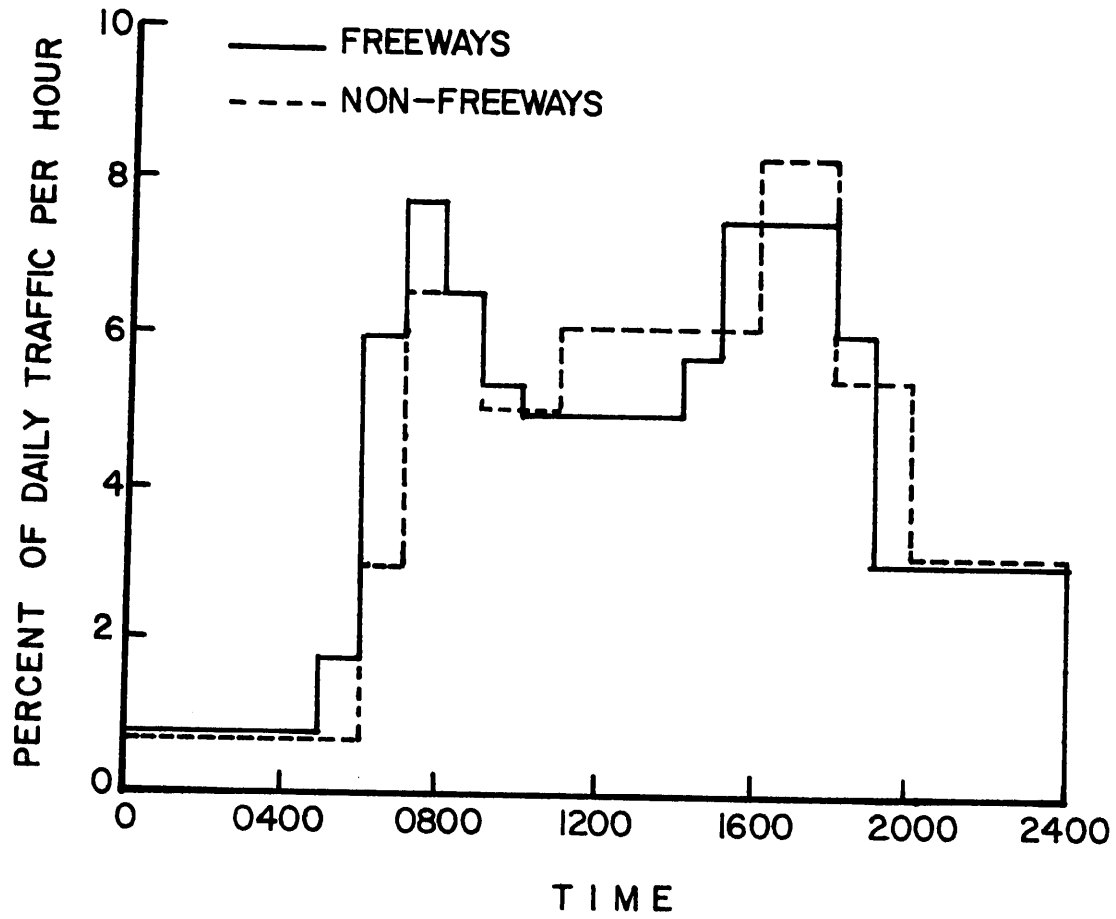
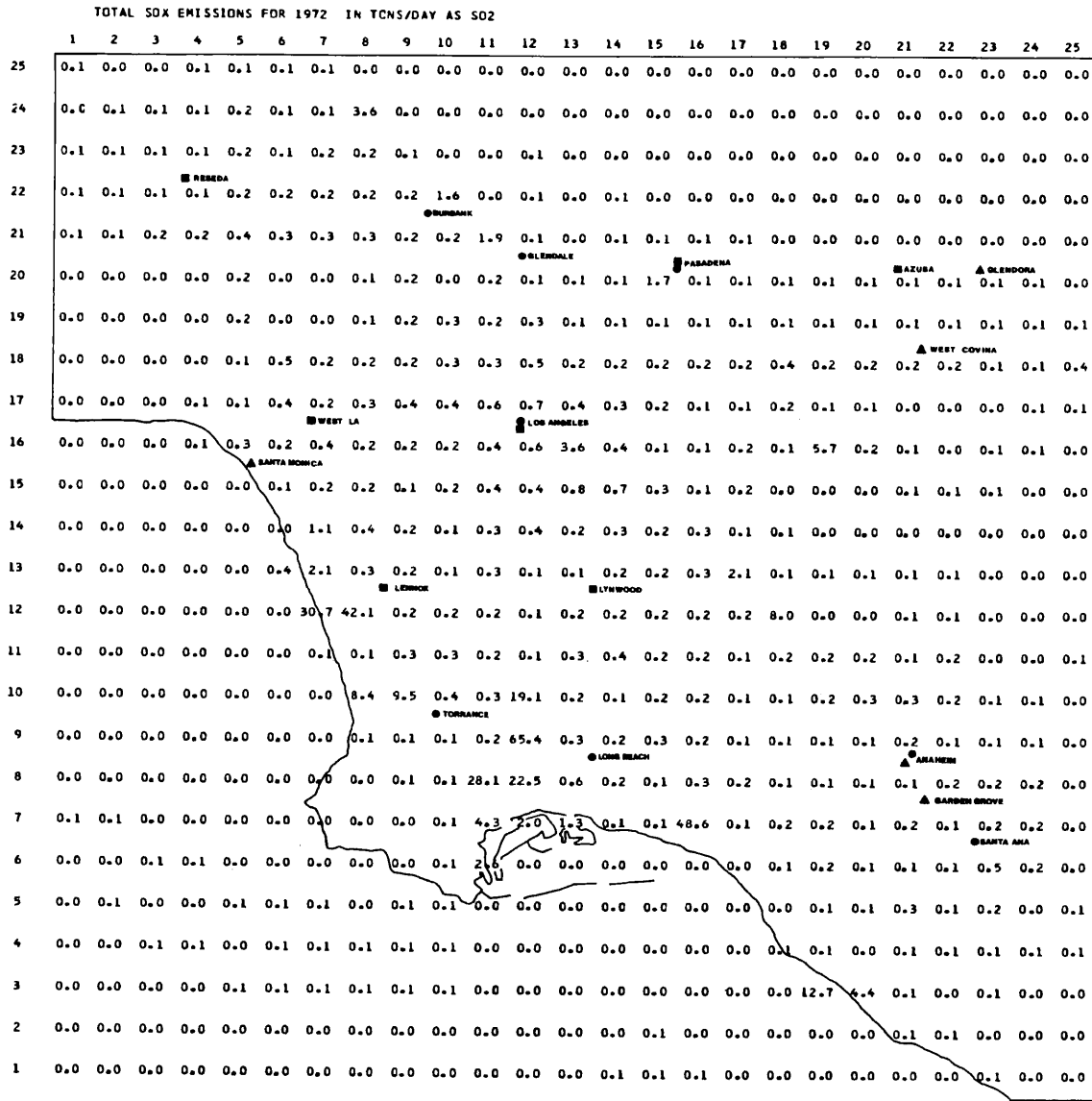


FIGURE 4.11  
Diurnal Variation of Los Angeles Traffic Flow  
(from Nordsieck, 1974)

TABLE 4.8  
 Diurnal Variations of Source Activities (1974)  
 (Fraction of Daily Total Assignable to a 1 Hour Period)

Local Time	Motor Vehicle Traffic			Power Plants
	Freeways	Surface Streets	Weighted Average (0.39 Freeways + 0.61 Surface)	
(Midnight) 2400-100	0.00776	0.00677	.00716	0.02756
100-200	0.00776	0.00677	.00716	0.01911
200-300	0.00776	0.00677	.00716	0.01695
300-400	0.00776	0.00677	.00716	0.01484
400-500	0.00776	0.00677	.00716	0.01381
500-600	0.0178	0.00677	.01107	0.01484
A.M. 600-700	0.0591	0.0293	.0409	0.01695
700-800	0.0768	0.0651	.0697	0.02334
800-900	0.0648	0.0651	.0650	0.03709
900-1000	0.0536	0.0502	.0515	0.04451
1000-1100	0.0494	0.0502	.0499	0.05095
1100-1200	0.0494	0.06088	.0564	0.05404
Noon 1200-1300	0.0494	0.06088	.0564	0.05616
1300-1400	0.0494	0.06088	.0564	0.06043
1400-1500	0.0569	0.06088	.0593	0.06146
1500-1600	0.0746	0.06088	.0662	0.06387
1600-1700	0.0746	0.0820	.0791	0.06043
1700-1800	0.0746	0.0820	.0791	0.05940
P.M. 1800-1900	0.0598	0.0540	.0563	0.05724
1900-2000	0.0302	0.0540	.0447	0.05306
2000-2100	0.0302	0.03077	.0306	0.05404
2100-2200	0.0302	0.03077	.0306	0.05616
2200-2300	0.0302	0.03077	.0306	0.04771
(Midnight) 2300-2400	0.0302	0.03077	.0306	0.03606

Reference: Nordsieck (1974)



SOX  
TONS/DAY  
389.130

FIGURE 4.12

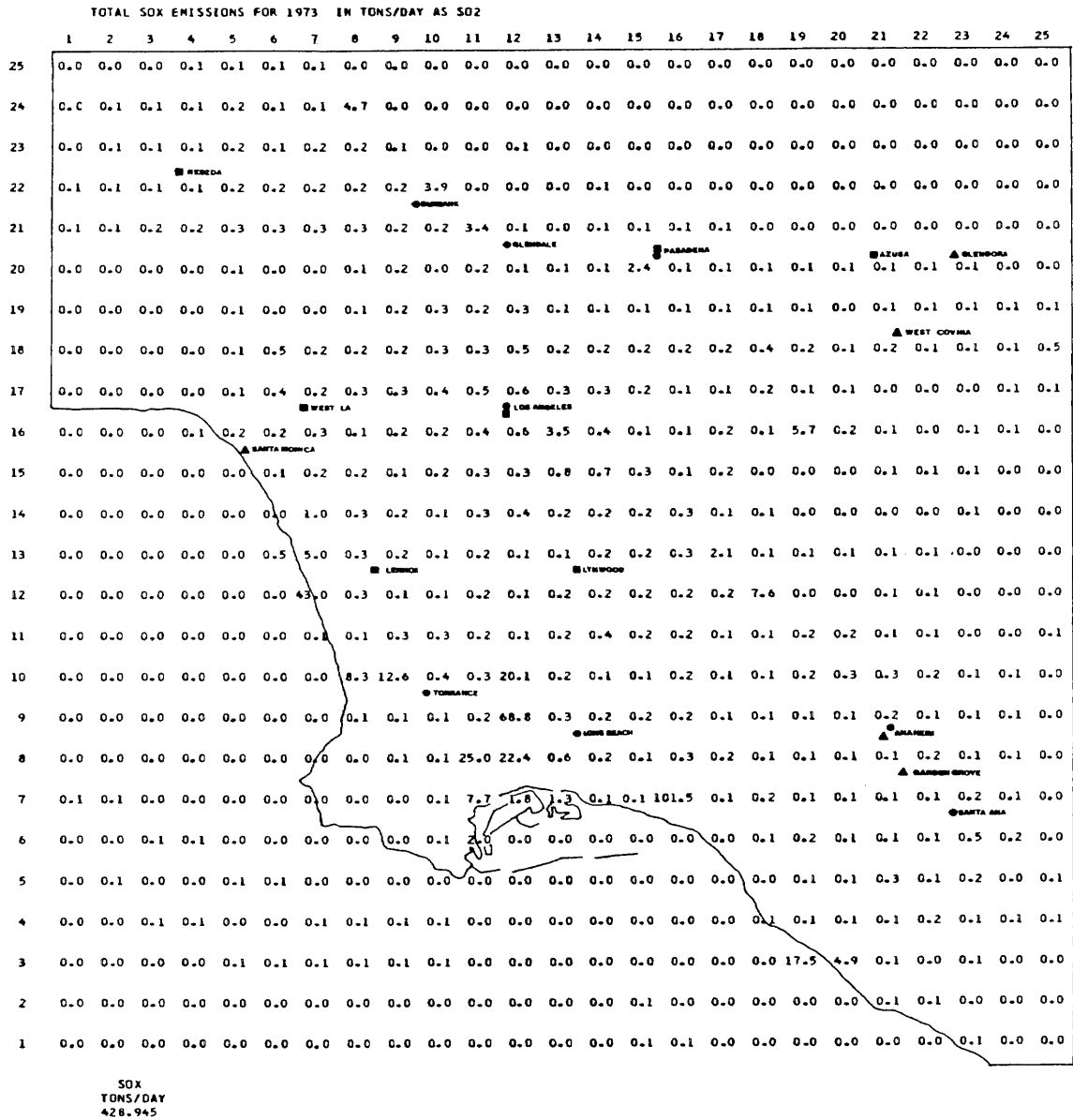


FIGURE 4.13

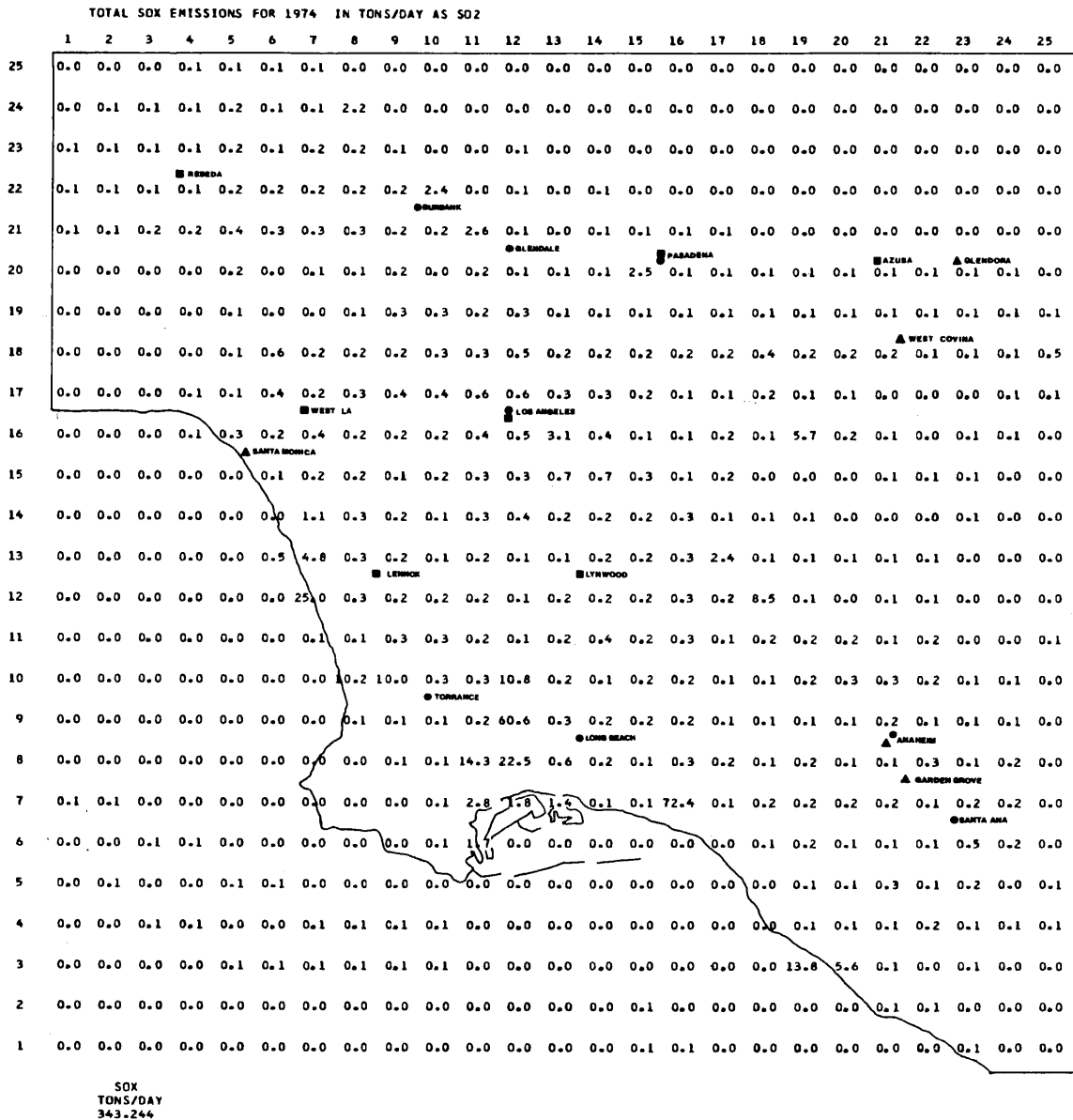


FIGURE 4.14

In Figures 4.15 through 4.20, the spatial distribution of  $\text{SO}_x$  emissions for the year 1973 has been broken down into several broad source categories. When this is done, it is seen that the high emission levels in the coastal zone are due largely to a high concentration of power plants, oil refineries and chemical plants.

An ability to add spatial resolution to the emission inventory in the vertical dimension is also important. In order to characterize the local air quality impact of emissions from a particular source, it is often necessary to estimate the source's effective stack height. Source effective stack height is the elevation above ground level at which a buoyant plume ceases to rise further into the atmosphere and instead equilibrates with its surroundings. Effective stack height can be thought of as having two components. An elevation is imparted to the emissions by the physical height of the stack or chimney. Then a further increment to effective source height is contributed by plume rise above the physical stack.

Typical values for physical stack height and plume rise for members of each source class of our emission inventory are given in Table 4.9. Plume rise estimates were first calculated for nearly one hundred major  $\text{SO}_x$  emission points in the South Coast Air Basin at a single set of reference meteorological conditions. Physical stack height and plume rise estimates for members of each source class were then averaged to obtain the typical values shown in Table 4.9. When data on stack parameters for a particular source class were unavailable,

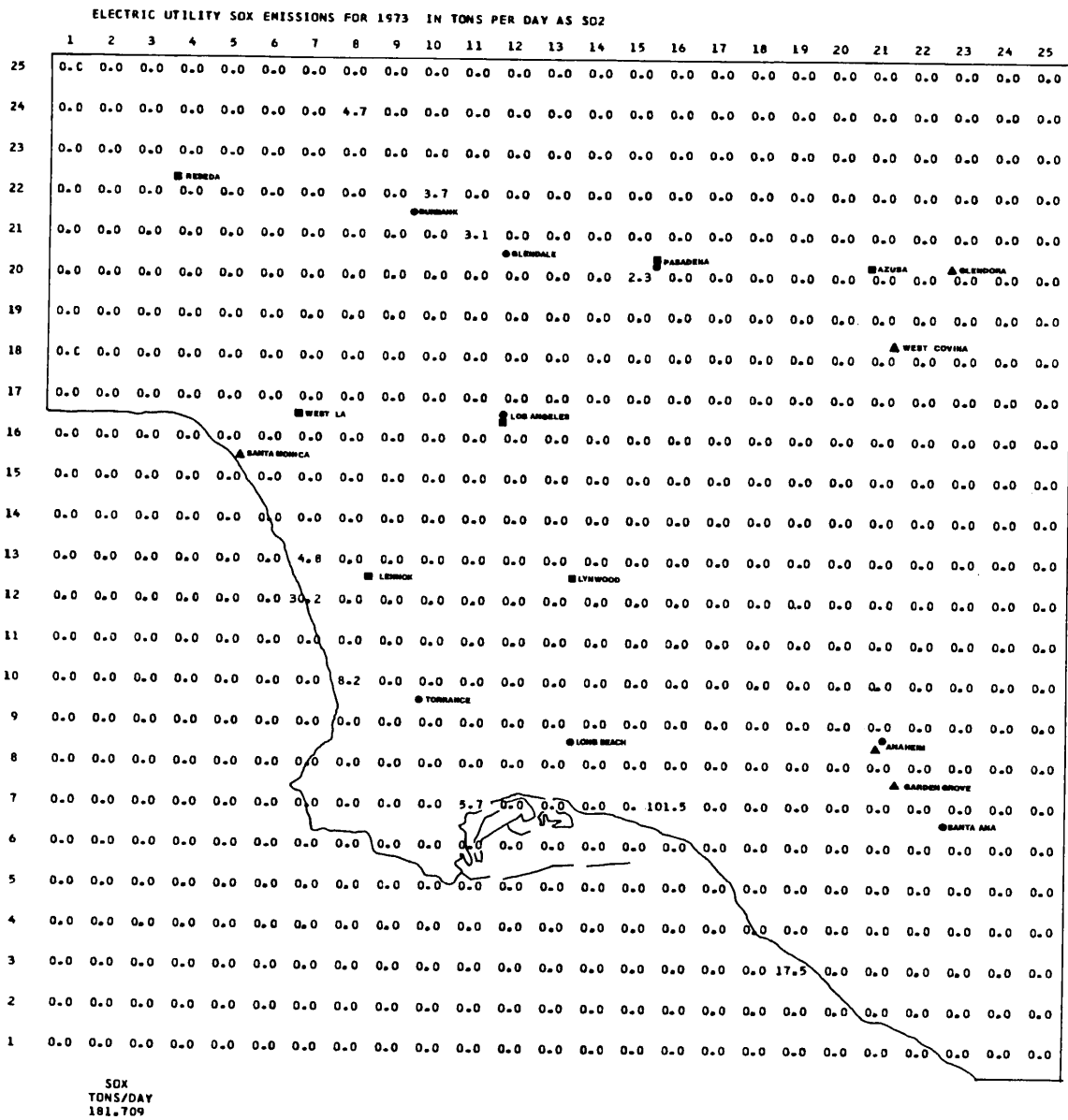
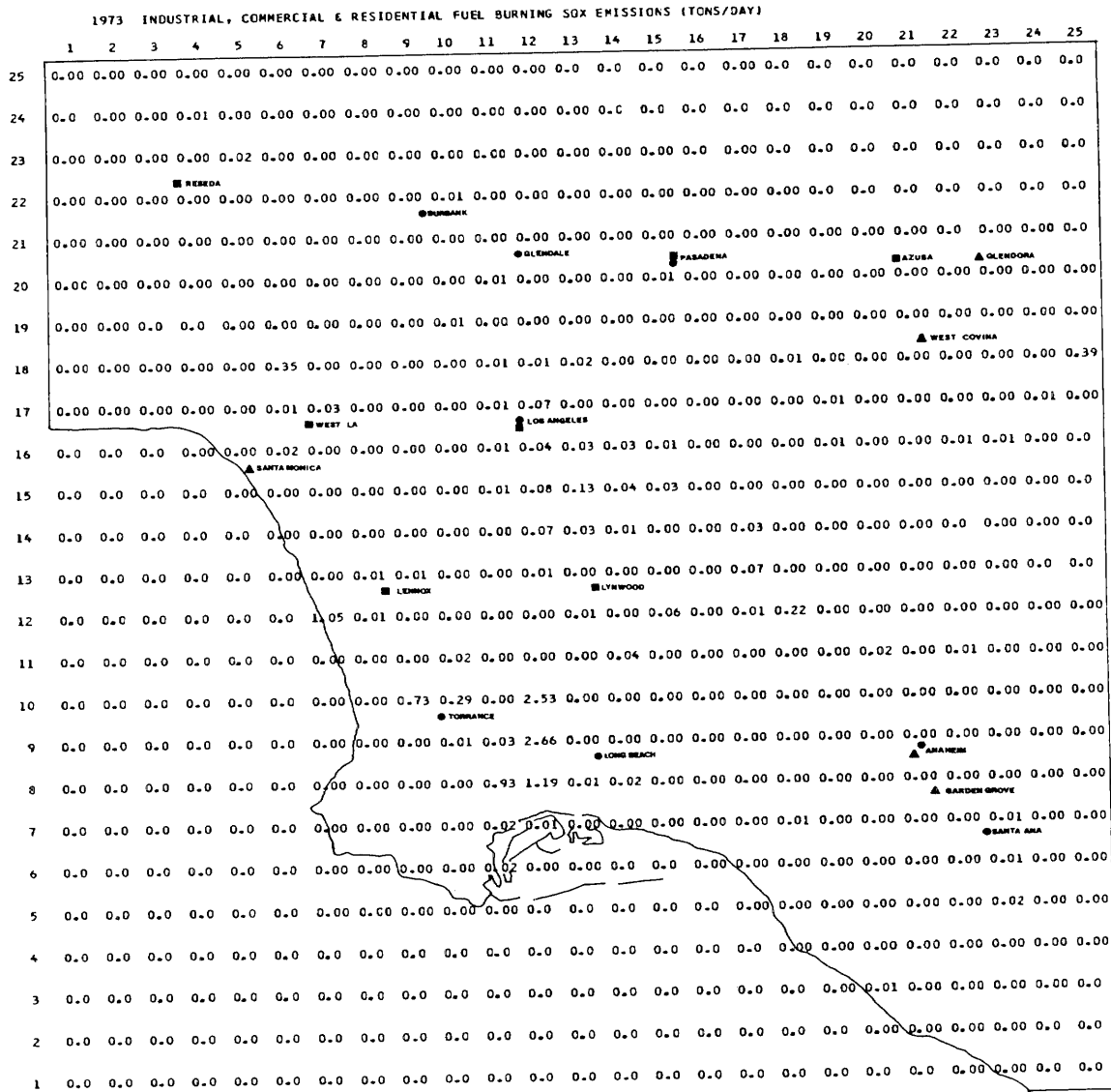


FIGURE 4.15



SOX  
TONS/DAY  
11.997

FIGURE 4.16

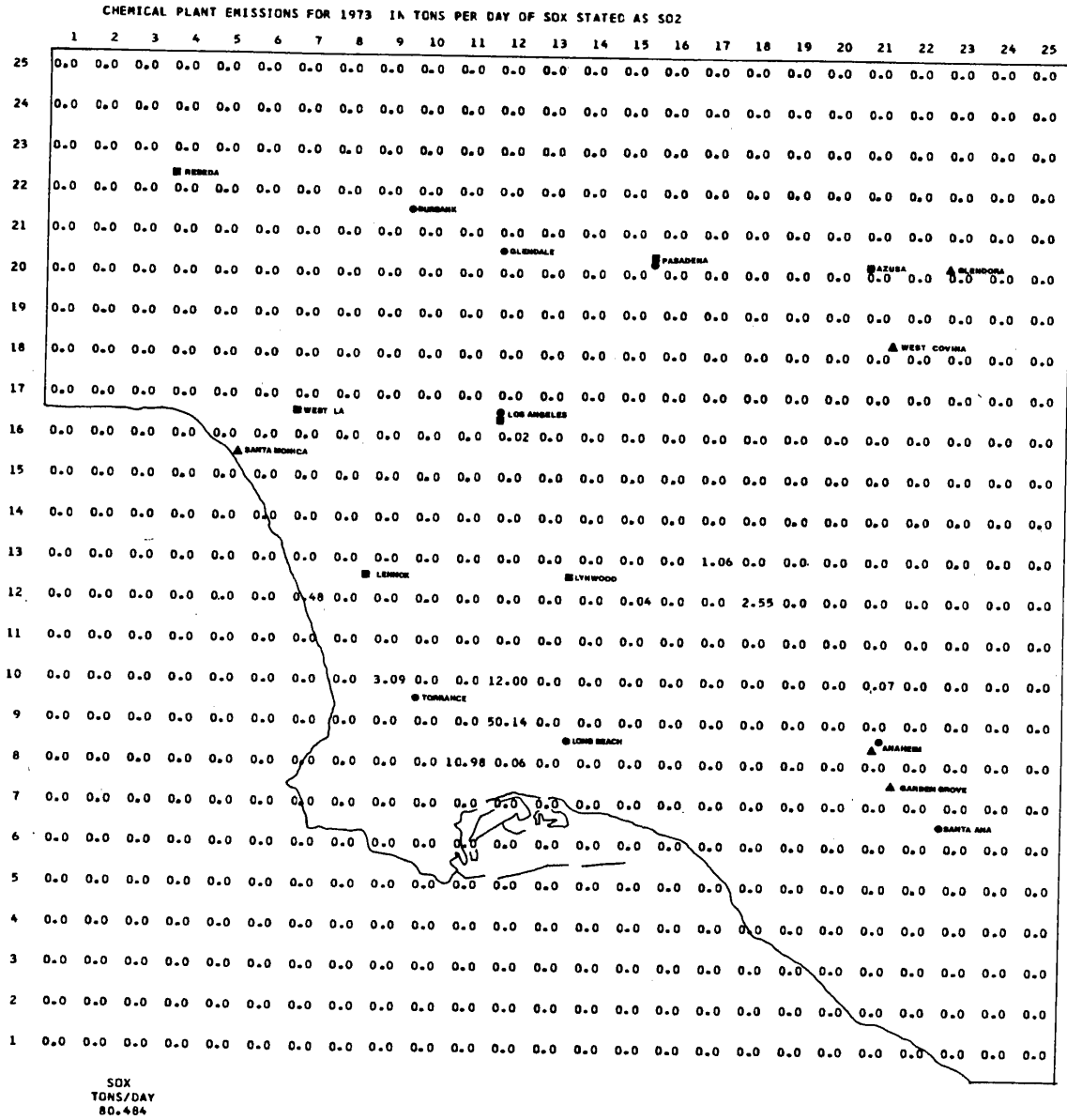


FIGURE 4.17

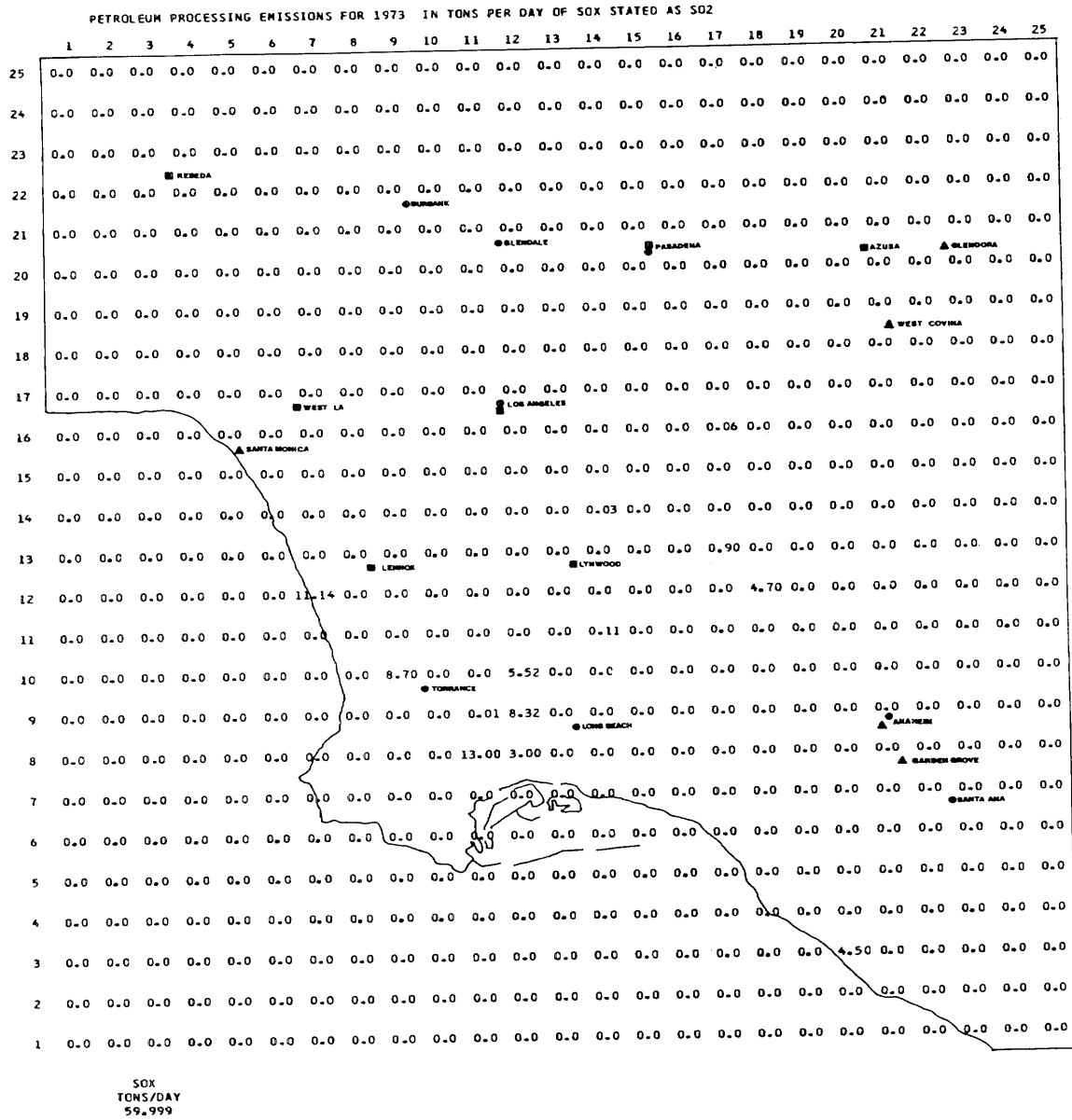


FIGURE 4.18

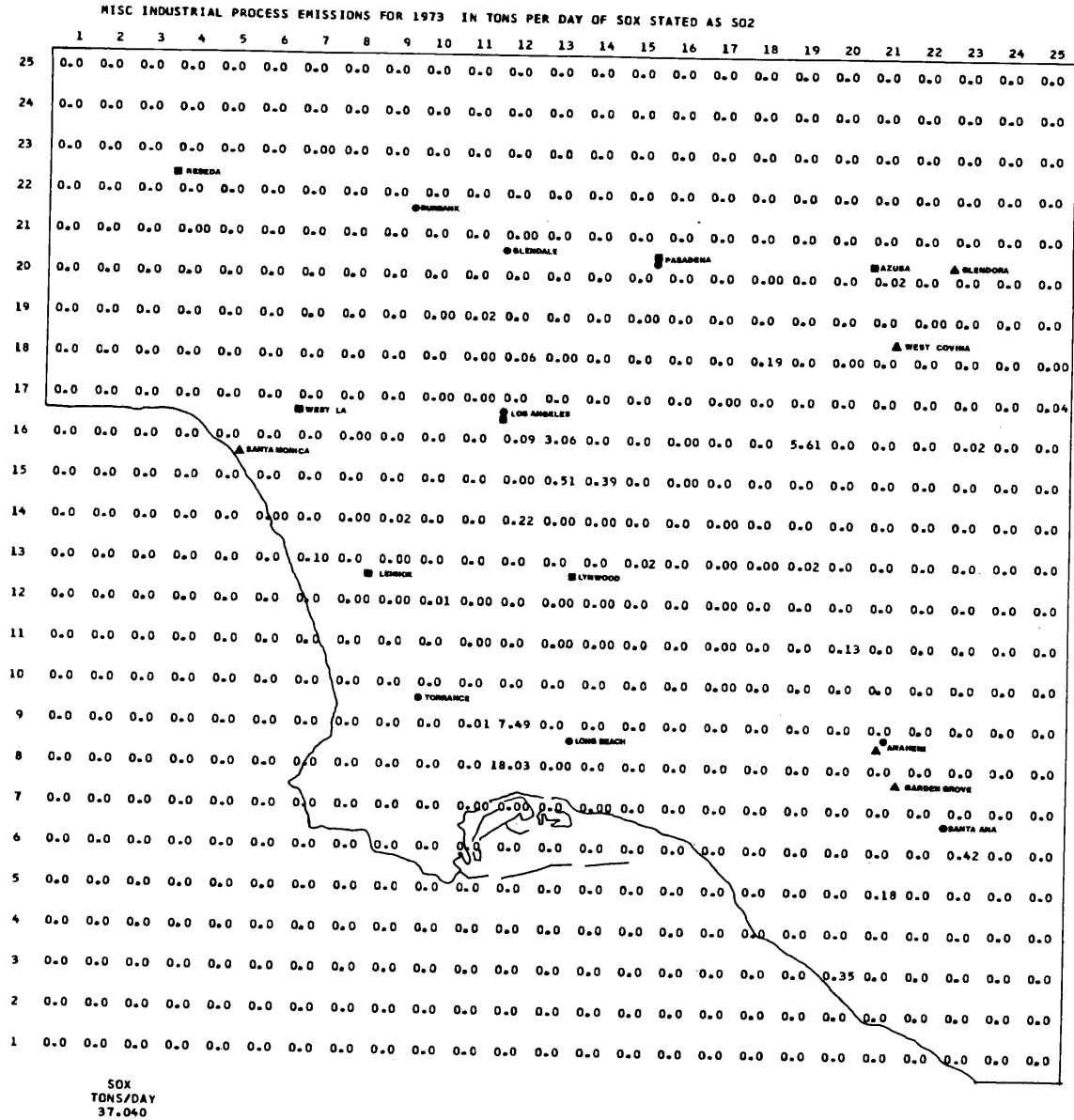
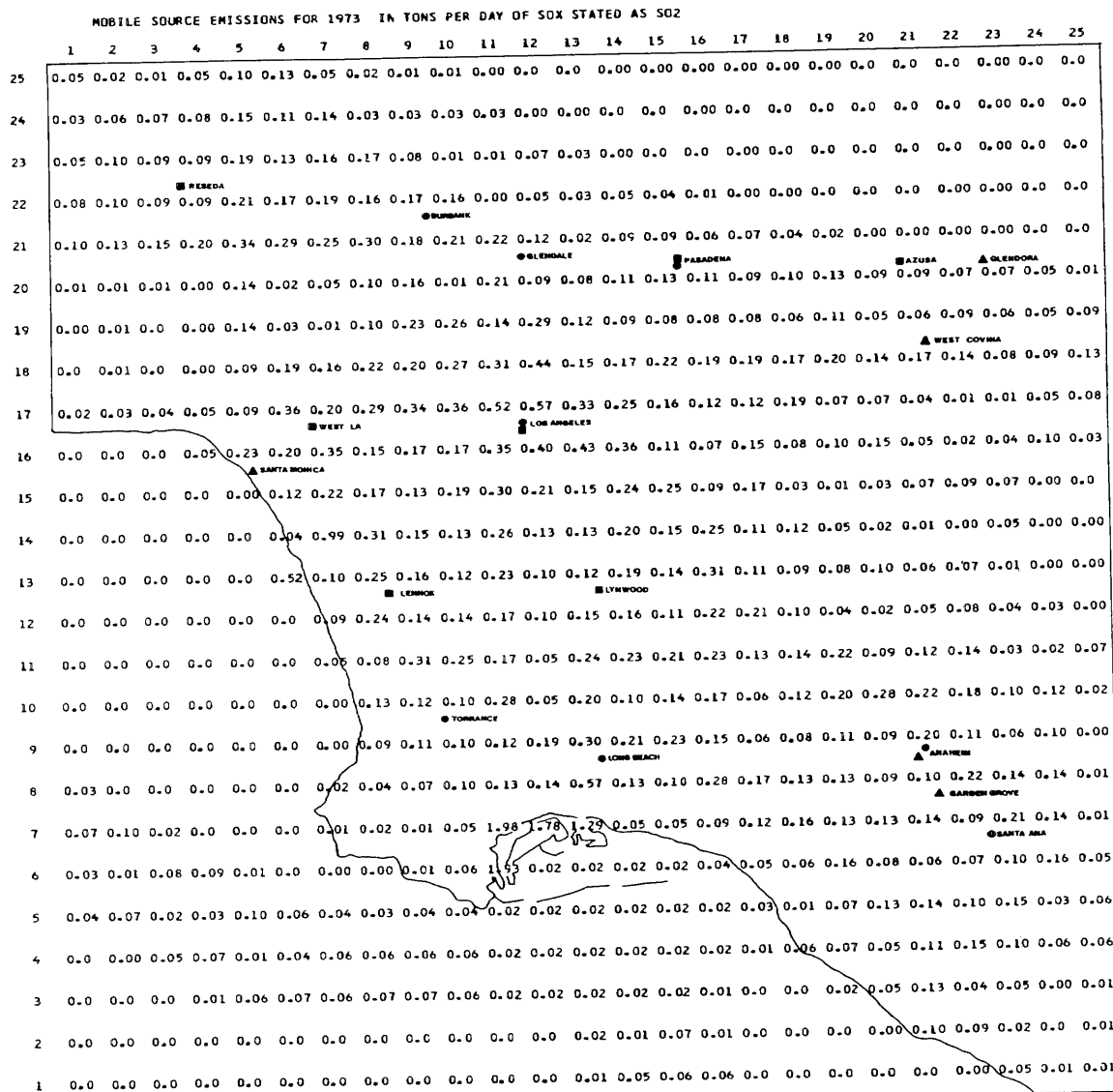


FIGURE 4.19



SOX  
TONS/DAY  
57.715

FIGURE 4.20

TABLE 4.9

Stack Height and Plume Rise  
for Individual Source Classes

(estimated at reference conditions: neutral stability;  
ambient temperature 64.4°F; wind speed 6.2 mph)

	Number of Cases Examined in Table A4.1	Notes	Range of Physical Stack Heights (ft)	Typical Physical Stack Height Adopted $H_p$ (ft)	Range of Plume Rise Calculated at Reference Conditions (ft)	Typical Plume Rise Adopted at Reference Conditions $\Delta H$ (ft)	Effective Stack Height Adopted at Reference Conditions $H_p + \Delta H$ (ft)
<b>Stationary Sources</b>							
<b>Fuel Combustion</b>							
Electric Utilities at 75% of Full Load							
Large Generating Units ( $H > 150$ ft)	28		176-300	225	409-1411	822	1047
Small Generating Units ( $H \leq 150$ ft)	16		60-150	102	58 - 342	189	291
Refinery Fuel Burning	--	(b)		100		180	280
Other Interruptible Gas Customers (Large)	2		45	45	166 - 199	182	227
Firm Gas Customers	--	(c)		12		24	36
<b>Chemical Plants</b>							
Sulfur Recovery Plants	9		50-200	127	61 - 578	181	308
Sulfuric Acid Plants	3		80-200	143	30 - 74	58	201
Other Chemicals	--	(c)		35		70	105
<b>Petroleum Refining and Production</b>							
Fluid Catalytic Crackers	9		89-181	122	282 - 794	540	662
Sour Water Strippers	--	(d)		130		367	497
Delayed Cokers	--	(d)		130		367	497
Miscellaneous Refinery Processes	--	(d)		130		367	497
Oil Field Production	--	(c)		20		72	92
<b>Miscellaneous Stationary Sources</b>							
Petroleum Coke Calcining Kilns	1		150	150	1261	1261	1411
Glass Furnaces	17		40-120	75	50 - 204	147	222
Secondary Metals Industries (On-Grid)	4	(a)	50 - 60	55		110	165
Sewage Treatment Plant Digesters	1		35	35	62	62	97
Other Industrial Processes	--	(c)		35		70	105
Permitted Incinerators	--	(c)		35		70	105
Primary Metals Industries (Off-Grid Steel Mill)	4		175-300	238	341 - 548	426	664
Mineral Products Industries (Off-Grid)	1		25	25	122	122	147
<b>Mobile Sources</b>							
Autos and Light Duty Trucks	--	(b)		1		2	3
Heavy Duty Vehicles	--	(b)		12		24	36
Airport Operations	--	(b)		20		40	60
Shipping Operations	--	(b)		90		180	270
Railroad Operations	--	(b)		18		36	54

- Notes: (a) Physical stack height known; plume rise assumed.  
 (b) Physical stack height estimated by observation of members of that source class; plume rise assumed.  
 (c) Physical stack height and plume rise assumed.  
 (d) Based on data for one refinery flare given in Table A4.1.

an assumed value has been noted in Table 4.9 based on a qualitative impression of the size of the sources involved.

The typical plume rise characteristics given in Table 4.9 provide a basis for visualizing the relative buoyancy of plumes from various source types. Petroleum coke calcining kilns and power plants are predicted to have by far the highest effective stack heights in the basin. Fluid catalytic crackers and a local steel mill display relatively tall effective stack heights. In contrast, sulfuric acid plants have non-buoyant plumes whose effective height of emission is due principally to their physical stack. Most small fuel burning sources and miscellaneous industrial processes display effective stack heights of between 100 and 300 feet above ground level at our reference conditions.

The brief discussion of effective stack height given here is supported in detail in Appendix A4. That appendix explains the calculation methods used. Stack parameters relevant to plume rise estimation for individual sources under a variety of meteorological conditions are tabulated. A method for dynamically allocating effective stack height as a function of wind speed within a simple air quality model is also described.

From the emissions estimates of Tables 4.5a and 4.5b, it is clear that at least 531 tons of sulfur oxides were emitted to the atmosphere on an average day in the South Coast Air Basin in 1973. That total, however, accounts for less than 15% of the sulfur thought to be entering local refineries in crude oil in that year. In order to account for

the rest of the sulfur, and thus to assess the accuracy of our emission inventory, an energy and sulfur balance was constructed for the South Coast Air Basin for the year 1973.

#### 4.4 Energy and Sulfur Balance

##### 4.4.1 Energy and Sulfur Balance -- Approach and Methods

The area under consideration is the entire South Coast Air Basin, which includes (using its 1973 boundaries) all of Orange and Ventura Counties, and portions of Los Angeles, Riverside, San Bernardino, and Santa Barbara Counties as shown in Figure 4.21. By determining the flows of energy resources across the boundaries of the basin, and by examining the transformations and uses of energy within the basin, an energy balance for this area can be derived. Similarly, by considering the sulfur content of these energy resources, flows of sulfur into and out of the basin, and points where sulfur is transformed or released to the atmosphere, a sulfur balance can also be determined. To the extent that energy intake can be balanced with energy consumption, one can build confidence that closure has been achieved over the fate of the sulfur accompanying those energy flows. Sulfur flows which were captured prior to becoming airborne can be identified. One can easily see what the potential emissions might be if one form of energy use were substituted for another.

The format of the energy balance is similar to that established by the Stanford Research Institute (1973). However in many cases our data sources, definitions and accounting conventions will differ significantly

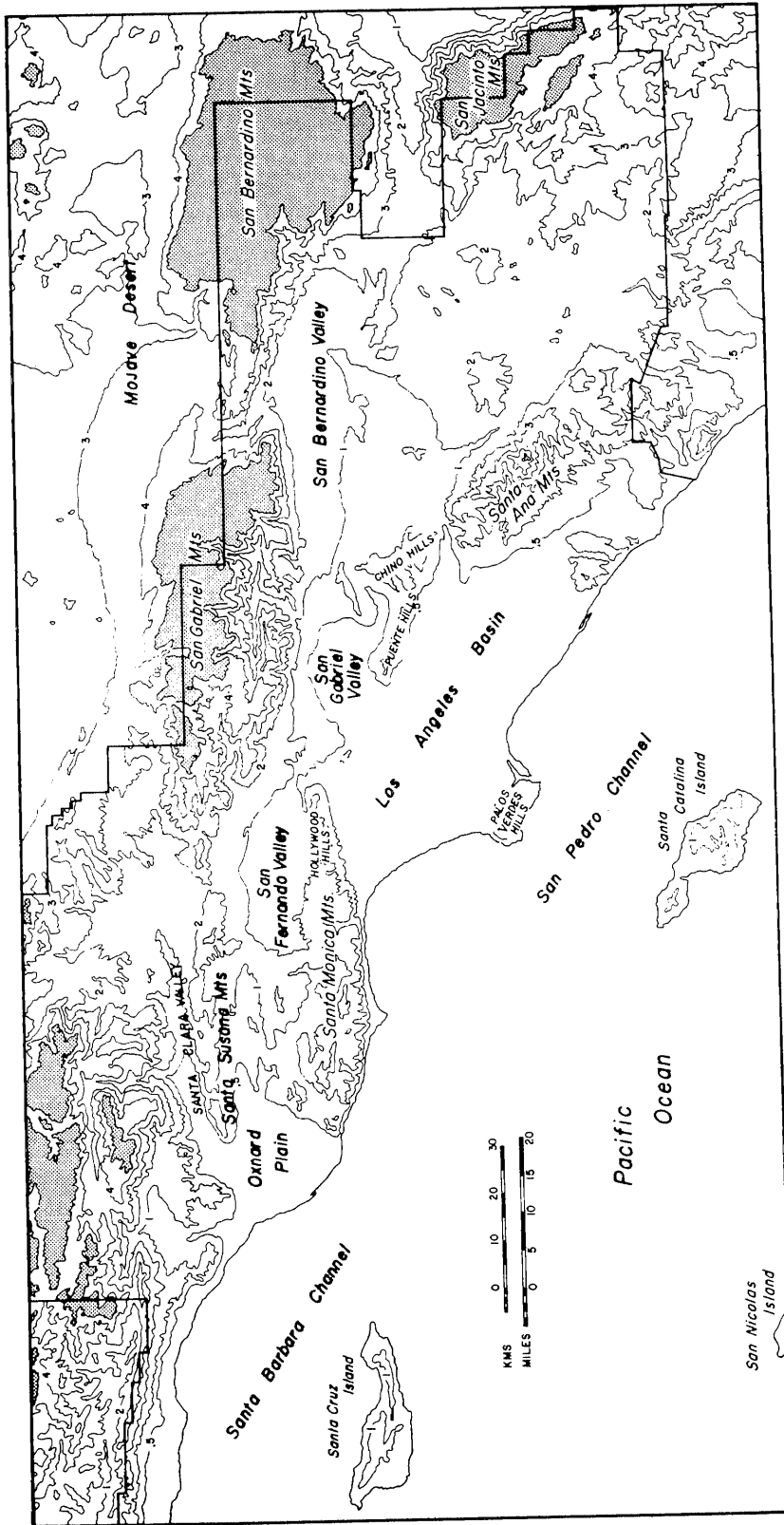


FIGURE 4.21  
The South Coast Air Basin  
(1973 Boundaries Shown by Heavy Outline)

from that prior survey of energy use in California. The energy balance is divided into four "sectors": sources, energy transformations, consumption, and exports. Energy sources include both local sources (i.e. those originating within the basin from crude oil and natural gas fields) and "imports" coming from outside the basin boundaries. These imports (the term will be used regardless of foreign or domestic origin) include items such as crude oil, refined petroleum products and other fuels, and electricity. In the transformation sector, two processes occur: crude oil is refined into a variety of petroleum products, and oil and natural gas are burned to generate electrical power. The consuming sector can be conveniently subdivided into six categories: raw materials use (e.g. use of natural gas in chemical fertilizer production), and five traditional energy use areas including residential/commercial, industrial, transportation, military, and miscellaneous energy consumption. Finally, energy can be exported from the basin in almost any form by pipeline or other overland transportation mode, by ship, or in the fuel tanks of various transportation media.

In each of the four sectors of the energy economy, a variety of energy forms are considered: natural gas, digester and refinery gas, LPG, natural gas liquids, crude oil, residual and distillate fuel oils, gasoline, jet fuel, petroleum coke, coal, and electricity. With such a wide variety of fuels to consider, and the need to study the sources, transformations, uses in a number of sectors, and exports for each fuel type, it has been necessary to employ a large number of data

sources. A complete discussion of the data sources used and the methods involved in their use is given in Appendix A3. In this section, only some general remarks about the types of information available and the treatment applied to them will be made. Appendix A3 should be consulted for a more detailed description of the methods and data sources employed.

The flow of natural gas through all four sectors of the energy balance was established from reports published jointly by the gas utilities serving the basin, and from additional information supplied to the California Air Resources Board by the Southern California Gas Company. Similarly, information on electrical energy within the basin was easily obtained from the annual reports of the utilities involved, and from the Federal Power Commission.

For other types of energy use, information had to come from a larger variety of sources. The U.S. Bureau of Mines publishes annual statistics on shipments of fuels, uses of various fuel types in different consuming sectors, and input and output at refineries. However, most of these data are reported on a state or district basis (California is a part of the West Coast district along with six other states). Thus, scaling factors must be developed, based on such statistics as refinery capacities, population, or industrial employment, to relate fuel sources and sinks at the basin level to those at the state or district levels.

For some items in the energy balance, state publications provided information on a county-by-county basis. Such data could be scaled

to the basin fairly easily, after making allowances for the out-of-basin portions of some counties. Some information was available on a point-by-point basis, e.g. operations at airports and fuel shipments received at various ports. In these cases, data for the basin were easily obtained by summation.

The purpose of the above discussion has been to give an introduction to the types of data sources and methods used to create the energy balance. Details on data, references, scaling factors, and assumptions made can be found in Appendix A3.

Much of the sulfur balance follows directly from the energy balance once the sulfur content of various fuels is known. The Bureau of Mines publishes yearly sulfur analyses for most of the fuels considered (see Appendix A3, Table A3.10). In some cases, local data on fuel sulfur content offer a better estimate of local fuel quality than do the regional analyses reported by the Bureau of Mines. These improved estimates of Los Angeles area fuel sulfur content have been used whenever possible. Data on the sulfur content of crude oils was adapted from the crude oil characterization study of Appendix A1.

In addition to fuel sulfur data, information is needed on sulfur flows occurring within certain industrial processes. Sulfur balance information on Los Angeles County refineries and chemical plants was obtained from the Southern California Air Pollution Control District (1976a). The refinery sulfur balance was used to confirm the quantity of sulfur received in crude oil by local refineries in 1973. That APCD refinery sulfur balance also permits comparison of sulfur flows leaving

the refineries in products to estimates of sulfur received in fuels by the consuming and export sectors of the Los Angeles energy economy. The APCD sulfur balance on local chemical plants was employed to gauge the amount of elemental sulfur and sulfuric acid produced in the basin from refinery wastes. Data on SO<sub>x</sub> emissions from other industrial processes were adapted to the sulfur balance from information given in Appendix A2.

A major strength of the energy and sulfur balance calculations is that independent estimates usually can be made of the amounts supplied and the amounts consumed of any given energy resource. Virtually every data point is estimated independently or has some degree of independence. Thus a summation of energy or sulfur sources and sinks, either for the entire system or for an individual fuel type, provides an assessment of the completeness and consistency of the information available.

#### 4.4.2 Caveat

A variety of conventions could have been adopted at many points within the energy and sulfur balance that would have yielded seemingly different numbers within the summary Tables 4.10 and 4.11 which follow. If the reader wishes to compare this energy and sulfur balance summary to other data at his or her disposal, it is absolutely necessary to digest Appendix A3 first.

The terms to be used in the energy and sulfur balance are defined in Appendix A3. As an incentive to the reader to consult that appendix,

consider the following examples in which detailed knowledge is necessary to a correct interpretation of the energy and sulfur balance summary.

It is often possible to account for energy flows (or for that matter cash flows) on either a gross or net basis.<sup>1</sup> Sometimes one method is more convenient than another. In this energy balance, gross imports and exports are given for most refined petroleum products and for natural gas. From the descriptions given in Appendix A3, the reader can tell whether an import or export figure is stated on a gross or net basis.

As a second example, consider the definition of transportation fuel "consumption" as distinguished from fuel sales in the basin. Large quantities of petroleum sold as fuel to long range transportation vehicles (ships and aircraft) are not "consumed" (burned) in the air basin within the definitions used in this study. Only a small fraction of that fuel is burned within the South Coast Air Basin as those vehicles exit the area. Instead, the bulk of these fuels are "exported"

---

<sup>1</sup>Crude oil flows from Ventura area oil fields provide an illustration of the accounting choices available. This oil first enters the air basin when produced from local wells. Then some of the Ventura area crude oil is exported to sea by ship. Part of those Ventura area crude oil shipments later reappear as domestic oil receipts at other South Coast Air Basin ports. In Appendix A1, all crude oil flows were counted as part of the air basin's crude oil supply only if they remained in the air basin on a net basis. In the following energy balance, all crude oils will be considered as part of the energy balance's "source" category if they ever resided in the basin. Then net shipments to sea of locally produced oil will be shown as an "export". The net crude oil supply remaining in the basin as developed in Appendix A1 may thus be determined by difference between crude oil sources and exports.

from the basin in the fuel tanks of transportation media. That distinction is built into the energy and sulfur balance as it is important to a correct computation of local air pollutant emissions from the results of the sulfur balance.

#### 4.4.3 The Energy Balance

Table 4.10 summarizes the energy balance on the South Coast Air Basin for the year 1973. A total of nearly  $3700 \times 10^{12}$  BTU's of energy resources entered the air basin's economy in that year. The ultimate fate of that energy supply is also apparent from Table 4.10:

- 15% of the energy supply is lost in transformation processes such as petroleum refining and electricity generation;
- 48% is expended for its heating value within the air basin by a final consumer of energy products;
- 4% of the energy content of the basin's energy resource base is tied-up in products that are used as industrial raw materials; and
- 33% of the gross energy supply passing through the air basin's economy is subsequently exported.

If the absolute value of all discrepancies between sources and sinks for various energy products appearing in Table 4.10 are added together, the total of all discrepancies is less than 5% of the gross energy input to the basin. On an aggregate basis, the energy balance actually balances with less than a 1% net surplus.

TABLE 4.10  
South Coast Air Basin Energy Balance--1973  
(10<sup>12</sup> BTUs per year)

	Electricity	Natural Gas	Crude and Unrefined Oils	NGL	LPG	Still Gas for Fuel	Gasoline	Jet Fuel	Light and Middle Distillate Fuel Oil	Residual and Heavy Distillate Fuel Oil	Petroleum Coke	Lubri-cants	Asphalt and Road Oil	Other Hydro-carbons	Coal	Digester Gas	TOTAL
<b>SOURCES</b>																	
Resource base: imports plus local crude oil and natural gas production	97.3	1050.3	2182.3	20.9	14.4		69.6	4.4	81.6	127.6	5.5	12.3	0.1	4.6	57.4	2.6	3732.9
Adjustments: change in gas storage; out-of-basin electric use	-13.1	-25.2															-38.3
Subtotal	84.2	1025.1	2182.3	20.9	14.4		69.6	4.4	81.6	127.6	5.5	12.3	0.1	4.6	57.4	2.6	3694.6
<b>TRANSFORMATION SECTOR</b>																	
Refinery feedstock (-)	-9.8	-48.5	-2124.8 <sup>(a)</sup>	-23.9	-8.7	-132.8								-16.9 <sup>(b)</sup>			-2174.3
Refinery fuels (-)						108.4											-219.9
Refinery production(+)							863.0	224.3	126.9	581.2	112.0	18.5	88.0	60.3			2218.7
Utility fuels (-)	179.9	-180.9							-2.7	-386.3						-0.3	-550.2
Utility production (+)																	179.9
Subtotal	170.1	-209.4	-2124.8	-23.9	-8.7	-14.0	863.0	224.3	124.2	183.1	112.0	18.5	88.0	43.4		-0.3	-545.8
<b>CONSUMED IN BASIN AS ENERGY RESOURCE</b>																	
System uses; losses	-28.8	-20.5															-49.3
Residential/commercial	-133.8	-431.4							-8.1	-8.1					-0.2		-588.2
Industrial (other than refinery)	-71.2	-153.9							-15.6	-19.5					-57.2		-320.7
Transportation (civilian)							-650.3	-17.3	-39.9	-9.1							-738.5
Military							-2.2	-6.1	-6.5	-0.1							-14.9
Miscellaneous	-21.9	-8.7							-16.5	-0.6							-48.7
Subtotal	-255.7	-614.5					-652.5	-23.4	-104.6	-27.4					-57.4		-1760.3
<b>CONSUMED AS A RAW MATERIAL (c)</b>																	
System uses; losses																	
As a commodity (by ship)																	
As a commodity (overland)																	
In transport mode fuel tanks																	
Subtotal																	
<b>EXPORTS</b>																	
As a commodity (by ship)																	
As a commodity (overland)																	
In transport mode fuel tanks																	
Subtotal																	
<b>SUBTOTAL</b>																	
Total sources (+ flows)	277.2	1050.3	2182.3	20.9	14.4	158.9	932.6	228.7	210.5	708.8	117.5	30.8	88.1	64.9	57.4	2.6	3732.9
Total sinks (- flows)	-278.6	-1054.5	-2182.3	-23.9	-8.7	-179.6	-898.9	-174.1	-232.6	-704.5	-109.4	-30.8	-88.1	-64.9	-57.4	-2.6	-3732.9
Absolute difference	-1.4	-4.2					33.7	54.6	-42.1	4.3	8.1	8.1	8.1	8.1	8.1	8.1	29.3
Difference as % of sources	-0.51%	-0.40%					3.61%	24.87%	-20.0%	0.61%	6.89%	6.89%	6.89%	6.89%	6.89%	6.89%	29.3
Difference as % of total energy resources	-0.04%	-0.11%					0.91%	1.48%	-1.14%	0.12%	0.22%	0.22%	0.22%	0.22%	0.22%	0.22%	0.79%

Notes: (a) Obtained by difference  
(b) May include some natural gas  
(c) Or put to other non-energy resource use  
(d) Includes exchange with out-of-basin utility

The degree to which the energy balance balances for individual product types is more variable, but still is considered to be acceptable. Three of the five largest energy flows in the system (i.e. natural gas, electricity and heavy fuel oil) balance to within less than a 1% discrepancy between sources and sinks. The gasoline summary balances to within 4%, and the crude oil supply balances by virtue of the fact that refinery input was determined by difference between crude oil supply and exports. In addition, the petroleum coke summary balances with only a 7% surplus. That is considered to be good agreement given that petroleum coke production had to be scaled in two stages from a West Coast refinery total. The unaccounted for petroleum coke may well have been lost in coke calcining processes which have not been investigated for their effect on product "shrinkage".

Major percentage discrepancies between individual product sources and sinks occur in the light and middle distillate fuel oil categories including both jet fuel and light fuel oil. These two product lines share overlapping hydrocarbon boiling ranges. Kerosene heating oil has much the same composition as certain jet and turbine fuels. Our estimated surpluses of jet fuel and deficiency of light and middle distillate heating oil are of corresponding magnitude and opposite sign. These two discrepancies could well be self-cancelling. The source of the estimation error is not readily apparent from the highly aggregated data on refinery output which are at our disposal. For the purposes of the forthcoming sulfur balance, jet fuel and light fuel oils must be merged because available data on refinery sulfur output are given only

for both product streams combined. If the source of the jet fuel surplus and light fuel oil deficit lies in the refinery output estimate made for each fuel, that problem alone will not affect the forthcoming sulfur balance's accuracy.

The energy balance also shows an excess of LPG and NGL consumption above known supply. This problem is felt to arise from an inadequate knowledge of the sources of supply for these materials. LPG is the product of natural gas processing plants and refinery processes. Harbor receipts show that very small quantities of liquified gases were imported into the South Coast Air Basin in 1973 by waterborne commerce. Refinery gas consumption for fuel appears to include virtually all potential local refinery LPG production. Therefore, it seems likely that LPG sufficient to meet residential, commercial, industrial, and feedstock demand may have been imported into the basin by intrastate overland transportation modes (e.g. tank trucks). If that were the case, a significant source of LPG supply would not be identifiable in our commerce statistics and would have been omitted from the energy balance. A similar situation is thought to mask NGL supply: it is either included within crude oil statistics, lumped with unidentified hydrocarbons or moved overland within California in a way that does not easily stand out in the interstate commerce records. Since the sulfur content of LPG and NGL is very low, this discrepancy between LPG and NGL supply and consumption will not jeopardize the forthcoming sulfur balance.

Turning our attention to product supplies and uses, it is seen that crude oil is the principal energy input to the basin, accounting for 59% of the original energy supply. Natural gas is in second place with about 28% of the total energy supply. Imported refined petroleum products and imported electricity follow in order of importance to the gross energy resource base of the basin.

From Table 4.10 it is seen that estimated refinery feedstocks and gross product yield are in good agreement on a net energy content basis. However, in order to obtain this transformation of feedstocks into products, fuels were consumed with an energy content equal to about 10% of gross refinery product output. The ratio of fuel use to product energy content is about the same for the South Coast Air Basin and for all refineries located in the Western United States. However, South Coast Air Basin refineries appear to depend much more heavily on refinery gases for fuel than is typical of West Coast Region (PAD District V) refineries as a whole.

The principal refinery product in the South Coast Air Basin is gasoline, which accounts for 39% of total refinery product output on an energy content basis. The next largest refinery product stream consists of heavy fuel oil. The principal customer for this heavy fuel oil is a second stage of the energy transformation sector: the electric utility industry.

Electric utilities consumed  $550.2 \times 10^{12}$  BTU's of fossil fuel within the South Coast Air Basin in 1973. Electricity generated from that fuel consumption amounted to  $179.9 \times 10^{12}$  BTU's for an overall

conversion efficiency of about 33%. Seventy percent of that electricity was generated by combustion of heavy fuel oil. If a typical refinery energy loss of 10% is associated with preparation of the fuel oils used by utilities, then the overall efficiency of generating electricity using liquid petroleum products falls even further.

The largest energy demand in the end use consumption sector is for transportation fuels, principally gasoline. Gasoline accounts for roughly one third of the total energy used in the air basin by final product customers. Residential and commercial customer demand for natural gas is second in magnitude, followed by industrial natural gas use and residential/commercial electricity demand.

Energy exports from the basin consist almost entirely of refinery products, plus natural gas in transit to other parts of the state. Net refinery product exports (i.e. exports less imports) have an energy content equal to about 30% of that of the initial crude oil runs to local refineries. That raises an interesting observation about the nature of trade patterns in the Southwest. For many years, persons living in areas outside of Los Angeles have complained that Los Angeles is exporting air pollution by locating some electric generating stations serving Los Angeles in desert areas to the east of the basin. As can be seen from Table 4.10, 33% of the electricity supply for the South Coast Air Basin comes from sources outside of the basin. From Table A3.2 in Appendix A3, it is seen that about half of that imported electricity is generated by fossil fuel fired steam plants located outside the air basin. However, it is also now apparent that a fairly

large fraction of the emissions caused by petroleum refining in Los Angeles are incurred within the South Coast Air Basin for the benefit of final product customers located elsewhere, principally in San Diego, Arizona and Nevada. It is obvious that the energy economies of all of Southern California, Arizona and Southern Nevada are so closely intertwined that the question of "exporting pollution" when siting a major energy transformation facility such as a power plant or refinery becomes nearly meaningless.

#### 4.4.4 The Sulfur Balance

Table 4.11 summarizes the sulfur balance on the South Coast Air Basin for the year 1973. An estimated total of 4.2 million pounds of sulfur per day was tracked through the basin's economy. Over ninety percent of that sulfur input accompanied crude oil.

The estimated fate of that sulfur supply is also given in Table 4.11:

- Nearly half of the sulfur was captured at sulfur recovery and sulfuric acid plants;
- Approximately one quarter of the sulfur was exported from the basin in finished petroleum products;
- 4.4% of the sulfur supply found its way into solid or liquid wastes;
- At least 14% of the sulfur was emitted to the atmosphere in the form of 586.51 tons per day of sulfur oxides air pollutants (stated as  $\text{SO}_2$ ); and
- The fate of 9.4% of the sulfur supply remains undetermined.

TABLE 4.11  
South Coast Air Basin Sulfur Balance-1973  
(1000's lbs sulfur per day)

	Refract Gas	Crude Oil; Refined Gasoline	LPG and Gasoline for Fuel	Light and Diesel Oil	Regional District Fuel Oil	Petroleum Coke	Non- Ferrous Products	Coal	Organic Solids	Sulfur Dioxide	Sulfur Trioxide	Sulfuric Acid	Waste Sulfur Products	Solid or Liquid Waste	Atmospheric Emissions From Processes	TOTAL
<b>SOXES</b>																
Resource base: impure plus local crude oil and natural gas production	0.81	3842.5	0.01	4.10	79.76	77.70	16.11	91.73	0.63	0.06			17.69			
Adjustments: change in gas storage	-5.02															
Subtotal	0.79	3842.5	0.01	4.10	79.76	77.70	16.11	91.73	0.63	0.06			17.69			4181.28
<b>TRANSFORMATION SECTOR</b>																
Refinery																
Feedstock sulfur																
Pulp sulfur																
Products and waste																
Sulfur Recovery and Sulfuric Acid																
Feedstock sulfur																
Products and waste																
Electric utilities																
Pulp sulfur																
Subtotal	-0.12	-3531.5	0.20	81.68	-20.18	-235.22	5.80	-0.07	-0.07	1390.4	0	353.4	134.95	53.77	11.68	
<b>END USE CONSUMPTION SECTOR</b>																
(Pulp Combustion in Basin)																
System uses: losses																
Residential/commercial																
Industrial (other than refinery)																
Transportation (aviation)																
Military																
Miscellaneous																
Subtotal	-0.01	-0.01	-0.01	-0.12	-26.74	-26.06	0	-0.22	-0.22	0	0	0	0	0	0	0
<b>ADJUSTMENT FOR EFFECT OF RAW MATERIALS PROCESSING INDUSTRIES</b>																
As a commodity (by ship)																
As a commodity (overland)																
In transport (with fuel tanks)																
Subtotal	0.07	-121.8	0	-3.03	-32.83	-302.37	-720.44	-91.73	-0.63	-1.67	unshown	0	0	0	0	0
<b>BASE FOR THIS AND OTHER SECTORS WHOSE ULTIMATE CONSUMER WILL NOT BE REPORTED</b>																
Subtotal	0.81	3842.5	2.66	86.28	165.41	879.01	348.22	91.73	0.63	1880.4	1700.76	353.4	17.69	185.00	368.31	17.69
<b>SUMMARY</b>																
Total sources (+ flows)	0.81	3842.5	2.66	86.28	165.41	879.01	348.22	91.73	0.63	1880.4	1700.76	353.4	17.69	185.00	368.31	17.69
Total sinks (- flows)	-0.81	-3842.5	-2.67	-86.88	-166.81	-880.25	-348.96	-91.73	-0.63	-1880.4	-1700.76	-353.4	-17.69	-185.00	-368.31	-17.69
Absolute difference	0	0	0	0	0	0	0	0	0	0	0	0	0	0	0	0
Difference as % of sources	0	0	0	0	0	0	0	0	0	0	0	0	0	0	0	0
Difference as % of total sulfur input of 481.38 thousand lbs/day	0	0	0	0	0	0	0	0	0	0	0	0	0	0	0	0

Notes: (a) This fuel burning total includes 41.36 thousand pounds of sulfur per day from the burning of fuel oil in industrial processes activities at Kaiser Steel.  
(b) These industrial process emissions include:  
- oil field production 4.50  
- steel mill 25.52  
- blast furnace 8.88  
- other industrial processes 0.07

In contrast to the energy balance, the sulfur balance at first glance does not appear to balance closely. The explanation for that problem, however, seems fairly straightforward.

The largest discrepancy between sulfur supply and consumption lies in the crude oil and refinery feedstocks column of Table 4.11. While sulfur supplied in that category exceeds known refinery feedstock sulfur intake plus exports by only 6.8%, that 6.8% difference is applied to two very large sulfur flows. One reason for this gap between estimated supply and demand lies in the fact that the APCD survey used to estimate sulfur intake by refineries did not include at least two small refineries which accounted for about 1% of the basin's daily crude oil demand in 1973. Refinery sulfur intake and products should be at least 1% higher than shown if more complete data were available on those small refineries. The remaining five to six percent surplus of sulfur in crude and unfinished oils probably represents an overestimate of either crude oil intake or crude oil sulfur content as part of the study conducted in Appendix A1 to this report. Considering the difficulty in estimating the origin of some of the crude oils received in the basin, that small percentage disagreement will be considered nearly unavoidable. Provided that the APCD refinery sulfur balance is correct, any overestimate of crude oil sulfur supply from Appendix A1 will not affect the rest of the sulfur flows shown in Table 4.11, nor will it inflate any atmospheric emissions estimates. With the crude oil sulfur discrepancy set aside, the remainder of the sulfur balance balances to within about 3%.

Turning to individual product streams, we note that the sulfur balances on the heavy petroleum products appear reasonable. Petroleum coke sulfur balances to within less than 1%, and heavy fuel oil balances to within 3.7%. Those two products account for about 28% of the total sulfur in the system. Heavy fuel oil combustion in the basin is the largest single source of sulfur oxides air pollutant emissions, accounting for just under half of the total  $SO_x$  emissions to the atmosphere. It is therefore reassuring to obtain a fairly close sulfur balance on supply and use for this product.

Petroleum coke is produced almost exclusively for export from the basin. However, a close balance on petroleum coke sulfur is still important because significant emissions to the atmosphere come from the petroleum coke calcining industry (25.22 tons/day as  $SO_2$ ; see adjustment for raw materials processing).

At the lightest product end of the sulfur balance, results also seem acceptable. Natural gas and refinery gases (LPG + still gas) contributed practically no sulfur oxides emissions even though they accounted for a third of the basin's total energy supply in 1973. Even a significant percentage error in estimating the sulfur content of either product would not change that conclusion.

In spite of the fact that the energy balance on gasoline closed almost exactly, the fate of 34% of the sulfur distributed in gasoline in 1973 remains undetermined. The apparent explanation is that the Bureau of Mines gasoline grab samples for that year were not

representative of a production-weighted average of local refinery products. Consider the following evidence to that effect.

Table 4.12 shows refinery sulfur output in gasoline for the years 1973 and 1974 as reported by refineries to the local air pollution control district. An estimate of the weight percent sulfur in gasoline implied by those refinery reports has been made for comparison with Bureau of Mines data. As can be seen, the refinery reports to the APCD closely follow the Bureau of Mines sulfur samples in 1974. But for 1973, either the Bureau of Mines samples are far too low, or the APCD sulfur balance is too high.

Since local refineries would be unlikely to overstate the total tonnage of sulfur distributed in gasoline by 47%, one tends to suspect the Bureau of Mines data. The Bureau of Mines appears to take grab samples of gasoline from a large number of refiners. These samples are first averaged for each refiner and then each refiner is weighted equally when computing the Southern California average gasoline sulfur content. But two of the eighteen refineries in the South Coast Air Basin accounted for about 40% of local refinery capacity in 1973. Unless the sulfur content of gasoline from the basin's large refineries is weighted by their market share, the Bureau of Mines would not compute a gasoline pool average sulfur content with any accuracy unless all gasoline samples were of about the same sulfur content. Bureau of Mines test results show wide variance in gasoline sulfur content between refineries. One therefore suspects that their average sulfur content

TABLE 4.12

Comparison of Bureau of Mines Gasoline Sulfur Content Data to the Sulfur Content of Gasoline Estimated from Refinery Reports to the Southern California APCD

Calendar Year	Sulfur distributed in gasoline (1000's lbs/day) (a)	Sulfur distributed as weight percent of gasoline production (approximate) (b)	Average weight percent sulfur in gasoline as implied by Bureau of Mines (c)
1973	81.88	0.070%	0.047%
1974	55.89	0.048%	0.049%

- Notes: (a) Based on refinery reports to the Southern California Air Pollution Control District (1976a).  
 (b) Based on an approximate gasoline production rate for local refineries of 450 thousand barrels per day in both years (estimated from Table A3.3).  
 (c) See Table A3.10.

values could be quite a bit in error if used to represent a gasoline pool average.

Unlike the discrepancy in the crude oil sulfur balance, the gasoline sulfur surplus probably represents a real uncertainty in the basin's atmospheric emissions estimates for 1973. Most gasoline produced in local refineries is actually burned in the basin. If the 1973 gasoline sulfur content were 47% higher than reported by the Bureau of Mines, then atmospheric emissions from gasoline combustion would have been close to 60 tons per day (as  $\text{SO}_2$ ) instead of the 41 tons per day calculated in Table 4.11.

A similar problem may have occurred with estimation of light and middle distillate fuel oil sulfur content in 1973. The average sulfur content of distillate oil products shown in Table A3.10 was given by the Bureau of Mines for the entire Western Region of the United States. Since several Southern California refineries handled very high sulfur crude oil, it would not be too surprising if Southern California distillate oil sulfur content were above the Western Region average. However, given the large variety of distillate oil products and the fact that our energy balance on these oils did not close exactly, it is not possible to pinpoint the nature of the imbalance in the distillate oil sulfur pool.

One of the most striking features of the sulfur balance is the relatively high degree of desulfurization of petroleum products that is already occurring at Los Angeles area refineries. Roughly half

of the sulfur entering those refineries is being captured as elemental sulfur or sulfuric acid, rather than leaving the refinery in products or waste discharges.

#### 4.5 Comparison of the Air Quality Modeling Emission Inventory to the Results of the Sulfur Balance

In Table 4.13, atmospheric emissions calculated from the sulfur balance on the South Coast Air Basin are compared to emissions identified in the air quality modeling inventory of Appendix A2. Emissions from electric utilities compare closely in both surveys even though one emissions total was calculated from utility annual reports while the other came from monthly data on each generating plant's fuel use. Refinery fuel burning estimates are in reasonable agreement, as are industrial process  $SO_x$  emissions levels. That is not too surprising since refinery and industrial process figures in both surveys were ultimately derived from local APCD records, with an independent check supplied by reference to Hunter and Helgeson (1976).

A comparison of mobile source emissions in Table 4.13 shows that about 36 tons per day of  $SO_x$  emissions were found by the sulfur balance beyond those identified in the modeling inventory. Most of that discrepancy represents emissions occurring within the air basin but located outside of the 50 by 50 mile square grid. However, most of these off-grid emissions may never be advected into the modeling region. They thus pose less of a hazard to air quality model results than would neglect of on-grid emissions of comparable size.

TABLE 4.13  
 Comparison of the Air Quality Modeling  
 Inventory of Appendix A2 to Emissions  
 Implied by the 1973 Sulfur Balance  
 on the South Coast Air Basin

Category	SO <sub>x</sub> Emissions from the Spatially Resolved Modeling Inventory -1973- (Tons/day as SO <sub>2</sub> )			SO <sub>x</sub> Emissions Implied by Sulfur Balance -1973- (Tons/day as SO <sub>2</sub> )
	On-Grid Sources	Off-Grid Sources	Total	
Stationary Sources				
Electric Utility Fuel	181.71	58.20	239.91	235.59
Refinery Fuel	9.42	(c)	9.42	11.68
Residential, Commercial and Industrial Fuel (*excluding Off-grid Steel Mill Fuel Use)	2.58	(c)	2.58	25.36*
Gas Utility System Fuel Use				0.02
Industrial Processes (including Off-Grid Steel Mill Fuel Burned)	177.52	43.59	221.11	219.80
Mobile Sources				
Civilian Transportation	57.71	(c)	57.71	85.82
Military Fuel <sup>(a)</sup>	---	(c)	---	3.26
Miscellaneous <sup>(b)</sup>	---	(c)	---	4.98
Total Emissions	428.94	101.79	530.73	586.51

Notes: (a) Military fuel is mostly for mobile sources.

(b) Miscellaneous uses are largely devoted to off-highway diesel fuel.

(c) Off-grid emissions in this category not inventoried.

In addition to the nearly certain 36 ton per day difference between the modeling inventory and actual basin-wide emissions, there are two uncertainties which are difficult to evaluate. The first is the 23 tons per day difference between residential, commercial and industrial fuel use  $SO_x$  emissions identified in the two competitive inventories. The second uncertainty involves approximately 20 tons per day of additional  $SO_x$  emissions which could have been missed by both survey techniques if the Bureau of Mines gasoline sulfur content data were too low.

The nature of the gasoline sulfur content issue has been explored previously and will not be pursued further at this time. However, the disagreement between survey methods in the area of residential, commercial and industrial stationary source fuel burning can be clarified somewhat.

Small stationary source fuel burning  $SO_x$  emissions estimated from Bureau of Mines fuel oil sales data are a full order of magnitude greater than emissions estimated from fuel burning records reported to the local air pollution control district. List (1971) also noted a similar discrepancy, and concluded that the APCD records must be wrong. In Appendix A2, however, a simulation model was constructed which calculated  $SO_x$  emissions within the 50 by 50 mile square grid from a combination of APCD reports and a knowledge of interruptible gas customers' sizes and locations in the basin. Natural gas use predicted by that simulation closely matched separate reports of total gas company dispatches to those customers. It is therefore concluded

that interruptible gas customers within the 50 by 50 mile grid have been correctly identified. Oil use estimates made for interruptible gas customers in Appendix A2 are known to be consistent with their gas curtailment status. Therefore oil burning  $SO_x$  emissions from those customers within the 50 by 50 mile square are thought to be calculated correctly in the modeling inventory. If the Bureau of Mines oil sales data are also correct, then the additional fuel burning sources involved are either located beyond our 50 by 50 mile square grid, or burn oil without regard for the level of gas service available to interruptible gas customers.

While neither the gasoline sulfur content nor the small stationary source fuel use uncertainties may be laid to rest completely, the absolute values of these uncertainties are fairly small. If only one of these two possible additional emission sources were actually to have existed in 1973, the modeling inventory would still reproduce total basin-wide emissions to within about 10.5%. Emissions within the 50 by 50 mile grid would be simulated much more closely. Reasonable assurance has been obtained that the modeling emission inventory reproduces average 1973  $SO_x$  emissions to within a few percent error.

#### 4.6 In Conclusion

Most of the sulfur entering the South Coast Air Basin's energy economy in 1973 arrived in a barrel of crude oil. Crude oils supplied to the basin in that year were characterized by origin, quantity and sulfur content. In the lowest sulfur category (< 0.25% S), 22% of the

total crude oil received contributed only 2% of the total sulfur input to local refineries. In contrast, 12% of the oil with the highest sulfur content accounted for 28.5% of the basin's sulfur supply. Well over 50% of the sulfur input to local refineries came from crude oils produced from oil fields located within the South Coast Air Basin. The South Coast Air Basin is saddled with a sulfur management problem which is likely to command considerable attention as long as local crude oils are processed in local refineries.

A spatially resolved sulfur oxides emission inventory has been constructed to advance an emissions-air quality modeling study of sulfate formation in the Los Angeles atmosphere. Emissions estimates were developed for each of 26 classes of mobile and stationary sources for each month of the years 1972 through 1974. The spatial distribution of total  $\text{SO}_x$  emissions from each source class in each month was determined within a 50 by 50 mile square laid over metropolitan Los Angeles and Orange Counties. Major off-grid stationary sources in the South Coast Air Basin were also inventoried. Information was presented on the fraction of each source class's  $\text{SO}_x$  emissions which are evolved as  $\text{SO}_3$  or sulfates rather than as gaseous  $\text{SO}_2$ . The diurnal variation of power plant and motor vehicle emissions was specified. The effective height of injection of emissions into the atmosphere has been investigated.

In the year 1973, for example, 82.6% of that  $\text{SO}_x$  emissions inventory was concentrated in a small number of point source classes, as shown in Table 4.14. Electric utility generating plants constituted

TABLE 4.14  
 SO<sub>x</sub> Emissions from Point Source Classes  
 Emitting over 20 tons/day in 1973  
 within the South Coast Air Basin

Equipment Type	Number of Plant Sites	1973 SO <sub>x</sub> Emissions tons/day	Percent of Total Modeling Inventory SO <sub>x</sub> Emissions* 1973
Electric Utility Generating Stations	18	239.91	45.2%
Sulfur Recovery Plants	9	60.40	11.4%
Refinery Fluid Catalytic Crackers	8	52.07	9.8%
Integrated Steel Mill	1	41.46	7.8%
Petroleum Coke Calcining Kilns	2	25.52	4.8%
Sulfuric Acid Plants	3	20.00	3.8%

Note: \*Based on modeling inventory total of 530.73 tons/day SO<sub>x</sub>

the largest source of total sulfur oxides emissions in the basin in recent years. Other major source classes emitting over 20 tons of  $\text{SO}_x$  per day in 1973 included refinery fluid catalytic crackers, chemical plants involved in recovering sulfur and sulfuric acid from refinery wastes, a local steel mill, and petroleum coke calcining kilns. All other stationary sources combined totaled only 6% of the modeling emission inventory in 1973. Mobile sources accounted for the remaining  $\text{SO}_x$  emissions surveyed.

From the results of the detailed emission inventory, it was estimated that less than 15% of the sulfur supplied to the basin daily in crude oil was being emitted to the atmosphere in the form of sulfur oxides air pollutants. In order to confirm that finding, an energy and sulfur balance was constructed for flows of energy and sulfur crossing a control surface drawn around the perimeter of the air basin. The findings of that sulfur balance indicated that about half of the sulfur arriving in crude oil in 1973 was recovered at the refinery level as elemental sulfur or sulfuric acid. Only 14% of the basin's original sulfur supply reached the atmosphere as sulfur oxides air pollutant emissions. Most of the remaining sulfur was diverted into solid materials like petroleum coke and asphalt that will not be burned within the basin for fuel, or was exported from the basin in heavy fuel oil or other petroleum products. The 1973 sulfur oxides emission control strategy for the South Coast Air Basin was found to entail about a 50% efficient overall desulfurization of products at local refineries,

followed by segregation of most of the remaining sulfur within products that will not be burned locally.